Helicity Density Matrix Formalism and Polarized Processes in QCD

by

Jian Tang

B.S., Peking University, P.R. China (1991)
M.S., Peking University, P.R. China (1994)
M.S., Massachusetts Institute of Technology (1996)

Submitted to the Department of Physics
in partial fulfillment of the requirements for the degree of

Doctor of Philosophy in Physics

at the

MASSACHUSETTS INSTITUTE OF TECHNOLOGY

June 1999

Author .....
Department of Physics
May 26, 1999

Certified by .....
Robert L. Jaffe
Professor
Thesis Supervisor

Accepted by .....
Thomas J. Greytak
Professor, Associate Department Head for Education

Helicity Density Matrix Formalism and Polarized Processes in QCD

by

Jian Tang

Submitted to the Department of Physics
on May 26, 1999, in partial fulfillment of the
requirements for the degree of
Doctor of Philosophy in Physics

Abstract

In this thesis, we shall first present *helicity density matrix formalism* to deal with the polarized processes in quantum chromodynamics(QCD), in which the calculations of the desired cross sections (or asymmetries in many cases) are simplified to take traces of products of helicity density matrices in the underlying particles' (partons, hadrons, etc.) helicity spaces. The parton distribution and fragmentation functions turn out to be the helicity density matrix elements which survive the QCD symmetries. The main advantages of this formalism are that it has very clear physical pictures, simplifies the calculation, and, most importantly, can be easily used to deal with interference effects between different partial waves in multiparticle production in semi-inclusive processes. Then this formalism will be used to propose new ways to measure nucleon's transversity, the least known quark distribution function inside the nucleon at leading twist (twist-two). The processes of interest are the two pion semi-inclusive productions in the transversely polarized deep inelastic scattering (only the target is polarized) and nucleon nucleon collisions (only one beam is polarized). A set of novel quark interference fragmentation functions are introduced in the framework of the helicity density matrix formalism and are used to probe the nucleon's transversity distribution function. The advantages of this method are that the effect is leading twist, meson pairs are abundantly produced in quark fragmentation, and the essential final state interaction phase is well studied.

Thesis Supervisor: Robert L. Jaffe
Title: Professor

Dedicated to My Family for Their Love and Supports

Acknowledgments

I would like to have this special opportunity to thank many people for their generous supports and helps, which make this thesis possible.

Primarily I would like to thank my thesis supervisor professor Bob Jaffe. This thesis truly could not be done without his useful advices, constant supports and encouragement. Bob showed incredible patience and understanding with me. He always had insightful suggestions and approaches to our research problems, which make this thesis much better. His determination and ingenious methods have won my highest respects. I am also particularly grateful for the time he devoted to me even though he was quite busy.

I would also like to thank professor Xiangdong Ji, with whom I have worked for two year from 1994 to 1996 while he was at MIT. His enthusiasm and dedication to physics really impressed me. His encouragement and supports helped me endure the most difficult two years at MIT. I thank him for the productive two years together.

I would also like to thank professor Uwe-Jens Wiese and professor Richard Milner for serving on my thesis committee as readers. Their comments and suggestions helps make this thesis better.

I would also like to thank professor John Negele for his supports and a lot of useful advices on my academical developments.

I would also like to thank Xuemin Jin for pleasant and productive collaborations.

I would also like to specially thank professor Kuangta Chao, my former advisor in Peking University of P.R.China, for his constant encouragements and the time and efforts he devoted to my intellectual and personal developments. Also thank my friends and former teachers and classmates at Peking University, whom I am unable to list one by one here.

I would also like to thank a lot of friends of mine here, Li Cai, Jiang Chen, Danning Dong, Juncai Gao, Shanhui Fan, Qiang Liu, Shiaobin Soong, ..., for their helps and advices and a lot of pleasant conversations, not to mention a lot of exciting and wonderful trips with some of them. They made my stay here much easier and much more enjoyable.

I would also thank CTP , LNS and Physics Department for their financial and other supports during my study here.

Finally, I would very much like to thank my family: my father Weijin Tang, my mother Nianbi Kang, my wife Zheng Liu, my brother Ping Tang and two sisters, Hong Tang and Yan Tang. Without their unselfish love and supports, this thesis could not be done. Nobody deserves more thanks from the bottom of my heart than them.

Thank everyone who ever helps me. May God bless you all.

Contents

List of Figures

Chapter 1

Introduction

The purpose of this thesis is to present a new helicity density matrix formalism to deal with the polarized processes in high energy physics, and then apply it to propose a new way to measure the nucleon's transversity distribution function, one of the three characterizing the quark states inside the nucleon.

This chapter acts as an introduction to this thesis. Our intention here is to walk through the theoretical backgrounds related to this thesis. Many topics will be touched but not detailedly in order to accommodate the concept of the *introduction.* One can refer to some standard textbooks for details[1].

For a long time it has been known that there are four kinds of forces mediated between elementary particles: (i) gravitation[1] ; (ii) electromagnetic interaction; (iii) weak interaction; (iv) strong interaction. The first two are long range forces because they basically have infinite ranges, although the potentials produced by them fall off as $1/r$ with distance r from the force sources. The weak and strong interactions have very short ranges, e.g. the strong interaction has a range of about 10^{-13}cm, and the weak force only has about 10^{-16}cm. This is one of the reasons why the gravitation and electromagnetic forces were discovered long before the other two.

Very roughly, the particles can be classified according to what types of interactions which they participate. All of the known particles so far are subject to gravi-

[1]it is believed to play a negligible role in particle physics since it is extremely weak.

tation and weak interaction. The particles which participate the strong interaction are called hadron, e.g. pion, proton, etc. The leptons are those particles which do not participate the strong interaction. Some typical leptons are electrons and neutrinos. All hadrons and leptons, except neutrinos, take part in the electromagnetic interaction[2]

Hadrons actually are not elementary particle as thought in the beginning. It is believed they are composed of six further constituents—*quarks*: u(up), d(down), s(strange), c(charm), b(bottom), t(top), which have spin 1/2 and fractional charges. These quarks and leptons are the fundamental fermions, which are grouped into three families, as summarized in the table1.1. The four interactions are mediated through

Families			Charge	Spin
ν_e	ν_μ	ν_τ	0	1/2
e	μ	τ	-1	1/2
u	c	t	2/3	1/2
d	s	b	-1/3	1/2

Table 1.1: Three families of fundamental fermions

the exchanges of the gauge bosons. For instance, strong interaction is exerted by gluons, electromagnetic interaction by photons, and weak interaction by W and Z bosons.

Over the past three decades, major progresses have been made in the particle physics. Two major theories have been developed: one is the electroweak theory, which unifies the weak and electromagnetic interactions (In reality, these two interactions are totally different because the symmetry is broken spontaneously.); another is quantum chromodynamics (QCD), which governs the color interaction between the quarks (or strong interaction at hadron level). These two theories together are called *standard model* of elementary particle physics[1]. Since this thesis deals mostly with the strong interaction, we will focus on QCD in this introduction.

[2]Even the hadrons with zero net charges feel the electromagnetic interaction through their charge distribution or magnetic moment.

1.1 Naive Quark Model[2]

As mentioned in last section, hadrons are not elementary particles, instead they are composed of quarks. There are two kinds of hadrons: one is called *meson*, which is the bound state of quark-antiquark pair ($q\bar{q}$); another is *baryon*, which is of three quarks (qqq).[3]

1.1.1 Flavor SU(3) symmetry

The observed hadrons are eigenstates of the strong interaction Hamiltonian $H_{\rm st}$. The fundamental assumptions of the naive quark model are

- Quark flavor independence of the strong interaction;
- Equality of the quark masses, i.e. $m_u = m_d = m_s$ [4].

Under these assumptions, $H_{\rm st}$ is invariant under SU(3) transformation of the quarks u, d and s—SU(3) flavor symmetry. The spectra of the hadrons can be understood from this symmetry. All hadrons can be classified according to the irreducible representations of the flavor SU(3) group, and all the particles in an SU(3) multiplet have same masses. For example, all mesons are either SU(3) singlet or octet, and all baryons act as SU(3) singlet, octet, and decuplet.

However, in reality the particles in the same multiplets do not have same masses, which indicates that flavor SU(3) symmetry is broken. There are no evidences of the violations of the first assumption thus far, however, $m_u \neq m_d \neq m_s$ has been proved.

1.1.2 Color SU(3) symmetry

An additional degree of freedom *color* for quarks was introduced by Gell-mann and Fritzsch [3] in order to avoid a problem in constructing wavefunctions for some hadrons

[3]However, other compositions are possible, e.g. glueball (made up of only gluons), although they are not yet confirmed by experiments.

[4]Only three light quarks u, d and s are considered here.

in quark model [5] . A quark is assumed to carry three kinds of colors: red(r), green(g), blue(b), which are the bases of a new SU(3) group — color SU(3). Only the singlet of this group can exist in nature. Therefore, a quark has to be confined in a hadron because it is a triplet in the color space. A quark with different flavors and colors is denoted by q_α, where $q = u,\ d,\ s$ indicates the flavor, and $\alpha = r,\ g,\ b$ is the color index. A more detailed discussion of the color SU(3) will be given in the appendix .3.

1.1.3 Hadron's wavefunctions

The quarks inside the hadrons have the following degrees of freedom: flavor, spin, color, and space. One should be able to construct the hadron's static wavefunction from its quark components, like in quantum mechanics. Here we are going to use the nucleon as an example to show how to do it.

The nucleon is composed of three quarks, proton $\sim uud$ and neutron $\sim udd$. Its wavefunction can be written as

$$\psi_N \sim \text{flavor} \otimes \text{spin} \otimes \text{color} \otimes \text{space} \ , \tag{1.1}$$

where ψ_N represents the nucleon's wavefunction. Due to the the fermionic nature of the quarks, the overall wavefunctions of the bound states of the quarks have to be totally antisymmetric, as required by Pauli principle. We will only discuss the ground states, in which the spatial wavefunctions are totally symmetric. The nucleon has to be a color singlet in the color SU(3) space, which means that the wavefunction is totally antisymmetric with respect to color

$$\psi_N \sim \epsilon_{\alpha\beta\gamma} q^\alpha q^\beta q^\gamma \ . \tag{1.2}$$

where α, β, γ are color indices, and $\epsilon_{\alpha\beta\gamma}$ is totally antisymmetric three dimensional tensor discussed in the appendix .1. Therefore flavor $\otimes$ spin part of the wavefunction

[5] For example, if there were no *color* degree of freedom, the total wavefunction for particle $\Omega^-(sss)$ would be totally symmetric, which contradicts the Pauli principle.

must be totally symmetric, i.e., the totally symmetric combinations of the basis states $u_\uparrow, u_\downarrow, d_\uparrow, d_\downarrow$ as follows

$$\begin{aligned} p(\tfrac{1}{2}\tfrac{1}{2}) = \quad & \frac{1}{\sqrt{18}}[2u_\uparrow u_\uparrow d_\downarrow + 2u_\uparrow d_\downarrow u_\uparrow + 2d_\downarrow u_\uparrow u_\uparrow \\ & -u_\uparrow u_\downarrow d_\uparrow - u_\downarrow u_\uparrow d_\uparrow - u_\downarrow d_\uparrow u_\uparrow - u_\uparrow d_\uparrow u_\downarrow - d_\uparrow u_\uparrow u_\downarrow - d_\uparrow u_\downarrow u_\uparrow] \ , \\ n(\tfrac{1}{2}\tfrac{1}{2}) = \quad & \frac{1}{\sqrt{18}}[2d_\uparrow d_\uparrow u_\downarrow + 2d_\uparrow u_\downarrow d_\uparrow + 2u_\downarrow d_\uparrow d_\uparrow \\ & -d_\uparrow d_\downarrow u_\uparrow - d_\downarrow d_\uparrow u_\uparrow - d_\downarrow u_\uparrow d_\uparrow - d_\uparrow u_\uparrow d_\downarrow - u_\uparrow d_\uparrow d_\downarrow - u_\uparrow d_\downarrow d_\uparrow] \ , \end{aligned} \tag{1.3}$$

where the up arrow means spin up and the down arrow means spin down. One can refer to an extensive table of such wavefunctions given by Thirring [4]. These wavefunctions can be used to calculate the static properties of the nucleon, for example, the magnetic moments of the proton and neutron which will be discussed in the following.

For a baryon in the ground state, the magnetic moment is the sum of the magnetic moment of the quarks because there is no orbital angular momentum. The operator of the magnetic moment is given by

$$\vec{\mu} = \frac{2}{3}\mu_u\vec{\sigma}_u - \frac{1}{3}\mu_d\vec{\sigma}_d - \frac{1}{3}\mu_s\vec{\sigma}_s \ , \tag{1.4}$$

where $\mu_q(q = u, d, s)$ is the quark magneton, which has the form of $\mu_q = e/2m_q$ $(q = u, d, s)$. $\vec{\sigma}$ is Pauli matrix.

Take the expectation value of the magnetic moment operator in Eq. (1.4) using the wavefunctions in Eq. (1.3), one can obtain

$$\begin{aligned} \mu_p &= \mu_u \ , \\ \mu_n &= -\frac{2}{3}\mu_u \ , \end{aligned} \tag{1.5}$$

if assuming $m_u = m_d$.

Thus the ratio predicted by the theory is

$$\frac{\mu_n}{\mu_p} = -\frac{2}{3} , \tag{1.6}$$

which agrees very well with the experiment value

$$\frac{\mu_n}{\mu_p} = \frac{-1.913}{2.793} = -0.685 . \tag{1.7}$$

This is a major achievement of the naive quark model.

From the Eq. (1.3), one can see that the nucleon's spin structure is quite simple. For example, a spin-up nucleon is made up of two quarks with spin-up and one spin-down. There is no orbital angular momentum. However, it is not this simple in QCD, as we will discuss later.

1.2 Quantum Chromodynamics: an Introduction

Like quantum electrodynamics (QED) in which the photon mediate the electromagnetic interaction between charged particles, the strong interaction between the quarks inside a hadron is believed to be mediated by exchanges of a flavor-independent spin-1 particle—gluon.

Likewise, one can also use the gauge minimal principle, which is used to obtain the QED Lagrangian $\mathcal{L}_{\text{QED}}$, to get the QCD Lagrangian $\mathcal{L}_{\text{QCD}}$,

$$\mathcal{L}_{\text{QCD}} = -\frac{1}{4}\text{Tr } \mathbf{F}_{\mu\nu}\mathbf{F}^{\mu\nu} + \bar{q}\ (i\gamma_\mu \mathbf{D}^\mu + m)\ q\ . \tag{1.8}$$

Here q represents the quark field. $\mathbf{D}_\mu = \partial_\mu + ig_s\mathbf{A}_\mu$ is the covariant derivative coming from the minimal principle, where g_s is the strong interaction coupling constant and $\mathbf{A}_\mu$ is the gluon gauge field, $\mathbf{A}_\mu = A^a_\mu(x)T^a$ with T^a being the Gell-Mann matrices for SU(3) group (see appendix .3). The trace Tr acts on the color space, e.g., Tr $\mathbf{A}_\mu(\mathbf{x}) =$

0. $\mathbf{F}_{\mu\nu}$ is the gluon field strength tensor,

$$\mathbf{F}_{\mu\nu}(x) = \partial_\mu \mathbf{A}_\nu(x) - \partial_\nu \mathbf{A}_\mu(x) + ig_s [\, \mathbf{A}_\mu(x), \mathbf{A}_\nu(x) \,] \;, \tag{1.9}$$

which is different from QED in that there is no analogous quadratic (the last term in Eq. (1.9)) in QED. This term is necessary to achieve a simple transformation behavior for the gluon field strength tensor $\mathbf{F}_{\mu\nu}(x)$ under local gauge transformations. It is also this term which makes QCD much more complicated than QED because it indicates the self interactions between gluons.

One of the most important properties of QCD is that it is asymptotically free [5]. The strong interaction coupling constant g_s gets smaller and smaller as the energy gets large. Therefore, one can use perturbation theory to do calculation at high energy (higher than some typical energy scale $\Lambda_{\rm QCD}$).

1.3 Deep Inelastic Scattering(DIS)

Deep inelastic scattering (DIS) has been playing essential roles in the development of the understanding of the sub-structure of elementary particles. It is the archetype for hard processes in QCD: a lepton (e.g. electron, muon or neutrino) with very high energy scatters off a target hadron (practically a nucleon) with a large quantities of invariant squared-four-momentum transferring from lepton to hadron. Because we are mainly interested in the experiments with polarized targets, we will devote ourselves to charged lepton scattering off a polarized nucleon, in which the dominant reaction mechanism is electromagnetism and one photon-exchange is a good approximation[1, 6].

1.3.1 Basic kinematic variables

We consider the process shown in Fig. (1-1). The initial lepton with momentum k and energy E exchange a photon of momentum q with a target with momentum P. The outgoing lepton's momentum is k' and its energy E'. The basic kinematic variables

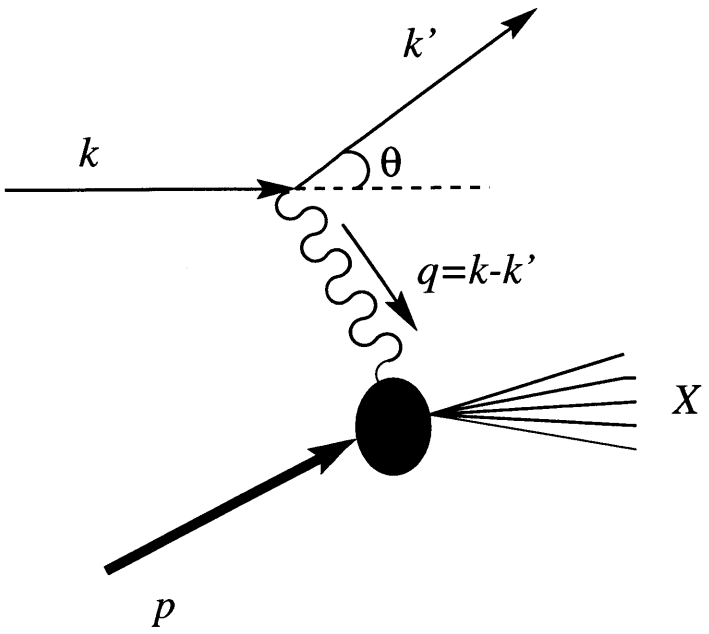

Figure 1-1: The basic diagram for lepton-hadron deep inelastic scattering in the target rest frame

are defined as below:

M	The mass of the target, which is the nucleon mass in the case of a nucleon target
E	The energy of the incident lepton
k	The momentum of the initial lepton.
P	The momentum of the target, $P = (M, 0, 0, 0)$ at its rest frame
E'	The energy of the scattered lepton
k'	The momentum of the scattered lepton.
Ω	The scattering solid angle
θ	the scattering angle illustrated in Fig. (1-1).
q	$= k - k'$, the momentum transfer in the scattering process, i.e. the momentum of the virtual photon
Q^2	$\equiv -(k - k')^2 = 4EE' \sin^2(\frac{\theta}{2})$, neglecting the lepton masses
W^2	$= (P + q)^2$, invariant squared mass of the hadrons(X) in the final state
ν	$\equiv P \cdot q$, which is equal to $M(E - E')$ in the target rest frame

x $= Q^2/2\nu$, Bjorken scaling variable$(0 \leq x \leq 1)$

ω $= 1/x$

y $= P \cdot q / P \cdot k$, the fractional energy loss of the lepton$(0 \leq y \leq 1)$.

where the lepton mass has been neglected. Unless otherwise noted, E, E', θ refer to the target rest frame, in which one has

$$P_\mu = (M, \vec{0}),\ k_\mu = (E, \vec{k}),\ k'_\mu = (E',\ \vec{k}')\ . \tag{1.10}$$

Bjorken limit is where Q^2 and ν both go to infinity with the ratio, $x = Q^2/2\nu$ fixed. x is the *Bjorken* scaling variable. Since the invariant mass of the hadronic final state is larger than or equal to that of the target, $(P+q)^2 \geq M^2$, one has kinetic range for x: $0 < x \leq 1$. The lepton energy loss must be between zero and E, hence $0 \leq y \leq 1$.

1.3.2 Cross Section and Hadronic Tensor

The differential cross-section for *inclusive* scattering ($eP \rightarrow e'X$, in which hadronic final states X are not observed) is given by:

$$d\sigma = \frac{1}{J}\frac{d^3k'}{2E'(2\pi)^3}\sum_X \prod_{i=1}^{n_X} \int \frac{d^3p_i}{(2\pi)^3 2p_{i0}} |\mathcal{T}|^2 (2\pi)^4 \delta^4 (P + q - \sum_{i=1}^{n_X} p_i). \tag{1.11}$$

The flux factor for the incoming nucleon and electron is denoted by $J = 4P \cdot k$, which is equal to $4ME$ in the rest frame of the nucleon. The sum runs over all unobserved hadronic final states X. Each hadronic final state consists of n_X particles with momenta p_i ($\sum_{i=1}^{n_X} p_i \equiv p_X$). The scattering amplitude is given by

$$\mathcal{T} = e^2 \bar{u}(k', s')\gamma^\mu u(k, s)\frac{1}{q^2}\langle X|J_\mu(0)|PS\rangle\ , \tag{1.12}$$

where J_μ is the hadronic electromagnetic current. $|X\rangle$ represents the unobserved final hadronic states. $|PS\rangle$ represents the nucleon state, which is normalized covariantly

as follows,

$$\langle P'S|PS\rangle = 2P^0(2\pi)^3\delta^3(\vec{P}-\vec{P}') \ , \tag{1.13}$$

s is the lepton spin vector which is normalized to $s^2 = -m^2$, while S is the nucleon spin vector normalized to $S^2 = -M^2$ and $S \cdot P = 0$.

The polarized differential cross-section can be written in terms of a leptonic ($l^{\mu\nu}$) and a hadronic ($W^{\mu\nu}$) tensor as follows

$$\frac{d^2\sigma}{d\Omega dE'} = \frac{\alpha^2}{Q^4}\left(\frac{E'}{ME}\right) l^{\mu\nu}W_{\mu\nu}, \tag{1.14}$$

where $\alpha = e^2/4\pi$ is the electromagnetic fine structure constant. The leptonic tensor $l^{\mu\nu}$ is given by the square of the elementary spin 1/2 current (summed over final spins):

$$\begin{aligned} l^{\mu\nu} &= \sum_{s'} \bar{u}(k,s)\gamma^\mu u(k',s')\bar{u}(k',s')\gamma^\nu u(k,s) \\ &= 2(k'^\mu k^\nu + k'^\nu k^\mu) - 2g^{\mu\nu}k\cdot k' + 2i\epsilon^{\mu\nu\lambda\sigma}q_\lambda s_\sigma, \end{aligned} \tag{1.15}$$

where we have used $u(k,s)\bar{u}(k,s) = \not{k}(1+\gamma_5\not{s})/2$. The hadronic tensor $W_{\mu\nu}$ is given by

$$\begin{aligned} W_{\mu\nu} &= \frac{1}{4\pi}\sum_X \prod_{i=1}^{n_X} \int \frac{d^3p_i}{(2\pi)^3 2p_{i0}} \langle PS|J^\mu|X\rangle\langle X|J^\nu|PS\rangle (2\pi)^4\delta^4(P+q-\sum_{i=1}^{n_X} p_i) \\ &= \frac{1}{4\pi}\int d^4\xi e^{iq\cdot\xi}\langle PS|[J^\mu(\xi), J^\nu(0)]|PS\rangle. \end{aligned} \tag{1.16}$$

In order to get Eq. (1.16) we have written the δ function as an exponential,

$$(2\pi)^4\delta^4(P) = \int d^4\xi e^{i\xi\cdot P}, \tag{1.17}$$

and used the completeness,

$$\sum_X \prod_{i=1}^{n_X} \int \frac{d^3p_i}{(2\pi)^3 2p_{i0}} |X\rangle\langle X| = 1, \tag{1.18}$$

and the translation invariance,

$$e^{i\xi\cdot(P-p_X)}\langle PS|J^\mu(0)|X\rangle = \langle PS|J^\mu(\xi)|X\rangle. \tag{1.19}$$

Note that another term

$$\frac{1}{4\pi}\int d^4\xi e^{iq\cdot\xi}\langle PS|J^\nu(0)J^\mu(\xi)|PS\rangle \tag{1.20}$$

has been subtracted to convert the current product into a commutator. It is easy to check that this new term vanishes for $q^0 > 0 (E > E')$ which is the case for physical lepton scattering from a stable target. The reason is because this term has a δ function: $\delta^4(q - P + p_X)$ when sandwiching the completeness condition Eq. (1.18) between two currents,

$$\begin{aligned} &\int d^4\xi e^{iq\cdot\xi}\langle PS|J^\nu(0)J^\mu(\xi)|PS\rangle \\ = &\sum_X \prod_{i=1}^{n_X}\int \frac{d^3p_i}{(2\pi)^3 2p_{i0}}\langle PS|J^\nu(0)|X\rangle\langle X|J^\mu(0)|PS\rangle(2\pi)^4\delta^4(q - P + p_X) \end{aligned} \tag{1.21}$$

However, we can show that $q-P+p_X \neq 0$. The reason is the following: Assume that $q-P+p_X = 0$ holds, then one has $p_X = P-q$ which leads to $p_X^0 = P^0 - q^0 = M - q^0$ in the target rest frame (laboratory frame). Thus one gets $p_X^0 < M$ at physical region $q^0 > 0$, which is impossible because proton is the lightest stable baryon.

[*Note:* $W^{\mu\nu}$ can be related to the imaginary part of the forward virtual Compton scattering amplitude T using the optical theorem:(see, for instance, Refs. [1])

$$2\pi W^{\mu\nu} = \mathrm{Im}T^{\mu\nu} \tag{1.22}$$

with

$$T^{\mu\nu} = i\int d^4\xi e^{iq\cdot\xi}\langle PS|TJ^\mu(\xi)J^\nu(0)|PS\rangle. \tag{1.23}$$

This relation will enable us to employ the Operator Product Expansion(OPE) [7] to discuss the perturbative properties of $W^{\mu\nu}$.]

1.3.3 Structure Functions and Bjorken Scaling

While the leptonic tensor is known completely, $W^{\mu\nu}$, which describes the internal structure of the nucleon, depends on the non-perturbative strong interaction dynamics, about which unfortunately we know little. Using Lorentz covariance, gauge invariance, parity conservation in electromagnetism and standard discrete symmetries of the strong interactions, $W^{\mu\nu}$ can be parameterized in terms of four scalar dimensionless structure functions $F_1(x,Q^2)$, $F_2(x,Q^2)$, $g_1(x,Q^2)$ and $g_2(x,Q^2)$. They depend only on the two invariants Q^2 and ν, or alternatively on Q^2 and the dimensionless *Bjorken* variable x,

$$\begin{aligned} W^{\mu\nu} &= \left(-g^{\mu\nu}+\frac{q^\mu q^\nu}{q^2}\right)F_1+\left[\left(P^\mu-\frac{\nu}{q^2}q^\mu\right)\left(P^\nu-\frac{\nu}{q^2}q^\nu\right)\right]\frac{F_2}{\nu} \\ &\quad -i\epsilon^{\mu\nu\lambda\sigma}q_\lambda\left(\frac{S_\sigma}{\nu}(g_1+g_2)-\frac{q\cdot SP_\sigma}{\nu^2}g_2\right), \end{aligned} \tag{1.24}$$

Note that here we explicitly have $q_\mu W^{\mu\nu}=q_\nu W^{\mu\nu}=0$, which is the consequence of the conservation of the electromagnetic current, $\partial_\mu J^\mu=0$.

The hadronic tensor defined in Eq. (1.16) is dimensionless, as are the structure functions in Eq. (1.24). The structure functions are functions of the Lorentz invariant variables $P^2=M^2$, $P\cdot q$ and Q^2 which can form two independent dimensionless combinations, e.g., $x=Q^2/2P\cdot q$ and Q^2/M^2 . The structure functions can be written as dimensionless functions of $x=Q^2/2P\cdot q$ and Q^2/M^2 . Bjorken first pointed out that if the hadron were composed of essentially free pointlike objects at high energies, then, up to logarithms, the structure functions only depend on x, but independent of the scale Q^2, in the Bjorken limit (where $Q^2\to\infty$ and $\nu\to\infty$, but $x=Q^2/2\nu$ fixed),

$$\begin{aligned} F_1(Q^2,\nu) &\to F_1(x,\ln Q^2), \quad F_2(Q^2,\nu) \to F_2(x,\ln Q^2) \\ g_1(Q^2,\nu) &\to g_1(x,\ln Q^2), \quad g_2(Q^2,\nu) \to g_2(x,\ln Q^2) \end{aligned} \tag{1.25}$$

This is the so-called *Bjorken* scaling[8]. [6] The Callan-Gross relation between F_1 and F_2,

$$F_2(x) = 2xF_1(x) \ , \tag{1.26}$$

indicates that the quark has spin $\frac{1}{2}$[9].

$F_1(x)$, $g_1(x)$ and $g_2(x)$ are related to quark unpolarized distribution, longitudinally polarized distribution and transversely polarized distribution functions inside the nucleon, respectively.

1.3.4 Cross Sections for DIS

The cross section for deep inelastic electron-nucleon scattering can be easily obtained by contracting the hadronic tensor $W_{\mu\nu}$ in Eq. (1.16) with the leptonic tensor $l_{\mu\nu}$ in Eq. (1.15). Here we list the results for the spin-average and polarized cross sections from Ref. [6]

$$\frac{d^3\bar{\sigma}}{dx\,dy\,d\phi} = \frac{e^4}{4\pi^2 Q^2}\left\{\frac{y}{2}F_1(x,Q^2) + \frac{1}{2xy}\left(1-y-\frac{y^2}{4}(\kappa-1)\right)F_2(x,Q^2)\right\} \tag{1.27}$$

and

$$\begin{aligned}\frac{d\Delta\sigma(\alpha)}{dx\,dy\,d\phi} &= \frac{e^4}{4\pi^2 Q^2}\left\{\cos\alpha\left\{\left[1-\frac{y}{2}-\frac{y^2}{4}(\kappa-1)\right]g_1(x,Q^2) - \frac{y}{2}(\kappa-1)g_2(x,Q^2)\right\}\right. \\ &- \left.\sin\alpha\cos\phi\sqrt{(\kappa-1)\left(1-y-\frac{y^2}{4}(\kappa-1)\right)}\left(\frac{y}{2}g_1(x,Q^2)+g_2(x,Q^2)\right)\right\}\end{aligned} \tag{1.28}$$

Here $\kappa \equiv 1 + 4x^2M^2/Q^2$ is a measure of approach to the scaling limit $Q^2 \to \infty$, ϕ is the azimuthal angle, α is the angle between the nucleon spin $\vec{S}$ and the momentum of the incident electron $\vec{k}$.

[6] This scaling invariance is violated in QCD due to quantum corrections, see, for example, Refs. [1]

1.3.5 Operator Product Expansion[7]

This is merely a very brief introduction to a very complicated topic in perturbative QCD[1]. Our goal here is to introduce some of the concepts relevant to this thesis.

The starting point in the derivation is the Eq. (1.23), the time-ordered product of two currents, which is not a local operator. Consider the product of two local operators $\mathcal{O}_a(x)\mathcal{O}_b(0)$ in coordinate space. [7] In the limit $x \to 0$, this product can be written as an expansion of some local operators

$$\lim_{x\to 0} \mathcal{O}_a(x)\mathcal{O}_b(0) = \sum_c C_{abc}(x)\mathcal{O}_c(0) \ , \tag{1.29}$$

in which $\mathcal{O}_c(0)$ is a local operator. All dependences on x, hence the singularities as $x \to 0$, are in the expansion coefficients $C_{abc}(x)$. The coefficients $C_{abc}(x)$ can be computed in the perturbation theory since all non-perturbative effects occur at scales which are much larger than x .

Usually, the operator product expansion is used in the momentum space, i.e., the Fourier transformation of Eq. (1.29),

$$\lim_{q\to\infty} \int d^4x e^{iq\cdot x} \mathcal{O}_a(x)\mathcal{O}_b(0) = \sum_c C_{abc}(q)\mathcal{O}_c(0) \ . \tag{1.30}$$

Now the limit $x \to 0$ is forced by $q \to \infty$. This expansion is valid provided that q is much larger than the typical hadronic mass scale $\Lambda_{\rm QCD}$.

The local operators in the operator product expansion in QCD are quark and gluon operators, e.g., a symmetric and traceless local operator with spin n and dimension d denoted by $\mathcal{O}_{d,n}^{\mu_1\cdots\mu_n}$. The matrix element has the following form

$$< P|\mathcal{O}_{d,n}^{\mu_1\cdots\mu_n}|P > \sim M^{d-n-2} P^{[\mu_1}\ldots P^{\mu_n]} A_n + \ldots \ , \tag{1.31}$$

where the square brackets [] in the superscript is to project the totally symmetric traceless part. The power of M follows from $< P'|P >= (2\pi)^3 2P^0\delta^3(\vec{P} - \vec{P}')$. A_n

[7] Note that x here is coordinate, not Bjorken scaling variable.

is non-perturbative structure function. ... indicates the less important terms in the expansion.

Then one can obtain the following form for the hadronic tensor $W_{\mu\nu}$,

$$W_{\mu\nu} \sim t_{\mu\nu} \sum_k \left(\frac{M}{Q}\right)^{t_{n_k}-2} \omega^{n_k} A_{n_k} \ , \tag{1.32}$$

where $\omega \equiv 1/x$ with x now being Bjorken variable, $Q \equiv \sqrt{-q^2}$, $t_{\mu\nu}$ is a rank-two tensor such as $g_{\mu\nu}, P_\mu P_\nu/Q^2$.

The *twist* t of a local operator defined as

$$t \equiv \text{dimension} - \text{spin} = d - n \tag{1.33}$$

is very important to classify the operators in OPE. Since usually $M \ll Q$, the importance of an operator is determined by its twist. We say that twist $t-1$ operators are suppressed by $\mathcal{O}(1/Q)$ compared to twist-t ones. The twist is also very important in categorizing the quark distribution and fragmentation functions, as discussed later.

The operator product expansion is very useful in deriving sum rules in parton model. It is so complicated issue that it is impossible to cover it in just about one page. One can refer to references[1] for details.

1.4 Parton Distribution and Fragmentation Functions

The parton distribution function $d(x)$ measures the probability to find a parton inside a hadron carrying longitudinal fraction x of the hadron's momentum. The parton fragmentation function $f(z)$ measure the probability to find a hadron carrying longitudinal fraction z of the parton's momentum in the parton fragmentation process. They are very important in understanding of the structure of the hadron. In the following we will focus on the quark distribution and fragmentation functions for spin-$\frac{1}{2}$ hadron. Readers can find more details in references[6, 10, 11, 12]

1.4.1 Distribution functions

The distribution functions are related to the quark-quark density matrix [6, 10, 11],

$$\mathcal{D}(x) = \int \frac{d\lambda}{2\pi} e^{i\lambda x} < PS|\bar{\psi}(0)\Gamma\psi(\lambda n)|PS > , \tag{1.34}$$

where n_μ are light-like null vector defined in appendix .6 . $|PS>$ is the wavefunction for the nucleon with normalization $< P'S|PS >= (2\pi)^3 2P^0\delta^3(\vec{P} - \vec{P}')$. P is the momentum of the nucleon, S is the polarization vector ($P^2 = M^2$, $S^2 = -M^2$, $P \cdot S = 0$). Γ is one of the 16 Dirac matrices, i.e. I, γ_5, γ_μ, $\gamma_\mu\gamma_5$, $\sigma_{\mu\nu}$(or $\sigma_{\mu\nu}\gamma_5$) .

Substitute those Dirac matrices into Eq. (1.34) and expand them according to their Lorentz structures, one obtains the following definitions for the quark distribution functions.

$$\begin{aligned}
\int \frac{d\lambda}{2\pi} e^{i\lambda x} \left\langle PS|\bar{\psi}(0)\psi(\lambda n)|PS\right\rangle &= 2Me(x), \\
\int \frac{d\lambda}{2\pi} e^{i\lambda x} \left\langle PS|\bar{\psi}(0)\gamma_\mu\psi(\lambda n)|PS\right\rangle &= 2\left\{f_1(x)p_\mu + M^2 f_4(x)n_\mu\right\}, \\
\int \frac{d\lambda}{2\pi} e^{i\lambda x} \left\langle PS|\bar{\psi}(0)\gamma_\mu\gamma_5\psi(\lambda n)|PS\right\rangle &= 2\left\{g_1(x)p_\mu S\cdot n + g_T(x)S_{\perp\mu} + M^2 g_3(x)n_\mu S\cdot n\right\}, \\
\int \frac{d\lambda}{2\pi} e^{i\lambda x} \left\langle PS|\bar{\psi}(0)i\sigma_{\mu\nu}\gamma_5\psi(\lambda n)|PS\right\rangle &= 2\{h_1(x)(S_{\perp\mu}p_\nu - S_{\perp\nu}p_\mu)/M \\
&\quad + h_L(x)M(p_\mu n_\nu - p_\nu n_\mu)S\cdot n \\
&\quad + h_3(x)M(S_{\perp\mu}n_\nu - S_{\perp\nu}n_\mu)\} .
\end{aligned} \tag{1.35}$$

Here p_μ is another light-like null vector($p^2 = 0$, $p^- = 0$, $p\cdot n = 1$, and $P = p + \frac{1}{2}M^2 n$). Also, we have written $S_\mu = S\cdot n p_\mu + S\cdot p n_\mu + S_{\perp\mu}$. Note that in principle there should be an expansion for $\Gamma = \gamma_5$, however, it vanishes since the only pseudo-scalar combination out of P and S is $P\cdot S$, which is zero.

The Eqs. (1.35) define nine quark distribution functions. However, they are not equally important in terms of their contributions to a hard process. As a matter of fact, they can be categorized according to their twist. $f_1(x)$, $g_1(x)$ and $h_1(x)$ are twist-two quantities; $e(x)$, $h_L(x)$ and $g_T(x)$ twist three; $f_4(x)$, $g_3(x)$ and $h_3(x)$ twist four. Therefore it is reasonable enough to discuss more about $f_1(x)$, $g_1(x)$ and $h_1(x)$.

In fact, only these three are relevant in this thesis.

It is easy to project out $f_1(x)$, $g_1(x)$ and $h_1(x)$ out of the decompositions,

$$\begin{aligned} f_1(x) &= \int \frac{d\lambda}{4\pi} e^{i\lambda x} \langle P|\bar{\psi}(0)\not{n}\psi(\lambda n)|P\rangle \\ g_1(x) &= \int \frac{d\lambda}{4\pi} e^{i\lambda x} \langle PS_\parallel|\bar{\psi}(0)\not{n}\gamma_5\psi(\lambda n)|PS_\parallel\rangle \\ h_1(x) &= \int \frac{d\lambda}{4\pi} e^{i\lambda x} \langle PS_\perp|\bar{\psi}(0)[\not{S}_\perp,\not{n}]\gamma_5\psi(\lambda n)|PS_\perp\rangle \end{aligned} \tag{1.36}$$

$f_1(x)$ is spin-average quark distribution function. $g_1(x)$ is helicity difference quark distribution function. $h_1(x)$ is called transversity distribution function. $f_1(x)$ and $g_1(x)$ are chiral-even, i.e. the chirality of the quark is not changed, whereas $h_1(x)$ is chiral-odd. [8] Chiral odd distribution functions are suppressed in ordinary DIS process since massless QCD conserves quark's chirality. Therefore it is harder to measure the transversity compared to the other two. How to probe it will be one of main topics of this thesis.

1.4.2 Fragmentation functions

The quark fragmentation function is more complicated than the distribution case in the sense that a quark can fragment into various particles, even multiple particles. Also, the fragmentation process might involve final state interaction such that the time reversal invariance is violated. We will give a very simple introduction here using as an example the quark fragmentation into spin-$\frac{1}{2}$ hadron. For more general discussions, e.g., fragmentation into spin-0, spin-1 hadrons, please refer to the references[6, 12].

The generic expression for a fragmentation function takes the form,

$$\hat{\mathcal{F}}(z) = \sum_X \int \frac{d\lambda}{2\pi} e^{-i\lambda/z} \langle 0|\Gamma_{\alpha\beta}\psi_\beta(0)|PX\rangle \left\langle PX|\bar{\psi}_\alpha(\lambda n)|0\right\rangle , \tag{1.37}$$

where $\Gamma_{\alpha\beta}$ stands for an arbitrary Dirac matrix. X represents the final states which are not observed.

[8] It is very easy to see this from the Eqs. (1.36)

Just like that in the distribution function case, one can easily obtain the twist two fragmentation functions $\hat{f}_1$, $\hat{g}_1$ and $\hat{h}_1$ if one chooses $\Gamma = \not{n}, \not{n}\gamma_5$ and $\sigma^j_\nu n^\nu i\gamma_5$ respectively,

$$\begin{aligned}
\hat{f}_1(z) &= \frac{1}{2}\sum_X \int \frac{d\lambda}{2\pi} e^{-i\lambda/z} \langle 0|\not{n}\psi(0)|PX\rangle \left\langle PX|\bar{\psi}(\lambda n)|0\right\rangle, \\
\hat{g}_1(z) &= \frac{1}{2}\sum_X \int \frac{d\lambda}{2\pi} e^{-i\lambda/z} \langle 0|\not{n}\gamma_5\psi(0)|PSX\rangle \left\langle PSX|\bar{\psi}(\lambda n)|0\right\rangle, \\
\frac{S_\perp{}^j}{M}\hat{h}_1(z) &= \frac{1}{2}\sum_X \int \frac{d\lambda}{2\pi} e^{-i\lambda/z} \left\langle 0|\sigma^j_\nu n^\nu i\gamma_5\psi(0)|PS_\perp X\right\rangle \left\langle PS_\perp X|\bar{\psi}(\lambda n)|0\right\rangle
\end{aligned} \tag{1.38}$$

Similarly, $\hat{f}_1(z)$ and $\hat{g}_1(z)$ are chiral even fragmentation functions, whereas $\hat{h}_1(z)$ is chiral-odd. $\hat{h}_1(z)$ can be coupled with $h_1(x)$ to measure the transversity distribution functions.

A twist three chiral-odd fragmentation function is $\hat{e}_1(z)$,

$$\hat{e}_1(z) = \frac{1}{2M}\sum_X \int \frac{d\lambda}{2\pi} e^{-i\lambda/z} \langle 0|\psi(0)|PX\rangle\langle PX|\bar{\psi}(\lambda n)|0\rangle \tag{1.39}$$

1.5 Spin Structures of the Nucleon

Together, f_1, g_1, and h_1 provide a complete description of quark distribution inside a nucleon at leading twist (twist 2). $f_1(x)$ has been well studied theoretically and experimentally for a long time[1]. $h_1(x)$ is hard to be accurately measured due to its chiral-odd property, so far there is no data on it although theoretical progresses have been made[6]. A big chunk of this thesis will be devoted to discuss how to probe it experimentally. The recently accurate measurement of $g_1(x)$ has given physics community a big surprise by declaring that, contrary to the naive quark model, quark spins only contribute a little to the nucleon's spin[13].

In this section, we shall give a brief review about the spin structure of the nucleon, which is closely related to the measurement of $g_1(x)$.

1.5.1 Ellis-Jaffe Sum Rule

$g_1(x)$ is related to the polarized quark distribution functions $\{q_\uparrow(x), q_\downarrow(x), \bar{q}_\uparrow(x), \bar{q}_\downarrow(x)\}$ as follows

$$g_1(x) = \frac{1}{2}\sum_q e_q^2[q_\uparrow(x) - q_\downarrow(x) + \bar{q}_\uparrow(x) - \bar{q}_\downarrow(x)] \tag{1.40}$$

where e_q is the quark electric charge measured in terms of the electron electric charge, $\uparrow$ and $\downarrow$ mean quark's helicity parallel and antiparallel to the nucleon's, respectively.

Much of the interest in the polarized structure function g_1 is due to its relation to axial vector current matrix elements:

$$\langle PS|A_\alpha^q|PS\rangle \mid_{\mu^2} \equiv \langle PS|\bar{q}\gamma_\alpha\gamma_5 q|PS\rangle \mid_{\mu^2} = \Delta q(\mu^2) S_\alpha \tag{1.41}$$

where the label μ refers to the mass scale at which the axial vector current operator is renormalized, and

$$\Delta q \equiv \int_0^1 dx[q_\uparrow(x) - q_\downarrow(x) + \bar{q}_\uparrow(x) - \bar{q}_\downarrow(x)] \ , \tag{1.42}$$

where the renormalization scale dependence μ is implicit. In naive quark model, the integrals of the g_1 structure functions for proton

$$\Gamma_1^p(Q^2) \equiv \int_0^1 dx g_1^p(x, Q^2) \tag{1.43}$$

are related to the combinations of the Δq

$$\Gamma_1^p(Q^2) = \frac{1}{2}\left(\frac{4}{9}\Delta u(Q^2) + \frac{1}{9}\Delta d(Q^2) + \frac{1}{9}\Delta s(Q^2)\right) \ . \tag{1.44}$$

The perturbative QCD corrections to the above relation have been calculated,

$$\begin{aligned}\Gamma_1^p(Q^2) \ &= \ \frac{1}{2}\left(\frac{4}{9}\Delta u(Q^2) + \frac{1}{9}\Delta d(Q^2) + \frac{1}{9}\Delta s(Q^2)\right) \\ &\quad \times\left(1 - \frac{\alpha_s(Q^2)}{\pi} + \mathcal{O}(\alpha_s^2)\right) + \mathcal{O}\left(\frac{\Lambda^2}{Q^2}\right) \ ,\end{aligned} \tag{1.45}$$

where the power series in $\alpha_s(Q^2)$ represents a perturbative calculation of the coefficient function of the axial vector currents[14, 15] and the $\mathcal{O}(\Lambda^2/Q^2)$ terms are higher-twist corrections.

The g_1^p sum rule is interesting because some of combinations of Δu, Δd and Δs can be independently measured, or inferred from data on nucleon and hyperon β-decays. The octet axial currents which mediate Gamow-Teller transitions between octet baryons are defined by

$$A_\mu^a \equiv \bar{\psi}\gamma_\mu\gamma_5 T^a \psi, \tag{1.46}$$

with $\mathrm{tr}T^aT^b = \frac{1}{2}\delta^{ab}$. The nucleon matrix element of the A_μ^3 determines the combination $\Delta u - \Delta d$;

$$(\Delta u - \Delta d)S_\mu = 2\langle PS|A_\mu^3|PS\rangle = g_A S_\mu = (F+D)S_\mu, \tag{1.47}$$

where g_A is the nucleon axial vector charge which can be measured in neutron β-decay. $F+D$ is its parameterization in terms of SU(3) invariant matrix elements for the axial current in the hyperon semileptonic decay,which is valid in the SU(3) symmetry limit. SU(3) symmetry is also responsible for determining the other linearly independent combination,

$$(\Delta u + \Delta d - 2\Delta s)S_\mu = 2\sqrt{3}\langle PS|A_\mu^8|PS\rangle = (3F-D)S_\mu, \tag{1.48}$$

The third combination, $\Delta\Sigma$, is related to the flavor singlet current operator A_μ^0 as follows

$$\Delta\Sigma(\mu^2)S_\mu \equiv (\Delta u + \Delta d + \Delta s)S_\mu = \langle PS|A_\mu^0|PS\rangle\ |_{\mu^2} \tag{1.49}$$

with

$$A_\mu^0 \equiv \sum_{f=1}^{3} \bar{\psi}_f\gamma_\mu\gamma_5\psi_f\ . \tag{1.50}$$

We can rewrite g_1^p sum rule in Eq. (1.45) in terms of F, D, and $\Delta\Sigma$ as below

$$\Gamma_1^p(Q^2) = \frac{1}{18}\left(3F + D + 2\Delta\Sigma(Q^2)\right)\left(1 - \frac{\alpha_s(Q^2)}{\pi} + \mathcal{O}(\alpha_s^2)\right) + \mathcal{O}\left(\frac{\Lambda^2}{Q^2}\right)\ . \tag{1.51}$$

Combining Eqs. (1.47), (1.48), and (1.49) together, we have

$$\begin{aligned} \Delta u(Q^2) - \Delta d(Q^2) &= F + D \ , \\ \Delta u(Q^2) + \Delta d(Q^2) - 2\Delta s(Q^2) &= 3F - D \ , \\ \Delta u(Q^2) + \Delta d(Q^2) + \Delta s(Q^2) &= \Delta\Sigma(Q^2) \ . \end{aligned} \tag{1.52}$$

Note that $\Delta\Sigma$ depends upon the renormalization scale μ^2 because the flavor singlet current A^0_μ is not conserved even when quarks are massless, due to the triangle anomaly[16]

$$\partial^\mu A^0_\mu = \frac{n_f \alpha_s}{2\pi} \mathrm{Tr} F\tilde{F} \ , \tag{1.53}$$

where n_f is flavor number.

It is not possible to derive sum rule for Γ_1^p without supplementary assumptions because there are three unknowns but only two experimental values (F and D, there was no experimental data on $\Delta\Sigma$ two decades ago). In 1973, J. Ellis and R. Jaffe assumed that $\Delta s = 0$ on the grounds that very possibly there were a negligible number of strange quarks in the nucleon wave function -OZI rule[17]. With this assumption, it was estimated that

$$\int_0^1 dx g_1^p(x, Q^2) = \frac{1}{18}(4\Delta u + \Delta d)(1 - \alpha_s/\pi + \mathcal{O}(\alpha_s^2)) = 0.17 \pm 0.01. \tag{1.54}$$

This is the so-called Ellis-Jaffe sum rule[18]. It based on two main assumptions: SU(3) symmetry and $\Delta s = 0$. It has become one of the most famous sum rules in spin physics due to the EMC experiment in 1987[13] that will be discussed in the following subsection.

1.5.2 EMC Experiment and Spin Crisis

In 1987 the EMC reported a measurement of $g_1^p(x, Q^2)$[13]. The quantity they measured is the spin asymmetry

$$A_1 \equiv \frac{\mu^\uparrow p^\uparrow - \mu^\uparrow p^\downarrow}{\mu^\uparrow p^\uparrow + \mu^\uparrow p^\downarrow} \tag{1.55}$$

in $\mu - p$ scattering, where the terms denote cross-sections and the arrows $\uparrow$ and $\downarrow$ denote polarizations along the beam direction. A_1 is related to g_1 by

$$g_1(x, Q^2) \simeq \frac{A_1(x) F_1(x, Q^2)}{1 + R(x, Q^2)} \tag{1.56}$$

where $R(x, Q^2)$ is the ratio of longitudinal to transverse virtual photon cross-section, which can be taken from parameterizations of unpolarized scattering data, and $F_1(x, Q^2)$ is the unpolarized structure function

$$F_1(x) = \frac{1}{2} \sum_q e_q^2 [q_\uparrow(x) + q_\downarrow(x) + \bar{q}_\uparrow(x) + \bar{q}_\downarrow(x)]. \tag{1.57}$$

EMC extrapolated their measured structure function from $x \simeq 0.02$ down to $x = 0$, and published a result for the first moment of $g_1(x)$,

$$\Gamma_1^p = \int_0^1 dx g_1^p(x) = 0.126 \pm 0.010 \pm 0.015, \tag{1.58}$$

at energy $Q^2 = 10.7\text{GeV}^2$. It is significantly smaller than the prediction of Ellis-Jaffe sum rule.

Fitting F and D to the hyperon semileptonic decays, and using the errors determined from the fit gives[21]

$$F = 0.47 \pm 0.004, \quad D = 0.81 \pm 0.003. \tag{1.59}$$

Substituting Eqs. (1.58) and (1.59) into Eq. (1.51), we find at EMC energy(about 10.7GeV^2)

$$\Delta\Sigma \equiv \Delta u + \Delta d + \Delta s = 0.13 \pm 0.19 \tag{1.60}$$

or equivalently,

$$\Delta u = 0.78 \pm 0.10, \ \Delta d = 0.50 \pm 0.10, \ \Delta s = -0.20 \pm 0.11, \tag{1.61}$$

by solving Eqs. (1.52).

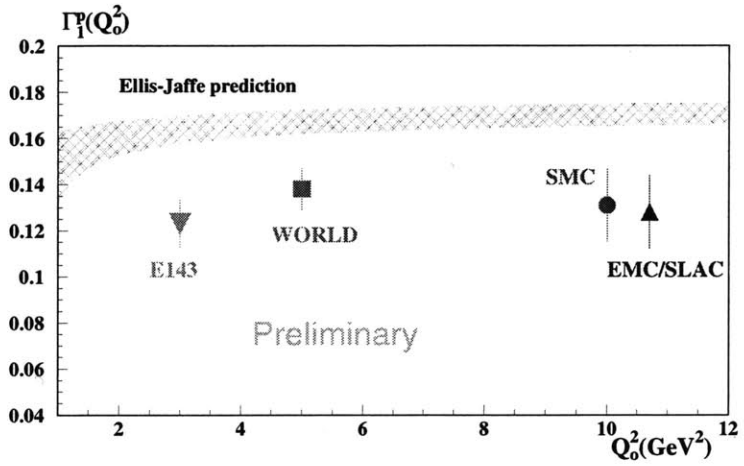

Figure 1-2: Comparison of data with the assumption $\Delta s = 0$ from SMC.

These results have shocked the particle community and aroused so much interest. Because according to the Ellis-Jaffe ansatz, $\Delta s = 0$[18], it would have predicted

$$\Delta\Sigma = 3F - D = 0.60 \pm 0.12. \tag{1.62}$$

The EMC data are about two standard deviations away from the prediction by Ellis-Jaffe sum rule. According to EMC data it seems that we can not attribute the nucleon's spin to only the spins of the quarks. Much of the nucleon's spin must lie elsewhere. This is the so-called "spin crisis". Since EMC announced their results, there have been further more accurate experiments done by EMC, SMC(at CERN), E142, E143(at SLAC)[22]. The comparison of the data with Ellis-Jaffe sum rule is shown in Fig. (1-2) [9]. From the figure, we can see clearly the deviation of Ellis-Jaffe sum rule from the experimental data. The values of $\Delta\Sigma$ at $Q^2 = 3\text{GeV}^2$ extracted

[9]It is extracted from Ref. [20]

Experiments	target	x	Q^2[GeV^2]
E130	p	0.180-0.7	3.5-10
EMC	p	0.010-0.7	1.5-70
SMC	p	0.003-0.70	1.0-60
E143	p	0.029-0.8	1.3-10
SMC-93	d	0.006-0.6	1.0-30
SMC-95	d	0.003-0.7	1.0-60
E143	d	0.029-0.8	1.0-30
E142	n	0.030-0.6	1.0-10

Table 1.2: Current experiments at CERN and SLAC.

from each experiment are shown in Fig. (1-3) [10]. The average value at $Q^2 = 3\text{GeV}^2$ is[23]

$$\Delta\Sigma = \Delta u + \Delta d + \Delta s = 0.27 \pm 0.04 \tag{1.63}$$

and

$$\Delta u = 0.82 \pm 0.03,\ \Delta d = -0.44 \pm 0.03,\ \Delta s = -0.11 \pm 0.03. \tag{1.64}$$

where the more recent $F + D = 1.2573 \pm 0.0028$ and $F/D = 0.575 \pm 0.016$ have been used.

One may also get a feeling for the expected range of $\Delta\Sigma$ and Δs by plotting the results for these two observables extracted from from each of the existing experiments, as shown in Fig. (1-4).

1.5.3 Theoretical Explanations

Then, what does the nucleon's spin come from if not just from quark's spin? Since the EMC experiment, there have been a lot of theoretical issues raised by the unexpected result. The following are some extracted from Ref. [21]:

- Violation of $SU(3)$ symmetry for octet axial charges could affect the evaluation of the sum rule. As we have pointed out, $SU(3)$ symmetry plays an important role in determining Δu, Δd and Δs(through the determination of F and D).

[10]Figs. (1-3) and (1-4) are extracted from Ref. [23]

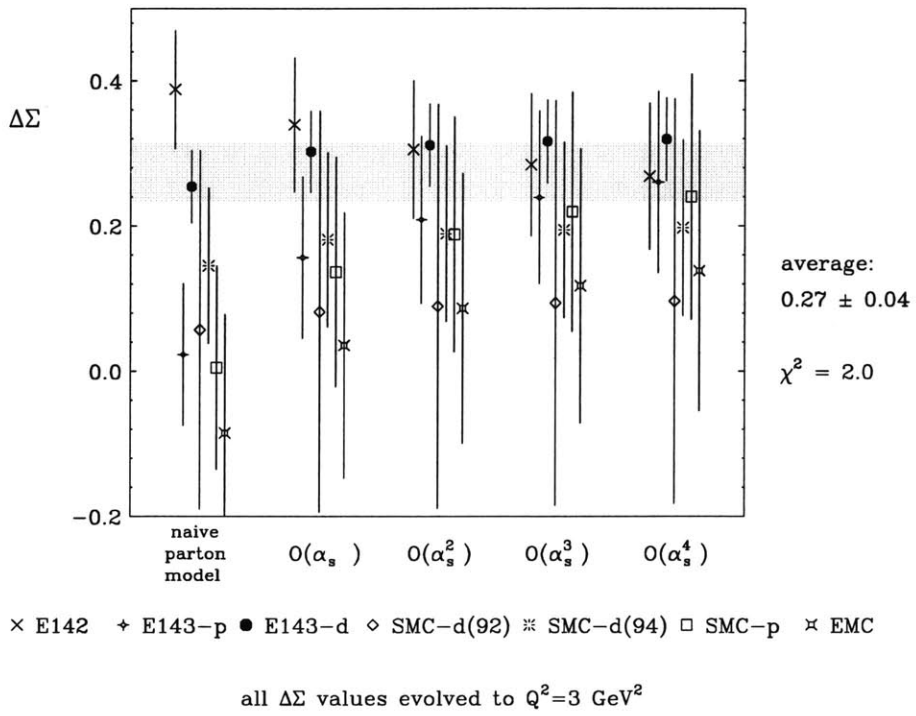

Figure 1-3: The values of $\Delta\Sigma(Q^2 = 3\text{GeV}^2)$ extracted from each experiment, plotted as the increasing order of QCD perturbation theory used in obtaining $\Delta\Sigma$ from the data.

However, we know that actually $SU(3)$ symmetry is broken badly. These large corrections may change the result significantly [24, 25, 26].

- Uncertainty of the extrapolation from the lowest measured $x(\sim 0.02)$ to $x = 0$. Unanticipated behavior of the functions $xg_1(x, Q^2)$ as $x \to 0$ could affect the sum rules [27].

- The possible non-perturbative evolution of $\Delta\Sigma$. As we have noted, $\Delta\Sigma$ does depend on the mass scale at which it is measured. It is possible that $\Delta\Sigma$ is large at the confinement scale($\mu \sim 1\text{GeV}$), but somehow evolves away to a very small value at EMC energy range[28].

- Ambiguity of the definition of $\Delta\Sigma$ due to the axial current anomaly[16]. Shortly after EMC published their results, Alterelli and Ross[29] and Carlitz et al.[30] pointed out that there is gluon contribution to the proton spin through the

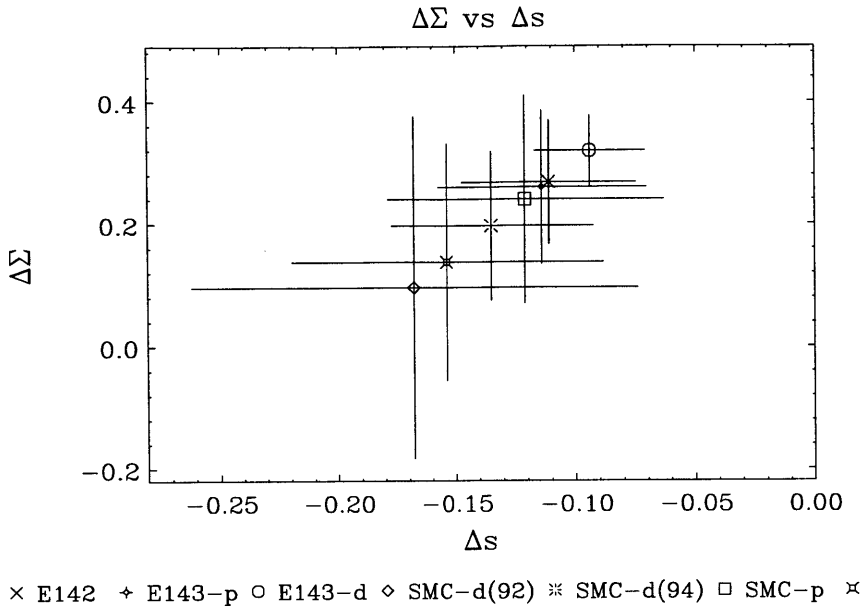

Figure 1-4: The values of $\Delta\Sigma$ and Δs extracted from each experiment, plotted against each other. All data have been evolved to common $Q^2 = 3$ GeV^2.

axial current anomaly[16]. What the EMC measured is actually the combination $\Delta q = \Delta q' - \frac{\alpha_s}{2\pi}\Delta g$ with $\Delta q'$ being identified to the naive quark model expectation and Δg being the integrated gluon helicity distribution. The small experimental value of $\Delta\Sigma$ can be interpreted due to large cancelation between $\Delta q'$ and Δg, which would require a rather large $\Delta g (\simeq 5 \sim 6)$ at the EMC energy.

These explanations focus on trying to point out what might go wrong in the experiment. However, a more modern view of the spin structure of the nucleon is that the nucleon's spin is separated into four terms [21, 31],

$$\frac{1}{2} = \frac{1}{2}\Delta\Sigma(\mu) + L_q(\mu) + \Delta G(\mu) + L_g(\mu) \ , \tag{1.65}$$

where ΔG is the gluon spin contribution, L_q and L_g are the quark and gluon orbital angular momenta, respectively.

$$\Delta\Sigma \ = \ \langle P+|\hat{S}_{3q}|P+\rangle = \langle P+|\int d^3x \ \bar{\psi}\gamma^3\gamma_5\psi \ |P+\rangle \ ,$$

$$\begin{aligned}
\Delta G &= \langle P+|\hat{S}_{3g}|P+\rangle = \langle P+|\int d^3x\ (E^1A^2 - E^2A^1)\ |P+\rangle\ , \\
L_q &= \langle P+|\hat{L}_{3q}|P+\rangle = \langle P+|\int d^3x\ i\bar{\psi}\gamma^0(x^1\partial^2 - x^2\partial^1)\psi\ |P+\rangle\ , \\
L_g &= \langle P+|\hat{L}_{3g}|P+\rangle = \langle P+|\int d^3x\ E^i(x^2\partial^1 - x^1\partial^2)A^i\ |P+\rangle\ , \qquad (1.66)
\end{aligned}$$

where for simplicity we have neglected the normalization of the state. $E^{ia} \equiv -F^{0ia} = -(\partial^0 A^{ia} - \partial^i A^{0a} + ig_s f^{abc} A^{0b} A^{ic})$ is the color electric field. These four terms are all dependent on renormalization scale μ . It would be very interesting to see how much these four terms contribute to the nucleon's spin $\frac{1}{2}$. However, unfortunately, only the first term $\Delta\Sigma$ is measured. There are still no any data on other three terms. While there are some plans to try to measure ΔG at RHIC, people are still clueless on how to probe the orbital angular momenta L_q and L_g experimentally although there are some theoretical attempts along this direction[32].

Ji, Tang and Hoodbhoy have found interesting results by studying the Q^2 evolution of the four terms[31], very similar to Altarelli and Parisi equations[33]

- Quark and gluon almost carry same amount of the nucleon's spin in the limit $Q^2 \to \infty$,

$$\begin{aligned}
\lim_{Q^2\to\infty} \frac{1}{2}\Delta\Sigma(Q^2) + L_q(Q^2) &= \frac{1}{2}\frac{3N_f}{16+3N_f}\ , \\
\lim_{Q^2\to\infty} \frac{1}{2}\Delta G(Q^2) + L_g(Q^2) &= \frac{1}{2}\frac{16}{16+3N_f}\ , \qquad (1.67)
\end{aligned}$$

  where N_f is the number of the quark flavors involved. It is exactly analogous to the result for the momentum sum rule[34]. If, like the momentum sum rule, these results hold even at relatively low Q^2, then one can conclude that $L_q \sim 0.1$ from the measurement of $\Delta\Sigma$.

- Another interesting result is that the net effect of the renormalization scheme dependence is just to shift some contribution between quark spin and its orbital angular momentum,

$$\frac{1}{2} = \frac{1}{2}\left(\Delta\Sigma(\mu) - \frac{\alpha_s}{2\pi}N_f\Gamma\right) + \left(L_q(\mu) + \frac{\alpha_s}{4\pi}N_f\Gamma\right) + \Delta G(\mu) + L_g(\mu)\ . \qquad (1.68)$$

However, the fraction of the nucleon spin carried by quarks is invariant under such shift.

More about this can be found in appendix .8 or Ref. [31].

1.6 Organization of This Thesis

The rest of this thesis is organized as follows. In the chapter 2, we shall present helicity density matrix formalism to deal with the polarized processes in QCD. Then we go on to discuss how to measure the transversity distribution function. First a detailed review of the transversity is presented in chapter 3. Since the measurement of transversity is one of the main topics of this thesis, we review it in a separate chapter instead of putting it in the chapter 1. Then we will introduce the interference fragmentation functions and use them to measure the transversity in DIS process in chapter 4 and in nucleon-nucleon collisions in chapter 5. In chapter 6, we will discuss the idea of using the interference fragmentation functions to measure the valence quark spin distribution functions. Chapter 7 is devoted to summarize the whole thesis. Part of this thesis is based on the works done or discussed with Bob Jaffe and Xuemin Jin[35, 36].

Chapter 2

Helicity Density Matrix Formalism

The operator product expansion[7] and cut diagram techniques have been traditionally used in dealing with high energy polarized processes in QCD[1]. However, these techniques are somewhat complicated and lack of clear physical pictures of the processes. In this chapter, we shall present a general helicity density matrix formalism, in which the calculations of the desired cross sections are simplified to be take traces of products of some helicity density matrices in the underlying particles'(partons, hadrons, etc.) helicity spaces [1]. The main advantages of this formalism are that it has very clear physical pictures, simplifies the calculation, and, most importantly, can be easily used to deal with multiparticle interferences.

Typically, the high-energy polarized processes in QCD are involved with soft QCD and hard QCD parts. The soft QCD parts are parton distribution functions in hadrons and parton fragmentation functions. The hard QCD parts are parton-parton or parton-electron hard processes (scattering, annihilation, etc.). For instance, a typical diagrams for a semi-inclusive single particle production process is shown in Fig. 2-1.

Accordingly, this chapter is divided into four sections. The first section is devoted to the parton distribution functions. We shall introduce the definitions of the QCD distribution density operators, and discuss how the conservation laws (angular

[1]Some early works about this formalism can be found in Refs.[37, 38]

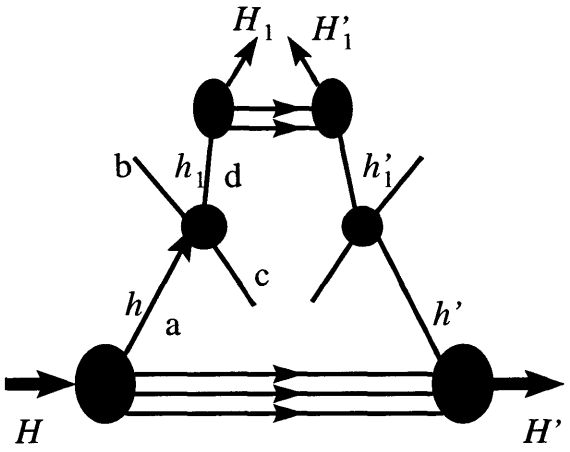

Figure 2-1: A generic semi-inclusive single particle production process at parton level. The top part is parton fragmentation into a single particle, the middle is the hard parton process, the bottom is the parton distribution in a hadron.

momentum, parity, time reversal) can reduce the number of the independent helicity amplitudes of processes. In the end, we shall show that the remaining independent amplitudes are related to the familiar parton distribution functions.

The second section is to discuss the parton fragmentation processes, which are more complicated than the distribution case due to the relaxation of the time-reversal symmetry and interference between different partial waves in the multiple particle production. We shall also introduce the definitions of QCD fragmentation density operators and discuss the symmetry constraints to the helicity matrix. We discuss the relations between the independent non-zero elements and the parton fragmentation functions in the end of this section.

The third section is to discuss the helicity amplitude approach to the hard QCD processes (e.g. parton parton scattering, etc.). We first review the Gastmanns and Wu's approach in the unpolarized processes[39]. Then we shall generalize their techniques to deal with the polarized processes in QCD.

The last section is to discuss the cross section density matrix in the formalism, and to summarize the whole chapter.

2.1 Distribution Functions as Helicity Density Matrix Elements

In this section, we shall discuss how to deal with the parton distribution functions in the helicity density matrix formalism. The purpose is to relate the helicity density matrix elements to the familiar distribution functions, in other words, to put the distribution functions into helicity density matrix.

The helicity density matrix elements are not independent of each other due to QCD symmetries. The symmetries (angular momentum, parity, time reversal) dramatically reduce the independent numbers of the helicity density matrix elements. The surviving independent elements are related to familiar parton distribution functions. Because the Cartesian operators are not irreducible under $SO(3)$ rotation, the irreducible tensor operators will be used in order to conveniently discuss the angular momentum conservation.

2.1.1 Helicity amplitudes

The parton distribution functions can be viewed as discontinuities in forward parton-(quark or gluon) hadron scattering: a hadron of helicity H emits a parton of helicity h which then participates in some hard scattering process. The resulting parton with helicity h' is reabsorbed by a hadron of helicity H', as shown in Fig. (2-2). This process can be represented by u-channel discontinuity of the forward parton-hadron scattering amplitude $\mathcal{F}_{H'h,Hh'}$, which will be called *helicity amplitude* in this thesis due to its close ties to the underlying particles' helicities.

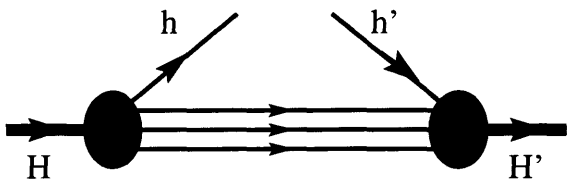

Figure 2-2: Parton distribution functions viewed as discontinuities in forward parton hadron scattering with explicit helicity labels.

The helicity amplitudes $\mathcal{F}_{H'h,Hh'}$ for quark distribution processes are defined in

QCD by[6, 10, 11]

$$\mathcal{F}_{H'h,Hh'} \equiv \int \frac{d\lambda}{2\pi} e^{i\lambda x} < PH'|T\bar{\psi}_{h'}(0)\psi_h(\lambda n)|PH > , \tag{2.1}$$

where the subscripts h and h' of the quark fields represent the helicities of the quarks. $|PH >$ is the helicity state of the hadron with momentum P and helicity H. ψ_h is the quark field operator in helicity h state. n is a light-cone vector defined in Eq. (93) of the appendix .6. T is the time order operator[1]. The dependences of helicity amplitudes upon x and Q^2 are suppressed for simplicity. Physically interesting $\mathcal{F}$ are diagonal in the hadron spin since they result from squaring something like $\langle X|\psi|PS\rangle$. However spin eigenstates are linear combinations of helicity eigenstates, so the matrix $\mathcal{F}$ do not have to be diagonal in the hadron helicity basis. Only forward scattering is of interest, thus angular momentum is conserved along the z-direction(defined by the problem at hand), so helicities of the initial and final states are same,

$$H + h' = H' + h \ . \tag{2.2}$$

The parity and time reversal are invariant in the strong interactions, which places constraints on $\mathcal{F}$,

$$\mathcal{F}_{H'h,Hh'} = \mathcal{F}_{-H'-h,-H-h'} \tag{2.3}$$

$$\mathcal{F}_{H'h,Hh'} = \mathcal{F}_{Hh',H'h} \tag{2.4}$$

respectively. Parity reverse the direction of momentum, but does not change spin, therefore the helicity change sign under parity transformation. Time reversal exchanges initial and final states, and reverse the directions of momentum and spin. Helicity is able to conserve its sign under time reversal.

These symmetry constraints dramatically reduce the independent numbers of non-zero helicity density matrix elements. For example, if $J_h = j = 1/2$, there are 16 elements for $\mathcal{F}$, however, under the symmetry constraints, there are only three

independent elements left:

$$\mathcal{F}_{\frac{1}{2}\frac{1}{2},\frac{1}{2}\frac{1}{2}} \ , \ \mathcal{F}_{-\frac{1}{2}-\frac{1}{2},-\frac{1}{2}-\frac{1}{2}} \ , \ \mathcal{F}_{\frac{1}{2}-\frac{1}{2},-\frac{1}{2}\frac{1}{2}} \ .$$

2.1.2 Parton distribution density operator

Definition

The helicity amplitudes $\mathcal{F}_{H'h,Hh'}$ can be seen as matrix elements of *parton distribution density operator* $\mathcal{F}$, which is defined as follows

$$\mathcal{F}_{H'h,Hh'} \equiv < JH'; jh| \ \mathcal{F} \ |JH; jh' > \ , \tag{2.5}$$

where $|JH; jh >$ is the helicity state for the hadron and parton system. J and j are the total angular momenta of the hadron and parton respectively. H and h represent the helicities of the hadron and parton respectively ($H = -J, ..., J,$ and $h = -j, ..., j$). [Note: j and J in distribution processes do not change, thus they are suppressed in the helicity amplitude $\mathcal{F}_{Hh',H'h}$for simplicity]. $\mathcal{F}$ is a $(2J+1) \times (2j+1)$ dimensional matrix in the helicity representation, e.g., if $J = 1/2$ and $j = 1/2$, $\mathcal{F}$ has $(2J+1)^2 \times (2j+1)^2 = 4 \times 4 = 16$ elements.

The helicity space formed by $|JH; jh >$ can be reduced into two subspaces: hadron helicity space and parton helicity space, i.e., the helicity state can be decomposed as a direct product of hadron and parton helicity states as follows

$$|JH; jh >= |JH > \ \otimes |jh > \ , \tag{2.6}$$

with $|JH >$ and $|jh >$ being helicity state bases for the hadron and parton helicity spaces,

$$\begin{aligned} < JH|J'H' >&= \delta_{JJ'}\delta_{HH'} \ , \\ < jh|j'h' >&= \delta_{jj'}\delta_{hh'} \ . \end{aligned} \tag{2.7}$$

Accordingly, the parton distribution density operator $\mathcal{F}$ can also be decomposed as a direct product of hadron density operator $\mathcal{F}_h$ and parton density operator $\mathcal{F}_p$

$$\mathcal{F} = \mathcal{F}_h \otimes \mathcal{F}_p \ . \tag{2.8}$$

The dimensions of operators $\mathcal{F}_h$ and $\mathcal{F}_p$ are $(2J+1)$ and $(2j+1)$, respectively. Hence, there are $(2J+1)^2$ and $(2j+1)^2$ basis operators for the hadron and parton helicity spaces, respectively, i.e., $\mathcal{F}_h$ and $\mathcal{F}_p$ can be expanded as linear combinations of the basis operators of their respective helicity spaces. In order to discuss the rotation transformation symmetry conveniently, we shall use *spherical irreducible tensor operators* as described later because the Cartesian operators are not irreducible under $SO(3)$ but *spherical irreducible tensor operators* do.

Symmetry properties

At the operator level, the parton distribution density operator $\mathcal{F}$ is invariant under the rotation along z-direction, that is,

$$e^{iJ_z\theta}\mathcal{F}e^{-iJ_z\theta} = \mathcal{F} \ , \tag{2.9}$$

where $J_z = I^q \otimes J_z^h + J_z^q \otimes I^h$ with I^q and I^h unit matrices in parton and hadron helicity space. In other words, under infinitesimal transformation(θ is infinitesimal) we have

$$[\ J_z, \mathcal{F}\ ] = 0 \ . \tag{2.10}$$

Strong interaction conserves parity and time reversal since there is no possible time-reversal-violating final state interaction in distribution process. Therefore the operator $\mathcal{F}$ is invariant under parity and time reversal transformation,

$$\mathcal{P}\mathcal{F}\mathcal{P}^{-1} = \mathcal{F} \ , \tag{2.11}$$

where $\mathcal{P}$ is parity operator, and

$$\mathcal{T}\mathcal{F}\mathcal{T}^{-1} = \mathcal{F}^{\dagger} , \tag{2.12}$$

where $\mathcal{T}$ is the time reversal operator.

Since the parton-hadron forward amplitude results from squaring something like $\langle X|\psi|PS\rangle$, $\mathcal{F}$ is hermitian

$$\mathcal{F}^{\dagger} = \mathcal{F} . \tag{2.13}$$

Eqs. (2.10)—(2.13) summarize the symmetry restrictions on $\mathcal{F}$, which will reduce the numbers of independent components of $\mathcal{F}_{H'h,Hh'}$.

2.1.3 Spherical irreducible tensor operator

The spherical irreducible *rank* k tensor operator $T^k_q(q = -k, ..., k)$ is defined under rotation transformation as [2]

$$D(R)T^k_q D(R)^{-1} = \sum_{q'=-k}^{k} T^k_{q'}\ \mathcal{D}^{(k)}_{q'q}(R) , \tag{2.14}$$

where $D(R) = e^{i\vec{J}\cdot\vec{\theta}}$ is the unitary transformation operator corresponding to rotation R along $\vec{\theta}$ direction and $\mathcal{D}^{(k)}_{q'q}(R) =< kq'|D(R)|kq >$, or under infinitesimal transformation

$$\begin{aligned} \left[J_{\pm}, T^k_q\right] &= \sqrt{k(k+1) \mp q(q \pm 1)}\ T^k_{q\pm 1} , \\ \left[J_z, T^k_q\right] &= q\ T^k_q , \end{aligned} \tag{2.15}$$

where $\vec{J}$ is the total angular momentum operator, with $J_{\pm} = J_x \pm iJ_y$.

[2] Only the properties relevant to our discussions are listed here. For more thorough discussions, please refer to[40] .

Take the Hermitian adjoint of the Eq. (2.14), we have

$$D(R)\ (T^k_q)^\dagger\ D(R)^{-1} = \sum_{q'=-k}^{k} (T^k_{q'})^\dagger\ \mathcal{D}^{(k)*}_{q'q}(R)\ . \tag{2.16}$$

The symmetry property of the $\mathcal{D}$'s

$$\mathcal{D}^{(k)*}_{q'q}(R) = (-)^{q'-q}\mathcal{D}^{(k)}_{-q'-q}(R) \tag{2.17}$$

gives us

$$D(R)(-)^q\ (T^k_q)^\dagger\ D(R)^{-1} = \sum_{q'=-k}^{k} (-)^{q'}(T^k_{q'})^\dagger\ \mathcal{D}^{(k)}_{-q'-q}(R)\ , \tag{2.18}$$

i.e. $(-)^q(T^k_{-q})^\dagger$ transforms under rotations in the same way as T^k_q . Therefore the concept of Hermitian adjoint of an operator may be generalized, and the Hermitian adjoint $\mathbf{T}^\dagger$ of a tensor operator $\mathbf{T}$ may be defined by

$$(T^\dagger)^k_q = (-)^q\ (T^k_{-q})^\dagger\ . \tag{2.19}$$

The components of a self-adjoint tensor $\mathbf{T}^\dagger = \mathbf{T}$ satisfies

$$(T^k_q)^\dagger = (-)^q\ T^k_{-q}\ . \tag{2.20}$$

2.1.4 The structure of parton distribution density operator under conservation laws

As mentioned in section (2.1.2), the hadron and parton density operators $\mathcal{F}_h$ and $\mathcal{F}_p$ can be expanded as sums of the basis generators of their corresponding helicity spaces (usually, Cartesian). On the other hand, the Cartesian operators can be expressed as linear combinations of the spherical irreducible tensor operators. Thus, the parton distribution density operator $\mathcal{F}$ can be written as a sum of direct products of hadron and parton irreducible tensor operators.

In general, there are $(2j+1)^2 \times (2J+1)^2$ elements in $\mathcal{F}$. This number quickly increases as j and J get large. For instance, if $j = J = 1$, there are already $3^2 \times 3^2 = 81$

elements. However, fortunately these matrix elements are not independent of each other in high energy processes. The QCD conservation laws give us several rules to dramatically reduce the numbers of the helicity density matrix elements. Those survivals will be identified as distribution functions.

Quark distribution density operator structure

$$\mathcal{F} = \sum_{k=0}^{1} \sum_{k'=0}^{2J} \sum_{q=-k}^{k} \sum_{q'=-k'}^{k'} C(kq;k'q')\ Q_q^k \otimes H_{q'}^{k'}\ , \tag{2.21}$$

where Q_q^k and H_q^k represent the irreducible tensor operators in quark and hadron helicity spaces respectively, $C(kq;k'q')$ are expansion coefficients.

One can deduce the following rules governing the relationships between the expansion coefficients $C(kq;k'q')$ in Eq. (2.21) from Eqs. (2.2) (2.3) (2.4) (2.10) (2.11) (2.12) (2.13) (2.20)

$$C(kq;k'q') = 0 \qquad \text{if} \quad q+q' \neq 0\ , \tag{2.22}$$

$$C(kq;k'q') = (-)^{k+k'} C(k-q;k'-q')\ , \tag{2.23}$$

$$C(kq;k'q') = (-)^{q+q'} C(k-q;k'-q')\ , \tag{2.24}$$

$$C^*(k,q;k',q') = (-)^{q+q'} C(k,-q;k',-q')\ . \tag{2.25}$$

Eq (2.22) is the result of the helicity conservation, Eq. (2.23) the parity invariance, Eq. (2.24) the time reversal invariance, and Eq. (2.25) the hermitian conjugate. In next subsection, we will show how to use these rules to simplify $\mathcal{F}$ and identify the surviving elements as parton distribution functions.

In massless theory the quark helicity is identical to its chirality, and Q_0^k will not change the helicity of quark while $Q_{\pm 1}^1$ change it by one unit, therefore the expansion coefficients in Eq. (2.21) in front of operator Q_0^k are chiral-even while those corresponding to $Q_{\pm 1}^1$ are chiral-odd.

Gluon distribution density operator structure

$$\mathcal{F} = \sum_{k=0}^{2} \sum_{k'=0}^{2J} \sum_{q=-k}^{k} \sum_{q'=-k'}^{k'} C(kq;k'q')\ G_q^k \otimes H_{q'}^{k'}\ , \tag{2.26}$$

where G_q^k and H_q^k represents the irreducible tensor operators in gluon and hadron helicity spaces respectively, $C(kq;k'q')$ are expansion coefficients.

One can get similar rules as those in Eqs. (2.22)—(2.25) for gluon distribution density operator. However, there is an additional constraint due to gauge invariance. The physical gluon can only have two polarization ($+1$ or -1), which means the only operators are G_0^0, G_0^1, G_2^2, and G_{-2}^2. [3]

2.1.5 Expansion coefficients as distribution functions

In this section, we shall apply our results on the structure of the density operator $\mathcal{F}$ to some well-known processes in order to show how the coefficients in the density operator expansion are related to the familiar distribution functions.

Quark distribution functions in the nucleon: $j = 1/2$ and $J = 1/2$

There are $(2j+1)^2 \times (2J+1)^2 = 16$ elements in the helicity density matrix $\mathcal{F}$. However, these number can be dramatically reduced by the rules in Eqs. (2.22)—(2.25), as we will show immediately.

We first apply the Eq. (2.22), there are only four nonzero elements left:

$$C(00;00),\ C(10;10),\ C(11;1-1),\ C(1-1;11),$$

which correspond to operators $Q_0^0 \otimes H_0^0$, $Q_0^1 \otimes H_0^1$, $Q_1^1 \otimes H_{-1}^1$, $Q_{-1}^1 \otimes H_1^1$, respectively. Then the Eq. (2.23) and Eq. (2.24) give us same relations in this case: $C(1,1;1,-1) = C(1,-1;1,1)$. The Eq. (2.25) requires $C^*(00;00) = C(00;00)$, $C^*(10;10) = C(10;10)$, and $C^*(1,1;1,-1) = C(1,-1;1,1)$. Therefore there are only *three* real independent nonzero elements left. The helicity operator $\mathcal{F}$ can be expanded by these three terms

[3] Note that we have use Q_q^k to represents the tensor operator for quark, H_q^k for hadron, and G_q^k for gluon.

as follows

$$\mathcal{F} = C(00;00)\ Q_0^0 \otimes H_0^0 + C(10;10)\ Q_0^1 \otimes H_0^1 + C(11;1-1)\ \left[\ Q_1^1 \otimes H_{-1}^1 + Q_{-1}^1 \otimes H_1^1\ \right]\ . \tag{2.27}$$

The matrices Qs and Hs are shown in the appendix .9. They are directly related to the well-known Pauli matrices: $Q_0^0 = I, Q_0^1 = \sigma_3, Q_1^1 = -\sqrt{2}\sigma^+, Q_{-1}^1 = \sqrt{2}\sigma^-$, where $\sigma^\pm \equiv (\sigma_1 \pm i\sigma_2)/2$. Therefore, the remaining three elements $C(00;00)$, $C(10;10)$, $C(11;1-1)$ can be related to the three familiar quark distribution functions as below[38]

$$\begin{aligned} C(00;00) &= \frac{1}{2}q\ , \\ C(10;10) &= \frac{1}{2}\Delta q\ , \\ C(11;1-1) &= -\frac{1}{4}\delta q\ . \end{aligned} \tag{2.28}$$

Then, we get the familiar formula[38]

$$\mathcal{F} = \frac{1}{2}q\ I_q \otimes I_N + \frac{1}{2}\Delta q\ \sigma_q^3 \otimes \sigma_N^3 + \frac{1}{2}\delta q\left(\sigma_q^+ \otimes \sigma_N^- + \sigma_q^- \otimes \sigma_N^+\right)\ , \tag{2.29}$$

where the subscripts q and N indicate quark and nucleon spaces respectively. The coefficients $C(00;00), C(10;10), C(11;1-1)$ correspond to tensor operators $Q_0^0, Q_0^1, Q_\pm^1$, respectively. Therefore, the quark distributions $q, \Delta q$ are chiral-even, and δq chiral-odd. q is unpolarized quark distribution function, Δq is quark helicity difference distribution function, and δq is quark transversity distribution function.

Quark distributions in a vector meson: $j = 1/2$ and $J = 1$

In this case, $2^2 \times 3^2 = 36$ matrix elements will be dramatically reduced to 4 after using the Eqs. (2.22)—(2.25).

Eq. (2.22) give only the following nonzero elements

$$C(00;00),\ C(10;10),\ C(00;20),$$

$$C(11;1-1),\ C(1-1;11),\ C(11;2-1),\ C(1-1;21)\ .$$

Eq. (2.23) requires

$$\begin{aligned} C(11;1-1) &= C(1-1;11)\ , \\ C(11;2-1) &= -C(1-1;21)\ . \end{aligned} \tag{2.30}$$

Finally Eq. (2.24) gives

$$C(11;2-1) = C(1-1;21)\ . \tag{2.31}$$

The combination of Eqs. (2.30) and (2.31) will give us $C(11;2-1) = C(1-1;21) = 0$. Combining these results with the Eq. (2.25) one can conclude that all the surviving amplitudes are real.

In the end, the symmetry constraints leave us only four independent nonzero coefficients, by which $\mathcal{F}$ can be expanded as follows

$$\begin{aligned} \mathcal{F} = C(00;00)\ Q_0^0 \otimes H_0^0 + C(10;10)\ Q_0^1 \otimes H_0^1 + C(00;20)\ Q_0^0 \otimes H_0^2 \\ + C(11;1-1) \left[\ Q_1^1 \otimes H_{-1}^1 + Q_{-1}^1 \otimes H_1^1\ \right]\ . \end{aligned} \tag{2.32}$$

One can relate the coefficients to the familiar quark distribution functions: $C(00;00) \sim q$ (the helicity average distribution), $C(10;10) \sim \Delta q$ (the helicity difference distribution), $C(00;20) \sim b_q$ (the quadrupole quark distributions[38]), and $C(11;1-1) \sim \delta q$ (the transversity distribution in a vector meson). After normalization, one can get the following formula

$$\mathcal{F} = \frac{1}{3} q\ I \otimes I - \frac{1}{4} b_q\ I \otimes Q + \frac{1}{2} \Delta q\ \sigma_3 \otimes S_3 + \frac{1}{2} \delta q\ \left[\ \sigma^+ \otimes \sigma^- + \sigma^- \otimes \sigma^+\ \right]\ , \tag{2.33}$$

where $Q = \text{diag}(1, -2, 1)$, $S_3 = \text{diag}(1, 0, -1)$. q, b_q, and Δq are chiral even, δq is chiral odd.

Gluon distributions in a nucleon: $J_g = 1$ and $J = 1/2$

The distribution density operator $\mathcal{F}$ can be written as follows after considering all the symmetry constraints[4]

$$\mathcal{F} = C(00;00)\ G_0^0 \otimes H_0^0 + C(10;10)\ G_0^1 \otimes H_0^1\ . \tag{2.34}$$

It can be shown that $C(00;00)$ is proportional to helicity average distribution function, and $C(10;10)$ is helicity difference distribution function. Both of them are real. The Eq. (2.34) can be written in more familiar terms

$$\mathcal{F} = \frac{1}{3} g\ I_g \otimes I_N + \frac{1}{2}\Delta g\ S_g^3 \otimes \sigma_N^3\ , \tag{2.35}$$

where I_g is 3×3 unit matrix in gluon helicity space, $S_g^3 = \text{diag}(1, 0, -1)$. I_N, σ_N^3 are pauli matrices in the nucleon helicity space. The distribution functions G and ΔG are both chiral even. It is worthwhile to point out that there is *no* gluon transversity distribution functions in the nucleon due to the helicity conservation.

2.2 Fragmentation Functions as Helicity Density Matrix Elements

In this section, we shall discuss the fragmentation functions in the frame of the helicity density matrix formalism. The parton fragmentation process is far more complicated than distribution because it is less constrained: the time reversal invariance must be relaxed in many processes due to final state interaction(FSI) between the production particles, and the angular momentum structures quickly get very complicated due to interference in multiple particle production processes

[4]Readers can easily show this by applying the rules in section 2.1.4

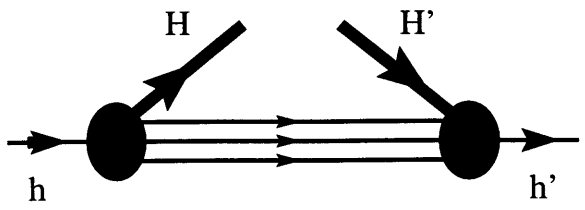

Figure 2-3: The parton fragmentation functions viewed as discontinuities in forward hadron parton scattering with explicit helicity labels.

The structure of this section is parallel to section 2.1. First we shall discuss the parton fragmentation density matrix. We will introduce the parton fragmentation density operator, and discuss its structures under QCD symmetries. In the end, we shall give some examples.

2.2.1 Helicity amplitudes

Just like parton distribution functions, the parton fragmentation functions can also be viewed as discontinuities in forward parton-(quark or gluon) hadron scattering: a parton of helicity h emits a hadron (or a bunch of hadrons) of helicity H and total angular momentum J. The resulting hadron (or hadron system) with helicity H' and total angular momentum J' is reabsorbed by a parton of helicity h', as shown in Fig. (2-3). This process can be represented by u-channel discontinuity of the forward parton-hadron scattering amplitude $\hat{\mathcal{F}}^{J'J}_{H'h,Hh'}$.

The quark fragmentation helicity density amplitude $\hat{\mathcal{F}}_{H'h,Hh'}$ is defined in QCD by[12, 6]

$$\hat{\mathcal{F}}^{J'J}_{H'h,Hh'} \equiv \sum_X \int \frac{d\lambda}{2\pi} e^{-i\lambda/z} \langle 0|\psi_{h'}(0)|JH;X\rangle_{\text{out}\,\text{out}}\langle X;J'H'|\bar{\psi}_h(\lambda n)|0\rangle \ , \qquad (2.36)$$

where the dependences of helicity amplitude on z, Q^2, and some internal momenta in the hadron system have been suppressed for simplicity. $|0\rangle$ represents the vacuum state. $|JH;X\rangle_{\text{out}}$ is the final state, where *out* means the outgoing state. The *out* states have been used because of possible final state interactions between the final particles.

$\hat{\mathcal{F}}$ is also subject to symmetry constraints. However, time reversal invariance

needs to be relaxed due to possible final state interaction among final hadrons,[5]

$$H + h' = H' + h \ . \tag{2.37}$$

$$\hat{\mathcal{F}}^{J'J}_{Hh',H'h} = \hat{\mathcal{F}}^{J'J}_{-H-h',-H'-h} \ . \tag{2.38}$$

2.2.2 Parton fragmentation density operator

Definition

Like in distribution case, the fragmentation helicity density operator $\hat{\mathcal{F}}$ is also related to the helicity density amplitude as follows

$$\hat{\mathcal{F}}^{J'J}_{H'h,Hh'} =< J'H'; jh|\ \hat{\mathcal{F}}\ |JH; jh' > \ , \tag{2.39}$$

where, once again, J and j are the total angular momenta of the hadron system(could be multiple hadrons) and parton respectively, H and h represent the helicities of the hadron system and parton respectively. J does not have to be equal to J', in which case interference between different partial waves occurs. [Note: j in fragmentation process do not change, thus they are suppressed in the helicity amplitude $\hat{\mathcal{F}}^{J'J}_{H'h,Hh'}$ for simplicity].

The helicity density operator $\hat{\mathcal{F}}$ can also be decomposed as a direct product of hadron helicity operator $\hat{\mathcal{F}}_h$ and parton helicity operator $\hat{\mathcal{F}}_p$

$$\hat{\mathcal{F}} = \hat{\mathcal{F}}_h \otimes \hat{\mathcal{F}}_p \ . \tag{2.40}$$

[5]For single particle semi-inclusive production, the final state interaction phase may be averaged out because of the summation over X state in Eq. (2.36)

Symmetry properties

At the operator level, the parton distribution density operator $\hat{\mathcal{F}}$ is invariant under the rotation along z-direction, that is,

$$e^{iJ_z\theta}\ \hat{\mathcal{F}}\ e^{-iJ_z\theta} = \hat{\mathcal{F}}\ , \tag{2.41}$$

where $J_z = I^q \otimes J_z^h + J_z^q \otimes I^h$ with I^q and I^h unit matrices in parton and hadron helicity space. In other words, under infinitesimal transformation(θ is infinitesimal) we have

$$[\ J_z,\ \hat{\mathcal{F}}\ ] = 0\ . \tag{2.42}$$

Strong interaction conserves parity, therefore the operator $\hat{\mathcal{F}}$ is invariant under parity transformation,

$$\mathcal{P}\ \hat{\mathcal{F}}\ \mathcal{P}^{-1} = \hat{\mathcal{F}}\ , \tag{2.43}$$

where $\mathcal{P}$ is parity operator.

Since the parton-hadron forward amplitude results from squaring something like $\langle X; JH|\psi|0\rangle$, $\hat{\mathcal{F}}$ is hermitian

$$\hat{\mathcal{F}}^\dagger = \hat{\mathcal{F}}\ . \tag{2.44}$$

The time reversal is no longer invariant due to the final state interaction which violates time reversal invariance.

2.2.3 Parton fragmentation density operator structure due to conservation laws

As in section 2.1, the fragmentation density operator $\hat{\mathcal{F}}$ can be expanded as sums of the spherical irreducible tensor operators as follows,

$$\hat{\mathcal{F}} = \sum_{J,J'} \sum_{k=0}^{2j} \sum_{k'=|J-J'|}^{J'+J} \sum_{q=-k}^{k} \sum_{q'=-k'}^{k'} \hat{C}(JJ';kq;k'q')\ Q_q^k \otimes H_{q'}^{k'}(JJ')\ , \tag{2.45}$$

where Q_q^k and $H_q^k(JJ')$ represent the irreducible tensor operators in the parton space and hadron space respectively.

Spherical irreducible tensor operator $H_q^k(JJ')$

The spherical irreducible tensor operator $H_q^k(JJ')$ is defined under rotation transformation just like T_q^k in Eqs. (2.14)(2.15) [6]

$$D(R)\ H_q^k(JJ')\ D(R)^{-1} = \sum_{q'=-k}^{k} H_{q'}^k(JJ')\ \mathcal{D}_{q'q}^{(k)}(R)\ , \tag{2.46}$$

or

$$\begin{aligned} \left[\ J_\pm,\ H_q^k(JJ')\ \right] &= \sqrt{k(k+1) \mp q(q\pm 1)}\ H_{q\pm 1}^k(JJ')\ , \\ \left[\ J_z,\ H_q^k(JJ')\ \right] &= q\ H_q^k(JJ')\ , \end{aligned} \tag{2.47}$$

where $\vec{J} = \vec{J} + \vec{J'}$ is the total angular momentum operator, $J_\pm = J_x \pm iJ_y$.

The operator $H_q^k(JJ')$ has an additional property—it will change not only the helicity but also the total angular momentum in the helicity state, i.e.,

$$H_q^k(JJ')\ |J'H\rangle \sim\ |J(H+q)\rangle\ . \tag{2.48}$$

Its hermitian conjugate can be defined as

$$\left(H_q^k(JJ')\right)^\dagger = (-)^q H_q^k(J'J) \tag{2.49}$$

Quark fragmentation density operator structure

$$\hat{\mathcal{F}} = \sum_{J,J'} \sum_{k=0}^{1} \sum_{k'=|J-J'|}^{J'+J} \sum_{q=-k}^{k} \sum_{q'=-k'}^{k'} \hat{C}(JJ';kq;k'q')\ Q_q^k \otimes H_{q'}^{k'}(JJ')\ , \tag{2.50}$$

One can deduce relations between the expansion coefficients $C(kq;k'q')$ in Eq. (2.50)

[6] In fact, H_q^k is a special case of $H_q^k(JJ')$ with $J = J'$

from Eqs. (2.37) (2.38) (2.42) (2.43) (2.44) (2.49)

$$\hat{C}(JJ';kq;k'q') = 0 \qquad \text{if} \quad q+q' = 0 \;, \tag{2.51}$$

$$\hat{C}(JJ';kq;k'q') = (-)^{k+k'}\hat{C}(JJ';k-q;k'-q') \;, \tag{2.52}$$

$$\hat{C}^*(JJ';kq;k'q') = (-)^{q+q'}\hat{C}(J'J;k-q;k'-q') \;. \tag{2.53}$$

Like in distribution case, Eq. (2.51) comes from helicity conservation, Eq. (2.52) from parity invariance, and Eq. (2.53) from hermitian conjugate. There is no relation from time reversal invariance because it is violated due to final state interactions. Therefore, some of the helicity amplitudes are not real.

Once again, the quark fragmentation functions corresponding to operator Q_0^k are chiral-even and those corresponding to $Q_{\pm 1}^1$ are chiral-odd.

Gluon fragmentation density operator structure

$$\hat{\mathcal{F}} = \sum_{J,J'}\sum_{k=0}^{2}\sum_{k'=|J-J'|}^{J'+J}\sum_{q=-k}^{k}\sum_{q'=-k'}^{k'} \hat{C}(JJ';kq;k'q')\; G_q^k \otimes H_{q'}^{k'}(JJ') \;. \tag{2.54}$$

where G_q^k represents the irreducible tensor operators in gluon helicity space.

One can get similar rules as those in Eqs. (2.51)—(2.52) for gluon distribution density operator. However, once again one has to take into account an additional constraint due to gauge invariance, as discussed in section 2.1.4.

2.2.4 Expansion coefficients as fragmentation functions

In this section, we shall apply our results to some processes in order to show how the coefficients in the density operator expansion are related to the familiar fragmentation functions.

Quark fragments into nucleon: $j = 1/2,\ J = 1/2,\ J' = 1/2$

Follow the procedure described in section 2.1.5, one can get [7]

$$\hat{\mathcal{F}} = \hat{C}(1/21/2;00;00)Q_0^0 \otimes H_0^0 + \hat{C}(1/21/2;10;10)Q_0^1 \otimes H_0^1 + \hat{C}(1/21/2;11;1-1)\ \left[\ Q_1^1 \otimes H_{-1}^1 + Q_{-1}^1 \otimes H_1^1\ \right]\ , \tag{2.55}$$

where $Q_0^0 = I, Q_0^1 = \sigma_3,\ Q_1^1 = -\sqrt{2}\sigma^+,\ Q_{-1}^1 = \sqrt{2}\sigma^-$. The same thing is true for H's. The coefficients $\hat{C}(1/21/2;00;00)$, $\hat{C}(1/21/2;10;10)$, $\hat{C}(1/21/2;11;1-1)$ can be identified as three familiar quark fragmentation functions as below[11, 38]

$$\begin{aligned} \hat{C}(1/21/2;00;00) &\equiv \frac{1}{2}\hat{q}\ , \\ \hat{C}(1/21/2;10;10) &\equiv \frac{1}{2}\Delta\hat{q}\ , \\ \hat{C}(1/21/2;11;1-1) &\equiv -\frac{1}{4}\delta\hat{q}\ . \end{aligned} \tag{2.56}$$

Since $\hat{C}(1/21/2;00;00)$, $\hat{C}(1/21/2;10;10)$, $\hat{C}(1/21/2;11;1-1)$ are the coefficients in front of the tensor operators Q_0^0, Q_0^1, $Q_\pm^1$, respectively, the quark distribution functions $\hat{q}$ and $\Delta\hat{q}$ are chiral-even, and $\delta\hat{q}$ chiral-odd. So, we get a familiar formula [38]

$$\hat{\mathcal{F}}_q = \frac{1}{2}\hat{q}\ I_q \otimes I_N + \frac{1}{2}\Delta\hat{q}\ \sigma_q^3 \otimes \sigma_N^3 + \frac{1}{2}\delta\hat{q}\left(\sigma_q^+ \otimes \sigma_N^- + \sigma_q^- \otimes \sigma_N^+\right)\ , \tag{2.57}$$

where $I_i, \sigma_i^3, \sigma_i^\pm (i = q, N)$ are Pauli matrices in the quark and nucleon helicity spaces, respectively. It is easy to show that all of the three functions are real.

Quark fragments into a vector meson: $j = 1/2,\ J = 1,\ J' = 1$

$$\begin{aligned} \hat{\mathcal{F}} = \hat{C}(11;00;00)\ Q_0^0 \otimes H_0^0 + \hat{C}(11;10;10)\ Q_0^1 \otimes H_0^1 + \\ \hat{C}(11;00;20)\ Q_0^0 \otimes H_0^2 + \\ \hat{C}(11;11;1-1)\ \left[\ Q_1^1 \otimes H_{-1}^1 + Q_{-1}^1 \otimes H_1^1\ \right] + \end{aligned}$$

[7] We will use H_q^k to represent $H_q^k(JJ')$ when $J = J'$ in the following discussions

$$\hat{C}(11;11;2-1)\left[\, Q_1^1 \otimes H_{-1}^2 - Q_{-1}^1 \otimes H_1^2 \,\right] . \tag{2.58}$$

Thus, we have 5 fragmentation functions: three chiral-even, two chiral-odd. It is easy to show that $\hat{C}(1,1;1,1;2,-1)$ is imaginary while others real. They can be identified to the familiar functions Ji used[12]

$$\begin{aligned}
\hat{C}(11;00;00) &\sim \hat{f}_1 , \\
\hat{C}(11;10;10) &\sim \hat{g}_1 , \\
\hat{C}(11;11;1-1) &\sim \hat{h}_1 , \\
\hat{C}(11;00;20) &\sim \hat{b}_1 , \\
\hat{C}(11;11;2-1) &\sim \hat{h}_{\bar{1}}
\end{aligned} \tag{2.59}$$

with $\hat{f}_1$, $\hat{g}_1$ and $\hat{b}_1$ chiral-even, $\hat{h}_1$ and $\hat{h}_{\bar{1}}$ chiral-odd.

From Eq. (2.58) one can see that the last fragmentation function $\hat{C}(11;11;2-1)$ or $\hat{h}_{\bar{1}}$ is time-reversal violating fragmentation function because it is proportional to the helicity amplitude combination $\mathcal{F}_{\frac{1}{2}0,-\frac{1}{2}1} - \mathcal{F}_{-\frac{1}{2}1,\frac{1}{2}0}$. Time reversal invariance would equal $\mathcal{F}_{\frac{1}{2}0,-\frac{1}{2}1}$ to $\mathcal{F}_{-\frac{1}{2}1,\frac{1}{2}0}$. X. Ji has shown the existence of such T-violating fragmentation function due to the nontrivial final state interaction[12]. However, the effect might be small due to possible final-state-interaction phase wash-out by summing over the intermediate state X in the definition of the fragmentation density operator in Eq. (2.36). Ignoring this T-violating fragmentation function, and using Jaffe's notations[38], we get

$$\hat{\mathcal{F}} = \frac{1}{3}\hat{q}\; I\otimes I - \frac{1}{4}\hat{b}_q\; I\otimes Q + \frac{1}{2}\Delta\hat{q}\;\sigma_3\otimes S_3 + \frac{1}{2}\delta\hat{q}\;\left[\,\sigma^+\otimes\sigma^- + \sigma^-\otimes\sigma^+\,\right] , \tag{2.60}$$

where $\hat{b}_q$ is quark quadruple fragmentation function.

Gluon fragment into nucleon: $J_g = 1,\ J = 1/2,\ J' = 1/2$

The fragmentation density operator $\mathcal{F}$ of gluon fragmenting into nucleon can be written as follows after considering all the symmetry constraints

$$\hat{\mathcal{F}} = \hat{C}(1/21/2;00;00)\ G_0^0 \otimes H_0^0 + \hat{C}(1/21/2;10;10)\ G_0^1 \otimes H_0^1\ . \tag{2.61}$$

There are two real chiral-even fragmentation functions. Express Eq. (2.61) in a more familiar way, one gets

$$\hat{\mathcal{F}} = \frac{1}{3}\hat{g}\ I_g \otimes I_N + \frac{1}{2}\Delta\hat{g}\ S_g^3 \otimes \sigma_N^3\ , \tag{2.62}$$

where $\hat{g}$ and $\Delta\hat{g}$ are gluon helicity average and difference fragmentation functions, respectively.

Gluon fragments into vector mesons: $J_g = 1,\ J = 1/2,\ J' = 1/2$

$$\begin{aligned}\hat{\mathcal{F}} = \hat{C}(11;00;00)\ G_0^0 \otimes H_0^0 + \hat{C}(11;10;10)\ G_0^1 \otimes H_0^1 + \\ \hat{C}(11;00;20)\ G_0^0 \otimes H_0^2 + \\ \hat{C}(11;22;2-2)\left[\ G_2^2 \otimes H_{-2}^2 + G_{-2}^2 \otimes H_2^2\ \right]\ .\end{aligned} \tag{2.63}$$

Two of the four real chiral-even fragmentation functions are new: $\hat{C}(1,1;0,0;2,0)$ and $\hat{C}(1,1;2,2;2,-2)$. $\hat{C}(1,1;0,0;2,0)$ is similar to quark quadruple fragmentation function $\hat{b}_q$, thus it can be called gluon quadruple fragmentation function denoted by $\hat{b}_g$. $\hat{C}(1,1;2,2;2,-2)$, on the other hand, can be called gluon transversity fragmentation function because the helicity of the gluon flips, which is very similar to quark transversity distribution function. We can denote it as $\delta\hat{g}$.

Interference Fragmentation Functions

In this subsection we shall discuss the interference fragmentation functions (in the case of $J \neq J'$) to show the power of the helicity density matrix formalism. The

interference fragmentation functions and their uses will be discussed in detail in the chapter 4.

We will use the fragmentation process $q \to \pi\pi X$ as an example. Only s and p wave interference is considered because they dominate other channels. In order to discuss the interference between s and p waves, we put the helicities of s and p together to form a 4-dimensional space, which is expanded by basis helicity state denoted by $|JH\rangle$. J is the total angular momentum of the two pion system, H is the helicity. The four basis states are $|00\rangle$, $|11\rangle$, $|10\rangle$, and $|1-1\rangle$. Therefore, there are $2^2 \times 4^2 = 64$ elements. Fortunately, these number will be reduced dramatically under symmetry constraints. In fact, one can get the following expansion for the density operator

$$\begin{aligned}
\hat{\mathcal{F}} = \hat{C}(00;00;00)\, Q_0^0 \otimes H_0^0(00) + \hat{C}(11;00;00)\, Q_0^0 \otimes H_0^0(11) + \\
\hat{C}(11;10;10)\, Q_0^1 \otimes H_0^1(11) + \hat{C}(11;00;20)\, Q_0^0 \otimes H_0^2(11) + \\
\hat{C}(11;11;1-1)\, \left[\, Q_1^1 \otimes H_{-1}^1(11) + Q_{-1}^1 \otimes H_1^1(11) \,\right] + \\
\hat{C}(11;11;2-1)\, \left[\, Q_1^1 \otimes H_{-1}^2(11) - Q_{-1}^1 \otimes H_1^2(11) \,\right] + \\
\hat{C}(10;10;10)\, Q_0^1 \otimes H_0^1(10) + \\
\hat{C}(10;11;1-1)\, \left[\, Q_1^1 \otimes H_{-1}^1(10) + Q_{-1}^1 \otimes H_1^1(10) \,\right] + \\
\hat{C}(01;10;10)\, Q_0^1 \otimes H_0^1(01) + \\
\hat{C}(01;11;1-1)\, \left[\, Q_1^1 \otimes H_{-1}^1(01) + Q_{-1}^1 \otimes H_1^1(01) \,\right] \,. \qquad (2.64)
\end{aligned}$$

There are only *ten* fragmentation functions, six of which are chiral-even and the others are chiral-odd. $\hat{C}(00;00;00)$ is proportional to the fragmentation function in $q \to \sigma X$. $\hat{C}(11;00;00)$, $\hat{C}(11;10;10)$, $\hat{C}(11;00;20)$, $\hat{C}(11;11;1-1)$, and $\hat{C}(11;11;2-1)$ are fragmentation functions for $q \to \rho X$, which are discussed before. The other four, $\hat{C}(10;10;10)$, $\hat{C}(01;10;10)$, $\hat{C}(10;11;1-1)$ and $\hat{C}(01;11;1-1)$, are new from s and p wave interference. Eq. (2.53) requires $\hat{C}^*(10;10;10) = \hat{C}(01;10;10)$ and $\hat{C}^*(10;11;1-1) = \hat{C}(01;1-1;11)$. In chapter 4, we will show that after separating out the final state interaction phases there are in fact only two real s and p wave

interference fragmentation functions, which will be denoted by $\hat{q}_I$ and $\delta\hat{q}_I$ respectively. $\hat{q}_I$ is chiral even because it is the coefficient in front of Q_0^1, which conserves the quark's chirality. On the other hand, $\delta\hat{q}_I$ is chiral odd because the operators $Q_\pm^1$ it relates to flip the quark's chirality. It is its chiral-odd property that makes $\delta\hat{q}_I$ useful in a new proposal to probe nucleon's transversity distribution functions.

2.3 Helicity Amplitude Approach to Hard QCD Processes

In the section, we shall discuss hard QCD processes (shown in Fig. 2-4) in the frame of helicity density matrix formalism. First, we will review the approach proposed by Gastmanns and Wu[39] in unpolarized processes. Then we will generalize their approach to polarized processes.

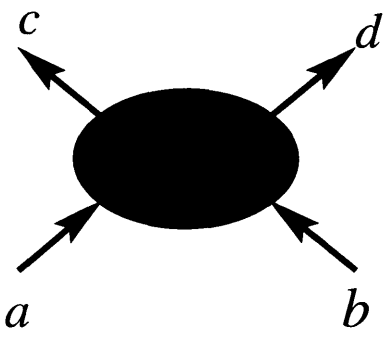

Figure 2-4: A generic parton parton interaction process $ab \longrightarrow cd$ at parton level.

2.3.1 Review of Gastmanns and Wu's approach

In their classical book *The Ubiquitous photon: The Helicity Method for QED and QCD*[39], Gastmanns and Wu propose the helicity amplitude approach to calculate the cross sections of high energy processes. Instead of following the standard procedure, in which one adds up all the Feynman amplitudes and then square it and then calculate the squared amplitudes using Dirac algebra, they propose that one first calculates the helicity amplitudes which are closely related to Feynman amplitudes, then adds their squared absolute values together to obtain the cross sections.

This method has the advantage over the standard procedure. In the standard procedure, since the Feynman amplitudes are squared before doing any calculations, when the numbers of the vertices and Feynman diagrams increase, this procedure in general becomes very lengthy and cumbersome. When a process is described by n Feynman diagrams, it amounts to writing down $n(n+1)/2$ traces. For instance, in the case of $e^+e^- \longrightarrow e^+e^-\gamma\gamma$, there are 40 Feynman diagrams, and if Z-exchange mechanism involved, this number increases to 80. Clearly ones does not like to calculate 3240 traces, not to mention for each trace there are a lot of Dirac matrices involved. However, in Gastmanns and Wu's helicity amplitude approach, the calculations are performed at the level of amplitudes. Hardly are there any Dirac traces involved. In the above example, it is described by 64 helicity amplitudes, of which one half can be obtained from a parity conjugation on the other 32 amplitudes. Obviously, it feels much better to just deal with 32 short expressions than 3240 long ones.

In the following, we shall have a review of their method. One can refer to their book for more details[39].

Helicity states for fermions

In high energy process like what we will examine in the following chapters, the fermion masses can be neglected. For massless fermion, helicity states are Lorentz invariant notions, which can be defined as below,

$$\begin{aligned} u_\pm(p) &= \frac{1}{2}(1 \pm \gamma_5)u_\pm(p) \\ v_\pm(p) &= \frac{1}{2}(1 \mp \gamma_5)v_\pm(p) \\ \bar{u}_\pm(p) &= \frac{1}{2}\bar{u}_\pm(p)(1 \mp \gamma_5) \\ \bar{v}_\pm(p) &= \frac{1}{2}\bar{v}_\pm(p)(1 \pm \gamma_5) \ , \end{aligned} \tag{2.65}$$

where the subscripts on the spinors denote the helicities of the corresponding fermions.

In the chiral representation of the Dirac matrix, one has

$$u_+(k) = v_-(k) = \begin{pmatrix} \sqrt{k_+} \\ \sqrt{k_-}e^{i\phi_k} \\ 0 \\ 0 \end{pmatrix}, \quad u_-(k) = v_+(k) = \begin{pmatrix} 0 \\ 0 \\ -\sqrt{k_-}e^{-i\phi_k} \\ \sqrt{k_+} \end{pmatrix} \tag{2.66}$$

for any light-like vector k_μ, where

$$k_\pm = k_0 \pm k_z, \qquad k_\perp = k_x + ik_y = |k_\perp|e^{i\phi_k} \ . \tag{2.67}$$

Helicity states for photons and gluons

It is critical to choose appropriate representation for photons and gluons' helicity states, which leads to great simplifications in the calculations.

Consider the case of a photon with four-momentum k. A convenient choice of the polarization vectors is

$$\begin{aligned} \epsilon_\mu^{\parallel} &= 2\sqrt{2}N\left[(q\cdot k)p_\mu - (p\cdot k)q_\mu\right], \\ \epsilon_\mu^{\perp} &= 2\sqrt{2}N\epsilon_{\mu\alpha\beta\gamma}q^\alpha p^\beta k^\gamma \ , \end{aligned} \tag{2.68}$$

where N is the normalization factor,

$$N = \frac{1}{4}\left[(p\cdot q)(p\cdot k)(q\cdot k)\right]^{-\frac{1}{2}} \ , \tag{2.69}$$

and $\epsilon_{\mu\alpha\beta\gamma}$ is the totally antisymmetric tensor in four dimensions with $\epsilon_{0123} = +1$. p and q are two arbitrary vectors, which are taken to be light-like, i.e., $p^2 = q^2 = 0$. The factor $2\sqrt{2}$ is merely introduced for the sake of the simplicity in the later formulae.

The polarization vectors $\epsilon_\mu^{\parallel}$ and $\epsilon_\mu^{\perp}$ are normalized as below,

$$\begin{aligned} (\epsilon^{\parallel})^2 &= (\epsilon^{\perp})^2 = -1 \ , \\ (k\cdot\epsilon^{\parallel}) &= (k\cdot\epsilon^{\perp}) = (\epsilon^{\parallel}\cdot\epsilon^{\perp}) = 0 \ . \end{aligned} \tag{2.70}$$

These polarization states can be alternatively combined into circularly polarized states,

$$\epsilon_\mu^\pm = \frac{1}{\sqrt{2}}\left(\epsilon_\mu^{\parallel} \pm i\epsilon_\mu^{\perp}\right) \ , \tag{2.71}$$

which can be rewritten as

$$\not{\epsilon}^\pm = -N\left[\not{k}\not{p}\not{q}(1 \pm \gamma_5) - \not{p}\not{q}\not{k}(1 \mp \gamma_5) \mp 2(p\cdot q)\not{k}\gamma_5\right] \ , \tag{2.72}$$

by using the identity

$$i\gamma^\mu \epsilon_{\mu\alpha\beta\gamma} = (\gamma_\alpha\gamma_\beta\gamma_\gamma - \gamma_\alpha g_{\beta\gamma} + \gamma_\beta g_{\alpha\gamma} - \gamma_\gamma g_{\alpha\beta})\gamma_5 \ . \tag{2.73}$$

Since the masses of the fermions are neglected in our calculations, the last term in Eq. (2.72) can be omitted because of the conservation of an axial current in QED. Accordingly, the polarization vectors $\epsilon_\mu^\pm$ can be rewritten as

$$\not{\epsilon}^\pm = -N\left[\not{k}\not{p}\not{q}(1 \pm \gamma_5) - \not{p}\not{q}\not{k}(1 \mp \gamma_5)\right] \ . \tag{2.74}$$

This is the basic formula for the photon polarization vectors in this approach.

The polarization vectors of the gluon in QCD can be treated in the similar way. However, the last term in Eq. (2.72) cannot be dropped now. Instead, one can write

$$\not{\epsilon}^\pm = -N\left[\not{k}\not{p}\not{q}(1 \pm \gamma_5) + \not{q}\not{p}\not{k}(1 \mp \gamma_5) - 2(p\cdot q)\not{k}\right] \ . \tag{2.75}$$

Now one can drop the last term due to the vector current conservation. Thus,

$$\not{\epsilon}^\pm = -N\left[\not{k}\not{p}\not{q}(1 \pm \gamma_5) + \not{q}\not{p}\not{k}(1 \mp \gamma_5)\right] \ . \tag{2.76}$$

There are several reasons why the formulae in Eq. (2.74) and Eq. (2.76) simplify the calculations in QED and QCD.

- The choices of the light-like four-momentum p and q are arbitrary. Thus when the photon or gluon line is next to an external fermion line, one can choose

either p or q to be the fermion momentum. In that case, only one of the terms contributes because of the Dirac equations.

$$\not{q}u(q) = 0, \qquad \bar{u}(p)\not{p} = 0 \ . \tag{2.77}$$

- In the case that the fermion helicities are fixed, either a factor $1+\gamma_5$ or $1-\gamma_5$ is associated with the fermion line. This will result in the survival of only one term in Eq. (2.74) and Eq. (2.76).

- When the photon or gluon line is next to the external fermion line, there is a cancelation of the denominator. For example,

$$\begin{aligned} \bar{u}(p)\not{\epsilon}^{\pm}\frac{\not{p}+\not{k}}{2(p\cdot k)} &= -N\bar{u}(p)\not{k}\not{p}\not{q}\frac{\not{p}+\not{k}}{2(p\cdot k)} \\ &= -N\bar{u}(p)\not{q}(\not{p}+\not{k}) \ . \end{aligned} \tag{2.78}$$

- There is one more trick one can use in the calculations. This is to do with the polarized projection operator.

$$\begin{aligned} (1\pm\gamma_5)u(p)\bar{u}(p)(1\mp\gamma_5) &= (1\pm\gamma_5)\left(\sum_{pol} u(p)\bar{u}(p)\right)(1\mp\gamma_5) \\ &= 2(1\pm\gamma_5)\not{p} \ . \end{aligned} \tag{2.79}$$

In the next subsection, we are going to use an example to show how one can benefit from this method. In particular, we shall focus on the polarized processes, which Gastmanns and Wu did not discuss much in their book[39]. Readers can refer to their book for plenty of examples for unpolarized processes.

2.3.2 Polarized processes

In Gastmanns and Wu's approach, they only concern about calculating the unpolarized cross-section, therefore they did not pay attention to phase of the helicity amplitudes. However, as we will see the phases of the helicity amplitudes are very

important in calculating polarized cross sections. In this subsection, we will generalize their approach to the polarized processes. We will use the process $qg \longrightarrow q'g'$ as an example to show how to deal with polarized processes using helicity amplitude approach.

The process of interest is the polarized $qg \longrightarrow q'g'$, which is very complicated to calculate using common trace method. However, it is relatively easy if we use the helicity amplitude method because most of the helicity amplitudes vanish due to helicity conservation, and the rest are not independent due to parity and time reversal conservation. Therefore it often happens that only a few elements are left, and they are easy to be computed as functions of the kinematical variables.

There are three Feynman diagrams contributing to the process at the first order, as shown in Fig. 2-5 The helicity amplitudes for the three diagrams are

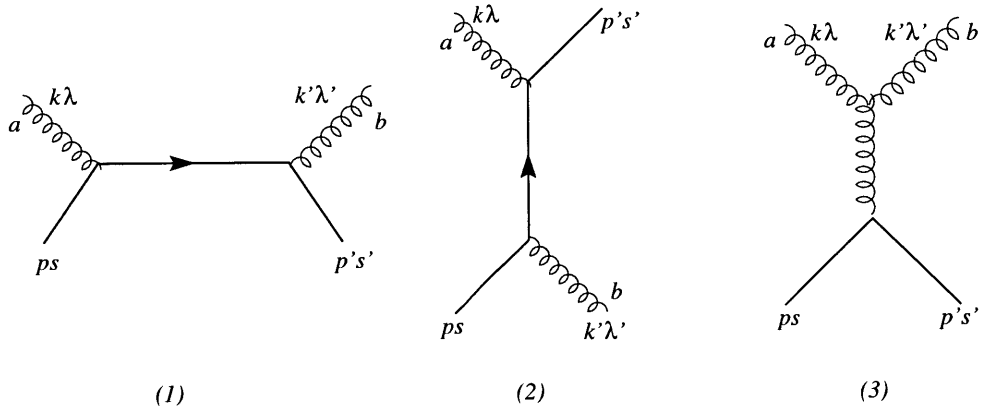

Figure 2-5: Feynman diagrams for the process $qg \longrightarrow q'g'$

$$
\begin{aligned}
M_1(\lambda s;\lambda' s') = \quad & -\frac{ig_s^2}{\hat{s}}(T_bT_a)_{ij}\bar{u}(p's')\not{\epsilon}^*(k'\lambda')(\not{p}+\not{k})\not{\epsilon}(k\lambda)u(ps)\ , \\
M_2(\lambda s;\lambda' s') = \quad & -\frac{ig_s^2}{\hat{u}}(T_aT_b)_{ij}\bar{u}(p's')\not{\epsilon}^*(k'\lambda')(\not{p}-\not{k}')\not{\epsilon}(k\lambda)u(ps)\ , \\
M_3(\lambda s;\lambda' s') = \quad & \frac{g_s^2}{\hat{t}}f_{bac}(T_c)_{ij}\bar{u}(p's')\gamma_\mu u(ps)\left[(k+k')^\mu\epsilon(k\lambda)\cdot\epsilon^*(k'\lambda')\right. \\
& \left.-2k\cdot\epsilon^*(k'\lambda')\epsilon^\mu(k\lambda)\ -2k'\cdot\epsilon(k\lambda')\epsilon^{*\mu}(k'\lambda')\right]\ ,
\end{aligned}
\tag{2.80}
$$

where

$$\begin{aligned}
\hat{s} &= (k+p)^2 = (k'+p')^2 = 2k\cdot p = 2k'\cdot p' \\
\hat{t} &= (p-p')^2 = (k-k')^2 = -2p\cdot p' = -2k\cdot k' \\
\hat{u} &= (p-k')^2 = (p'-k)^2 = -2p\cdot k' = -2p'\cdot k \ , \qquad (2.81)
\end{aligned}$$

neglecting the masses of the partons. g_s is the strong interaction coupling constant with $\alpha_s \equiv g_s^2/4\pi = 0.117 \pm 0.005$ at energy of M_Z[41]. $T_a(a = 1..8)$ is the infinitesimal operators of $SU(3)$ group, $(T_aT_b - T_bT_a)_{ij} = if_{abc}(T_c)_{ij}$ with subscripts $i, j = 1, 2, 3$, and f_{abc} the structure constant[1]. λ, s are the helicity labels for the incoming gluon and quark, λ', s' for the outgoing ones, respectively. $u(ps)$ is Dirac spinor for a quark with momentum p and helicity s and $\bar{u}(ps) \equiv u^\dagger(ps)\gamma^0$, which satisfies the Dirac equations $\not{p}u(ps) = 0$, $\bar{u}(ps)\not{p} = 0$.

The gluon polarizations ϵ_μ can be chosen to be the following[39]

$$\begin{aligned}
\not{\epsilon}(k\pm) &= N\left[\not{p}\not{p}'\not{k}(1\pm\gamma_5) + \not{k}\not{p}'\not{p}(1\mp\gamma_5)\right] \ , \\
\not{\epsilon}^\star(k'\pm) &= N\left[\not{k}'\not{p}'\not{p}(1\pm\gamma_5) + \not{p}\not{p}'\not{k}'(1\mp\gamma_5)\right] \ , \qquad (2.82)
\end{aligned}$$

where $N = (2\hat{s}\hat{t}\hat{u})^{-1/2}$ is the normalization factor.

In principle, we can add the above three parts together, square it, and then calculate the traces of a very complicated expressions. It is already hard to do this in unpolarized processes, even much harder in polarized processes. Therefore, we shall first calculate the helicity amplitudes (into either a number or a very simple expression which we can easily handle) using Gastmanns and Wu's approach[39].

The quark has two helicity state $+1/2$ or $-1/2$, the gluon also have only two helicity states due to gauge invariance, $+1$ or -1. [For simplicity, we will use only $+, -$ to represent the positive, negative helicity states for both quark and gluon.] Therefore, there are $2 \times 2 \times 2 \times 2 = 16$ helicity amplitudes.

However, these 16 helicity amplitudes are not independent of each other, some of them actually vanish due to the constraints of QCD symmetries.

Since the quark's chirality is same as its helicity and the strong interaction does not change the quark's chirality, the quark's helicity conserves, i.e., $s' = s$. On the other hand, the helicities conserve in the scattering, $\lambda + s = \lambda' + s'$, thus the helicities of the gluon also conserve, i.e. $\lambda' = \lambda$. Hence, only the helicity amplitudes $M(\lambda s; \lambda s)$ survive. Therefore, only four elements $M(++;++)$, $M(--;--)$, $M(+-;+-)$, $M(-+;-+)$ are left. Actually, these four elements are not independent of each other. Under parity, $+ \longleftrightarrow -$, hence $M(++;++) = M(--;--)$, $M(+-;+-) = M(-+;-+)$. Thus, only two helicity amplitudes $M(++;++)$ and $M(-+;-+)$ need to be computed. Substitute Eq. (2.82) into Eqs. (2.80), and use the Dirac equations for the quarks, we can simplify the two independent non-zero helicity amplitudes as follows

$$\begin{aligned} M(++;++) = & \quad \frac{2ig_s^2}{\hat{t}\hat{u}} \left[\hat{s}(T_aT_b)_{ij} + \hat{u}(T_bT_a)_{ij}\right] \bar{u}(p'+) \not{k} u(p+) \\ M(-+;-+) = & \quad \frac{2ig_s^2}{\hat{t}\hat{s}} \left[\hat{s}(T_aT_b)_{ij} + \hat{u}(T_bT_a)_{ij}\right] \bar{u}(p'+) \not{k} u(p+) \ . \end{aligned} \tag{2.83}$$

We can simplify the above helicity amplitudes further to just some c-numbers in Dirac space. However, now there are only a few Dirac matrices involved, which is very easy to compute. Now we can square the above helicity amplitudes. For instance,

$$\begin{aligned} |M(++;++)|^2 = & \quad \frac{1}{8\times 3}\frac{4g_s^4}{\hat{t}^2\hat{u}^2}\left[\hat{s}^2\mathrm{Tr}(T_aT_bT_bT_a) + \hat{u}^2\mathrm{Tr}(T_bT_aT_aT_b) + 2\hat{s}\hat{u}\mathrm{Tr}(T_aT_bT_aT_b)\right] \\ & \mathrm{Tr}\not{k} u(p+)\bar{u}(p+)\not{k} u(p'+)\bar{u}(p'+) \ , \end{aligned} \tag{2.84}$$

where $1/(8\times 3)$ is the color normalization factor of the color state of the initial gluon and quark. $\mathrm{Tr}(T_aT_bT_bT_a) = 16/3$, $\mathrm{Tr}(T_aT_bT_aT_b) = -2/3$, thus,

$$\begin{aligned} |M(++;++)|^2 &= -\frac{2}{9}\frac{g_s^4}{\hat{t}^2\hat{u}^2}\left[4\hat{s}^2 + 4\hat{u}^2 - \hat{s}\hat{u}\right] \mathrm{Tr}\not{k} u(p+)\bar{u}(p+)\not{k} u(p'+)\bar{u}(p'+) \\ &= -\frac{2}{9}\frac{g_s^4}{\hat{t}^2\hat{u}^2}\left[4\hat{s}^2 + 4\hat{u}^2 - \hat{s}\hat{u}\right] \mathrm{Tr}\not{k}\frac{1}{2}(1+\gamma_5)\not{p}\not{k}\frac{1}{2}(1+\gamma_5)\not{p}' \\ &= -\frac{2}{9}\frac{g_s^4}{\hat{t}^2\hat{u}^2}\left[4\hat{s}^2 + 4\hat{u}^2 - \hat{s}\hat{u}\right] \hat{s}\hat{u} \\ &= 2g_s^4\left(\frac{\hat{s}^2}{\hat{t}^2} - \frac{4}{9}\frac{\hat{s}}{\hat{u}}\right) \ , \end{aligned} \tag{2.85}$$

where we have use the fact $\hat{s}+\hat{u}+\hat{t}=0$, and Eq. 2.79: $u(p\pm)\bar{u}(p\pm)=(1\pm\gamma_5)\not{p}/2$. Likewise, $|M(-+;-+)|^2$ can be calculated as below

$$|M(-+;-+)|^2 = 2g_s^4\left(\frac{\hat{u}^2}{\hat{t}^2}-\frac{4}{9}\frac{\hat{u}}{\hat{s}}\right) . \tag{2.86}$$

Hence, we can get the unpolarized cross section which is proportional to $|\bar{M}|^2$,

$$\begin{aligned} |\bar{M}|^2 &= \frac{1}{4}\left[\, |M(++;++)|^2+|M(--;--)|^2+|M(+-;+-)|^2+|M(-+;-+)|^2 \,\right] \\ &= g_s^4\left(\frac{\hat{s}^2+\hat{u}^2}{\hat{t}^2}-\frac{4}{9}\frac{\hat{s}^2+\hat{u}^2}{\hat{s}\hat{u}}\right) , \end{aligned} \tag{2.87}$$

where the factor $\frac{1}{4}$ comes from the average of the helicities of the initial quark and gluon. This result is consistent with that in the textbooks [1, 39].

Now we are ready to discuss the polarized case. In chapter 5 of this thesis we are going to discuss $pp\longrightarrow(\pi\pi)X$ to measure the nucleon's transversity, in which we are going to consider the two pions only from quark fragmentation, thus the final gluon state will be summed over. Therefore, in the following we are going to discuss the helicity density matrix for $qg\longrightarrow qg$ with the final gluon helicity states are summed over. We define the helicity density matrix S as follows

$$S(\lambda_i\lambda_i';s_is_i';s_f's_f)\equiv\frac{1}{24}\left(M^\star(\lambda_i's_i';+s_f')M(\lambda_is_i;+s_f)+M^\star(\lambda_i's_i';-s_f')M(\lambda_is_i;-s_f)\right) \tag{2.88}$$

where the subscript i represents *initial*, f *final*, $1/24$ is the initial state color average factor.

Substitute Eq. (2.83) into Eq. (2.88) and perform the same calculations as in calculating the unpolarized cross section, we get

$$\begin{aligned} S=\frac{1}{2}g_s^4\left(\frac{1}{\hat{t}^2}-\frac{4}{9}\frac{1}{\hat{s}\hat{u}}\right) \quad & \Big[\, (\hat{s}^2+\hat{u}^2)\; I_g\otimes(I_q\otimes I_q+\sigma_q^3\otimes\sigma_q^3) \\ & +4\hat{s}\hat{u}\; I_g\otimes(\sigma_q^+\otimes\sigma_q^-+\sigma_q^-\otimes\sigma_q^+) \\ & +(\hat{s}^2-\hat{u}^2)\; G\otimes(I_q\otimes\sigma_q^3+\sigma_q^3\otimes I_q)\,\Big] , \end{aligned} \tag{2.89}$$

where $I_q, \sigma_q^3, \sigma_q^\pm$ are Pauli matrices in the quark helicity space, whereas I_g is unit matrix in gluon helicity space and $G = \mathrm{diag}(1, 0, -1)$.

The differential cross section can be obtained as follows

$$\begin{aligned}\frac{d\hat{\sigma}(qg \longrightarrow qg)}{d\hat{t}} &= \frac{1}{16\pi\hat{s}^2} S \\ &= \frac{\pi\alpha_s^2}{2\hat{s}^2}\left(\frac{1}{\hat{t}^2} - \frac{4}{9}\frac{1}{\hat{s}\hat{u}}\right)\Big[(\hat{s}^2+\hat{u}^2) I_g \otimes (I_q \otimes I_q + \sigma_q^3 \otimes \sigma_q^3) \\ &\quad +4\hat{s}\hat{u} I_g \otimes (\sigma_q^+ \otimes \sigma_q^- + \sigma_q^- \otimes \sigma_q^+) \\ &\quad +(\hat{s}^2 - \hat{u}^2) G \otimes (I_q \otimes \sigma_q^3 + \sigma_q^3 \otimes I_q)\Big] \ , \end{aligned} \tag{2.90}$$

from which one can easily get the the cross sections he wants. For example, the unpolarized cross section $d\hat{\sigma}/d\hat{t}$ can be obtained as below

$$\begin{aligned}\frac{d\hat{\sigma}}{d\hat{t}} &= \frac{1}{3}\frac{1}{2}\mathrm{Tr}\left[\frac{d\hat{\sigma}(qg \longrightarrow qg)}{d\hat{t}}(I_g \otimes I_q \otimes I_q)\right] \\ &= \frac{\pi\alpha_s^2}{\hat{s}^2}\left(\frac{\hat{s}^2+\hat{u}^2}{\hat{t}^2} - \frac{4}{9}\frac{\hat{s}^2+\hat{u}^2}{\hat{s}\hat{u}}\right) \ . \end{aligned} \tag{2.91}$$

One can also easily get the longitudinally polarized cross section $d\Delta\hat{\sigma}/d\hat{t}$

$$\begin{aligned}\frac{d\Delta\hat{\sigma}}{d\hat{t}} &= \frac{1}{2}\frac{1}{2}\mathrm{Tr}\left[\frac{d\hat{\sigma}(qg \longrightarrow qg)}{d\hat{t}}(G \otimes \sigma_q^3 \otimes I_q)\right] \\ &= \frac{\pi\alpha_s^2}{\hat{s}^2}\left(\frac{\hat{s}^2-\hat{u}^2}{\hat{t}^2} - \frac{4}{9}\frac{\hat{s}^2-\hat{u}^2}{\hat{s}\hat{u}}\right) \ . \end{aligned} \tag{2.92}$$

2.4 Cross Sections

Now put all the ingredients together one can get the cross section density matrix in Fig. 2-1, all as density matrices in helicity basis:

$$\left[\frac{d\sigma}{dxdzd\Omega}\right]^{H_1 H_1'}_{H'H} = \mathcal{F}(x)^{hh'}_{H'H}\left[\frac{d\sigma(ab \longrightarrow cd)}{d\Omega}\right]^{h_1 h_1'}_{h'h} \mathcal{D}(z)^{H_1 H_1'}_{h_1' h_1} \ , \tag{2.93}$$

where x is the longitudinal momentum fraction of the hadron carried by the parton, z the longitudinal momentum fraction of the parton carried by the hadron produced in

the fragmentation process, Ω represents the kinematical variables in the underlying process $ab \longrightarrow cd$.

Any physical cross sections can be obtained by taking trace of the cross section density matrix with parton and hadron helicity density matrices. For example, if one wants to calculate the cross section for single particle semi-inclusive in the unpolarized DIS process, one can have,

$$\frac{d\sigma(eN \longrightarrow e'HX)}{dxdzd\Omega} = \frac{1}{4}\mathrm{Tr}\left[\frac{d\sigma}{dxdzd\Omega}(I_e \otimes I_N)\right] , \tag{2.94}$$

where the factor $1/4$ comes from the helicity average of the initial states, I_e, I_N are the unit matrix in the electron and nucleon helicity space, respectively.

The Eq. (2.93) is our basic formula in the helicity density matrix formalism, which will be used repeatly in the following chapters.

To summarize this chapter, we present the helicity density matrix formalism in the polarized processes. We first discuss parton distribution functions in hadron. We show the distribution functions can be related to the independent non-zero helicity density matrix elements. In order to discuss the helicity operator's symmetry properties, we use the spherical irreducible tensor operator. Then, we go on to discuss the parton fragmentation functions. We show it is more complicated because of the possible time reversal violation due to final state interaction (FSI). Finally, we discuss how to compute the helicity density matrix in hard QCD. In particular, we show that the usage of Gastmanns and Wu's helicity amplitude approach dramatically reduce the complication of the calculations.

In the following chapters, we shall show how to use the helicity density matrix formalism. In particular, we shall use it to discuss the s and p wave interference between two pion productions in deep inelastic scattering and high energy pp scattering. We shall show how this mechanism can be used to probe nucleon's transversity, one of the three important distribution functions inside the nucleon at leading twist level.

Chapter 3

Nucleon's Transversity Distribution

In this chapter, we shall briefly review the quark transversity distributions inside the nucleon. (A very good summary about transversity can be found in Ref. [42], from which much of this section is taken.) First, the definition of the transversity and its interesting and important properties are reviewed. Then we go on to discuss the existing proposals to measure the quark transversity, especially focusing on their advantages and disadvantages. This chapter is justified because we will propose new ways to probe the nucleon's transversity in the following chapters using the helicity density matrix formalism which was discussed in chapter 2.

3.1 Transversity

3.1.1 What is transversity

Accurate measurements of quark unpolarized distribution function $q(x, Q^2)$ and longitudinally polarized distribution function $\Delta q(x, Q^2)$ have shed considerable light upon the quark-gluon substructure of the nucleon. The unpolarized quark distribution $q(x, Q^2)$, which characterizes the quark momentum distribution in the nucleon, has been well studied theoretically and experimentally for a long time[1]. The integral of

$q(x, Q^2)$ over x from 0 to 1 at asymptotic limit ($Q^2 \to \infty$) leads to a momentum sum rule[34], in which the quarks carry approximately 1/2 of the nucleon's momentum. The longitudinally polarized quark distribution $\Delta q(x, Q^2)$ has just been accurately measured recently. The results shocked spin physicist community by discovering that the quarks' spin only contribute to about one-third of the nucleon's spin[43], which generated a lot of interests among nucleon spin theorists and experimentalists. For example, one of the theoretical progresses found that similar to the momentum sum rule, the quarks' contributions (including spin and orbital angular momentum) to the nucleon's spin is about half in the asymptotic limit[31].

The quark transversity distribution δq [1] is one of the three quark distribution functions characterizing the quarks inside the nucleon at leading twist level (twist-two). It measures the probability difference to find a quark polarized along versus opposite to the polarization of a nucleon polarized transversely to its (infinite) momentum, It was first found by Ralston and Soper in their study of polarized Drell-Yan process[44]. But its place along with q and Δq in the complete description of the nucleon spin was not realized until after measurements of Δq had spurred interest in QCD spin physics[10, 45, 46].

Quark distribution functions can be regarded as particular discontinuities in forward quark-nucleon scattering[6]. The scattering amplitude and the discontinuity that defines a distribution function are shown in Fig. 2-2 [2]. The quark (h, h') and hadron (H, H') helicities take on the values $\pm 1/2$. Helicity conservation requires $H + h' = H' + h$. Parity sends $h \to -h$, *etc.*, and time-reversal interchanges initial (H, h') and final (H', h) helicities. This leaves exactly three independent quark distribution

[1] Although the name *transversity* is fairly universal, the notation is not. In addition to δq, the notations $\Delta_T q$ and h_1 are also commonly used in the literatures.

[2] Transverse momenta enter only at higher twist. Therefore, the whole process is collinear, so the angular momentum along the $\hat{P}$-axis(i.e., helicity), is conserved.

functions corresponding to the helicity labels as discussed in chapter 2,

$$\begin{array}{cccc} H & h' & \longrightarrow & H' \quad h \\ \frac{1}{2} & \frac{1}{2} & \longrightarrow & \frac{1}{2} \quad \frac{1}{2} \\ \frac{1}{2} & -\frac{1}{2} & \longrightarrow & \frac{1}{2} \quad -\frac{1}{2} \\ \frac{1}{2} & -\frac{1}{2} & \longrightarrow & -\frac{1}{2} \quad \frac{1}{2} \end{array} \tag{3.1}$$

These three helicity amplitudes can be regrouped into combinations that measure spin average (q), helicity difference (Δq), and helicity flip transversity (δq) distribution,

$$\begin{aligned} q &\sim \mathcal{F}_{\frac{1}{2}\frac{1}{2}\to\frac{1}{2}\frac{1}{2}} + \mathcal{F}_{\frac{1}{2}-\frac{1}{2}\to\frac{1}{2}-\frac{1}{2}} \\ \Delta q &\sim \mathcal{F}_{\frac{1}{2}\frac{1}{2}\to\frac{1}{2}\frac{1}{2}} - \mathcal{F}_{\frac{1}{2}-\frac{1}{2}\to\frac{1}{2}-\frac{1}{2}} \\ \delta q &\sim \mathcal{F}_{\frac{1}{2}-\frac{1}{2}\to-\frac{1}{2}\frac{1}{2}} \ , \end{aligned} \tag{3.2}$$

where $\mathcal{F}$ means the helicity amplitude. Together, q, Δq, and δq provide a complete description of quark momentum and spin at leading twist[6]. This can be seen from a spin-density matrix representation of the leading twist quark distribution functions

$$\mathcal{F}(x,Q^2) = \frac{1}{2}q(x,Q^2)\ I\otimes I + \frac{1}{2}\Delta q(x,Q^2)\ \sigma_3\otimes\sigma_3 + \frac{1}{2}\delta q(x,Q^2)\ (\sigma_+\otimes\sigma_- + \sigma_-\otimes\sigma_+) \tag{3.3}$$

where the Pauli matrices lie in the quark and nucleon helicity spaces respectively.

3.1.2 The properties of the transversity

There are reasons behind why the transversity escapes the spin physicists' attentions for such a long period of time. In this section, we shall discuss the properties of the transversity, with emphasis on the differences between the transversity and the other two distributions.

Odd chirality

There are fundamental differences between δq and the other two distributions q, Δq when we look at their chirality properties. It is illustrated in the Eq. (3.2) that the transversity is associated with the helicity flipping amplitudes while the other two conserve the quark's helicity. On the other hand, helicity and chirality are identical for "good" light-cone components of the Dirac field (they are opposite for the "bad" components)[6]. Therefore, the transversity δq flips the chirality of the quark. It is this property that makes the transversity very difficult to be measured experimentally since all perturbative QCD process and all interactions with external electroweak currents conserve chirality (up to corrections of order m/Q). δq decouples from all hard processes that involve only one quark distribution function at leading twist (twist 2), such as deep inelastic scattering process $ep \to e'X$. Instead, in order to probe the transversity, one has to have two soft (chiral-odd) QCD parts involved in the process. So far, the chiral-odd soft QCD functions(up to twist-three) available are 1) twist-two: $\delta q(x, Q^2)$ and $\delta\hat{q}(z, Q^2)$; 2) twist-three: $e(x, Q^2)$, $\hat{e}(z, Q^2)$, $h_L(x, Q^2)$, $\hat{h}_L(z, Q^2)$. See the introduction in the chapter 1 in this thesis, or Refs. [6, 10, 11, 12]

.

Significance

For non-relativistic quarks, where boosts and rotations commute[3], $\Delta q_a(x, Q^2) = \delta q_a(x, Q^2)$, $g_A/g_V = 5/3$ and $\Delta\Sigma = 1$. However, we have learned from $g_A/g_V \approx 1.26$ and $\Delta q \approx 0.2$[47] that the quarks inside the nucleon cannot be non-relativistic. Therefore, the difference between the nucleon's helicity difference and transversity distributions provides a further and more detailed measure of the relativistic nature of the quarks inside the nucleon.

[3]a transversely polarized nucleon with momentum $\vec{P}$ first can be boosted to its rest frame, then its transverse polarization can be rotated to be along its original momentum direction, finally it can boosted back to original momentum. Now a transversely polarized nucleon with momentum becomes longitudinally polarized.

Evolution

$\delta q(x, Q^2)$ does not mix with gluons under evolution. All its anomalous dimensions are positive. Thus it evolves very simply with Q^2 — it goes slowly and inexorably to zero. The anomalous dimensions for δq were first calculated by Artru and Mekhfi[45] in leading order. NLO anomalous dimensions have now been calculated by three groups[48].

Inequalities

The transversity obeys some important inequalities. The first, $|\delta q_a(x, Q^2)| \leq q_a(x, Q^2)$, follows from its interpretation as a difference of probabilities. The second is the so-called *Soffer's inequality* which comes from the positivity properties of helicity amplitudes, $|2\delta q_a(x, Q^2)| \leq q_a(x, Q^2) + \Delta q_a(x, Q^2)$[49]. Saturation of Soffer's inequality along with simple model calculations would suggest $|\delta q_a| > |\Delta q_a|$.

Tensor charge and its evolution

The first moment of δq measures a simple local operator analogous to the axial charge,

$$\begin{aligned} \int_{-1}^{1} dx\, \delta q_a(x, Q^2) &= \int_0^1 dx\, (\delta q_a(x, Q^2) - \delta \bar{q}_a(x, Q^2)) \equiv \delta q_a(Q^2) \\ &\sim \langle PS|\bar{q}_a \sigma^{0i} \gamma_5 q_a|_{Q^2}|PS\rangle \end{aligned} \tag{3.4}$$

known as the "tensor charge". [4] Unlike its vector and axial equivalents, the tensor charge is not conserved in QCD, so it has an anomalous dimension at one-loop. The leading-log evolution of the tensor charge is[50]

$$\delta q_a(\mu^2) = \left[\alpha(\mu^2)/\alpha(\mu_0^2)\right]^{\frac{4}{33-2n_f}} \delta_a(\mu_0^2)\ , \tag{3.5}$$

[4]The first moment of Δq, known as axial charge, measures $\langle PS|\bar{q}_a \gamma^i \gamma_5 q_a|_{Q^2}|PS\rangle$. In non-relativistic limit, the tensor charge is equal to axial charge because for a non-relativistic quark, which has only upper components, $\bar{\psi} = \psi$, both charges measure same quantity $\langle PS|q_a^\dagger \gamma^i \gamma_5 q_a|_{Q^2}|PS\rangle$. Therefore the differences between tensor charge and axial charge also provide a measure of the relativistic nature of the quarks inside the nucleon.

where n_f is the quark flavor number, $\alpha(\mu) \equiv g_s^2(\mu)/4\pi$ with $g_s(\mu)$ the strong interaction coupling at energy μ .

Initial efforts have been made to calculate the tensor charge on the lattice[51]. Although the lattice is small ($16^3 \times 20$) and the coupling is relatively strong ($\beta = 5.7$), the results are intriguing[51]. Also, there have been a lot of model discussions about tensor charge in the literatures[50].

3.2 Proposals to Measure Transversity

In this section, we shall discuss the existing proposals to measure the transversity, with emphasis on their advantages and disadvantages. The processes to be discussed here are transversely polarized Drell-Yan process[44], Λ production in deep inelastic scattering process(DIS) [45, 38], A_{TT}/A_{LL} in polarized jet production in PP scattering [52, 53], twist-three single pion production in DIS [11], azimuthal asymmetry in single particle semi-inclusive DIS[54].

As mentioned before, one has to measure the product of the transversity and another chiral-odd soft QCD quantity in order to probe the transversity. A generic (and complicated) example is shown in Fig. [2-1]. The lower soft vertex might be the transversity distribution of the target. The compensating chirality flip can be provided by a distribution or fragmentation at the upper vertex. The available chiral-odd (*i.e.* chirality flip) quantities up to twist three are listed in section 3.1.2. With these building blocks, it is possible to construct the proposals to measure δq.

3.2.1 Transversely Polarized Drell-Yan in PP Collisions

As a matter of fact, the transversity first caught physicists' attentions when J. Ralston and D. E. Soper discussed the transversely polarized Drell-Yan process in PP collisions decades ago[44]. The process of interest is $\vec{P}_\perp \vec{P}_\perp \longrightarrow l\bar{l}X$. This process measure the combination of $\delta q(x_1) \otimes \delta\bar{q}(x_2)$, where $\bar{q}(x)$ is the antiquark transversity distribution. The advantages of this approach are

- Drell-Yan is well understood through next to leading order in perturbative QCD[55].
- The RHIC Collider in its polarized mode will provide the beams.

However, there are several disadvantages which make it hard to probe the transversity.

- $\delta\bar{q}$ is presumably small in the nucleon.
- Drell-Yan rates are generically low compared to purely hadronic processes at colliders.

3.2.2 Λ Production in DIS

This method was first examined by Artru and Mekhfi[45], and then discussed more thoroughly by Jaffe[38]. The process of interest is $e\vec{P}_\perp \longrightarrow e'\vec{\Lambda}_\perp X$, where the nucleon beam is transversely polarized but electron beam unpolarized. This process enables us to measure the product of $\delta q(x) \otimes \delta\hat{q}(z)$. The advantages of this process are

- Polarized u-quarks exists at large x in N and small x in Λ, s-quarks also at small-x in N and large-x in Λ .

The disadvantages are

- Λ may be rare in current fragmentation region.
- Quark$\longrightarrow \Lambda$ fragmentation spin transfer is unknown at present.

3.2.3 Twist-three Single Pion Production in DIS

This process is proposed by Jaffe and Ji[11]. The process of interest is $e\vec{p}_\perp \rightarrow e'\pi X$, single pion production when unpolarized electron hit a transversely polarized nucleon. This process measure the transversity through the product of $\delta q(x) \otimes \hat{e}(z) \oplus g_T(x) \otimes \hat{q}(z)$, where $g_T(x) = g_1(x) + g_2(x)$ and $\hat{q}(z)$ is unpolarized fragmentation function. The advantages for this process are

- Pions are abundant in the fragmentation region of DIS.

- Accessible to HERMES or COMPASS with a transversely polarized target.

The disadvantages are

- The process is twist-three, suppressed by $\mathcal{O}(1/Q)$.
- The competing (twist-three) chiral-even mechanism, $g_T(x) \otimes \hat{q}(z)$, must be subtracted away to expose the process of interest.

3.2.4 A_{TT}/A_{LL} in Polarized Jet Production

This method has been examined by several people[52, 53, 56]. The process of interest is $P_\perp P_\perp \to \text{jet(s)}X$, in which both proton beams are transversely polarized. This process measures the quantity

$$\frac{\delta q(x_1) \otimes \delta q(x_2)}{\Delta G(x_1) \otimes \Delta G(x_2) \oplus \Delta G(x_1) \otimes \Delta q(x_2) + \cdots}$$

where $G(x)$ is the unpolarized gluon distribution, $\cdots$ indicates other possible terms. The advantages for this process are

- Jets are abundant in the final state at colliders.
- Accessible to RHIC in the polarized collider mode.

But the disadvantages are

- The production of jets in collisions of transversely polarized protons is suppressed for a variety of reasons. Most important is the fact that there is no analog of transversity for gluons. Furthermore the quark-quark contribution is suppressed by a color exchange factor[52].

3.2.5 Azimuthal Asymmetry in Semi-inclusive Single Particle Production in polarized DIS

Collins and his collaborators proposed to look for an asymmetry associated with a plane defined in the current fragmentation region in DIS[54]. They suggested to

measure the following azimuthal distribution

$$\cos\phi = \frac{\vec{p}\times\vec{q}\cdot\vec{S}_\perp}{|\vec{p}\times\vec{q}||\vec{S}_\perp|}\ , \tag{3.6}$$

which is sensitive to the transversity of the struck quark. Here $\vec{q}$ is the virtual photon momentum, which defines the fragmentation axis; $\vec{p}$ is the momentum of the leading meson; $\vec{S}_\perp$ is the polarization vector of the nucleon target. ϕ is the so-called "Collins angle".

This process measure the combination of $\cos\phi \times \delta q(x) \otimes \delta\hat{q}(z)$, which requires there be significant phases generated by final state interactions (FSI) in the fragmentation process because otherwise application of "naive time-reversal" symmetry[57], $(\vec{p},\ \vec{q},\ \vec{s}) \rightarrow -\ (\vec{p},\ \vec{q},\ \vec{s})$ would forbid a Collins angle asymmetry($< \cos\phi >= 0$). The advantages for this process are:

- The effect is twist-two.
- Every DIS event has a current fragmentation region.
- Accessible to HERMES or COMPASS running with a transversely polarized target.

But there are also some disadvantages:

- Requires a FSI phase that does not average to zero summed over unobserved hadrons, X.

3.3 Summary

The transversity distribution provides a further and more detailed measure of the relativistic nature of the quarks inside the nucleon. However, it is hard to measure it experimentally due to its odd chirality, which makes it decouple from the ordinary DIS at leading twist. The difficulties of the existing processes so far to probe the transversity propel people to continue to pursue new feasible ways. In the following several chapters, we shall describe a brand-new way to access the nucleon's

transversity in semi-inclusive DIS or PP collisions. The basic idea is to consider the interference between s and p waves of the two meson productions in polarized DIS or PP collisions. The mechanism can also be used to probe valence quark distributions in DIS.

Chapter 4

Interference Fragmentation Functions and the Nucleon's Transversity

As discussed in chapter 3, the transversity distribution measures the correlation of quarks with opposite chirality in the nucleon. Since hard scattering processes in QCD preserve chirality at leading twist, transversity is difficult to measure experimentally. For example, it is suppressed like $\mathcal{O}(m_q/Q)$ in totally-inclusive deep inelastic scattering (DIS). Ways have been suggested to measure the transversity distribution. These include transversely polarized Drell-Yan [44], twist-three pion production in DIS [10], the so-called "Collins effect" [54], and polarized Λ production in DIS [45, 6]. However, each of these has drawbacks, as discussed in chapter 3. For example, the Drell-Yan cross section is small and requires both transversely polarized quarks and antiquarks in the nucleon; twist-three pion production is suppressed by $\mathcal{O}(1/Q)$, and a $g_T \hat{f}_1$ term must be subtracted to reveal the transversity dependence; the Collins effect requires a residual final state interaction phase in an inclusive process which we believe to be unlikely (see below); the polarized Λ production suffers from a likely low production rate for hyperons in the current fragmentation region and an as yet unknown and possibly small polarization transfer from u-quarks to the Λ.

In this chapter we describe another way to isolate the quark transversity distri-

bution in the nucleon that is free from many of these shortcomings. The process of interest is two-meson (*e.g.* $\pi^+\pi^-$ or $K\overline{K}$) production in the current fragmentation region in deep inelastic scattering on a transversely polarized nucleon. Our analysis focuses on the *interference* between the s- and p-wave of the two-meson system around the ρ (for pions) or the ϕ (for kaons). Such an interference effect allows the quark's polarization information to be carried through $\vec{k}_+ \times \vec{k}_- \cdot \vec{S}_\perp$, where $\vec{k}_+$, $\vec{k}_-$, and $\vec{S}_\perp$ are the three-momenta of π^+ (K), π^- ($\overline{K}$), and the nucleon's transverse spin, respectively. This effect is at the leading twist level, and the production rates for pions and kaons are large in the current fragmentation region. However, it would vanish by T-invariance in the absence of final state interactions($\vec{k}_+ \to -\vec{k}_+$, $\vec{k}_- \to -\vec{k}_-$, $\vec{S}_\perp \to -\vec{S}_\perp$) or by C-invariance($\pi^+ \leftrightarrow \pi^-$) if the two-meson state were an eigenstate of C-parity. Both suppressions are evaded in the ρ ($\pi^+\pi^-$) and ϕ ($K\overline{K}$) mass regions.

The final state interactions of $\pi\pi$ and $K\overline{K}$ are known in terms of meson-meson phase shifts. From these phase shifts we know that s- and p-wave production channels interfere strongly in the mass region around the ρ and ϕ meson resonances. Since the s- and p-waves have opposite C-parity, the interference provides exactly the charge conjugation mixing necessary. Combining perturbative QCD, final state interaction theory, and data on the meson-meson phase shifts, we can relate this asymmetry to known quantities, the transversity distribution we seek, and to a new type of fragmentation function that describes the s- and p-wave interference in the process $q \to \pi^+\pi^-(K\overline{K})$. Unless this fragmentation is anomalously small, the measurement of this asymmetry may be the most promising way to measure the quark transversity distribution.

Earlier works[54] have explored angular correlations of the form $\vec{k}_1 \times \vec{k}_2 \cdot \vec{S}_\perp$, where $\vec{k}_1$ and $\vec{k}_2$ are vectors characterizing the final state in DIS. The simplest example would be $\vec{k}_1 = \vec{q}$ and $\vec{k}_1 = \vec{k}_\pi$, the momentum of a pion. These asymmetries, however, require that the final state interaction phase between the observed hadron(s) and the rest of the hadronic final state must not vanish when the unobserved states are summed over. We believe this to be unlikely. We utilize a final state phase generated by the two-meson final state interaction, which is well understood theoretically and well

measured experimentally.

The results of our analysis are summarized by Eq. (4.14) where we present the asymmetry for $\pi^+\pi^-(K\overline{K})$ production in the current fragmentation region. Current data on $\pi\pi$ and $K\overline{K}$ phase shifts are used to estimate the magnitude of the effect as a function of the two-meson invariant mass (see Fig. 4-2).

The advantages of this method are: the effect is leading twist, hence there is no $1/Q$ suppresion; the meson pairs are copiously produced in the quark fragmentation; the final state interaction phase can be measured in meson-meson scattering; the final state interaction phase remains fixed even after the summation on the X states is performed; it can be done at HERMES and COMPASS. The disadvantage is that the cross section must be held differential to avoid the possible phase averaging to zero.

We consider the semi-inclusive deep inelastic scattering process with two-pion final states being detected: $eN \to e'\pi^+\pi^-X$. The analysis to follow applies as well to $K\overline{K}$ production. The nucleon target is transversely polarized with polarization vector S_μ. The electron beam is unpolarized. The four-momenta of the initial and final electron are denoted by $k = (E, \vec{k})$ and $k' = (E', \vec{k'})$, and the nucleon's momentum is P_μ. The momentum of the virtual photon is $q = k - k'$, and $Q^2 = -q^2 = -4EE'\sin^2\theta/2$, where θ is the electron scattering angle. The electron mass will be neglected throughout. We adopt the standard variables in DIS, $x = Q^2/2P\cdot q$ and $y = P\cdot q/P\cdot k$. The $\sigma[(\pi\pi)^{I=0}_{l=0}]$ and $\rho[(\pi\pi)^{I=1}_{l=1}]$ resonances are produced in the current fragmentation region with momentum P_h and momentum fraction $z = P_h\cdot q/q^2$. We recognize that the $\pi\pi$ s-wave is not resonant in the vicinity of the ρ and our analysis does not depend on a resonance approximation. For simplicity we refer to the non-resonant s-wave as the "σ".

The invariant squared mass of the two-pion system is $m^2 = (k_+ + k_-)^2$, with k_+ and k_- the momentum of π^+ and π^-, respectively. The decay polar angle in the rest frame of the two-meson system is denoted by Θ, and the azimuthal angle ϕ is defined as the angle of the normal of two-pion plane with respect to the polarization vector $\vec{S}_\perp$ of the nucleon, $\cos\phi = \vec{k}_+ \times \vec{k}_- \cdot \vec{S}_\perp/|\vec{k}_+ \times \vec{k}_-||\vec{S}_\perp|$. This is the analog of

the "Collins angle" defined by the $\pi^+\pi^-$ system[54].

To simplify our analysis we make a collinear approximation, i.e., $\theta \approx 0$, in referring the fragmentation coordinate system to the axis defined by the incident electron (the complete analysis will be published elsewhere[58]). At SLAC, HERMES, and COMPASS energies, a typical value for θ is less than 0.1. Complexities in the analysis of fragmentation turn out to be proportional to $\sin^2\theta$ and can be ignored at fixed target facilities of interest. In this approximation the production of two pions can be viewed as a collinear process with the electron beam defining the common $\hat{e}_3$ axis. Also we take $\vec{S}_\perp$ along the $\hat{e}_1$ axis.

Since we are only interested in a result at the leading twist, we follow the helicity density matrix formalism developed in Refs. [37, 6], in which all spin dependence is summarized in a *double* helicity density matrix. We factor the process at hand into basic ingredients: the $N \to q$ distribution function, the hard partonic $eq \to e'q'$ cross section, the $q \to (\sigma, \rho)$ fragmentation, and the decay $(\sigma, \rho) \to \pi\pi$, all as density matrices in helicity basis:

$$\left[\frac{d^6\sigma}{dx\,dy\,dz\,dm^2\,d\cos\Theta\,d\phi}\right]_{H'H} = \mathcal{F}^{h_1h_1'}_{H'H}\left[\frac{d^2\sigma(eq\to e'q')}{dx\,dy}\right]^{h_2h_2'}_{h_1'h_1}\left[\frac{d^2\hat{\mathcal{M}}}{dz\,dm^2}\right]^{H_1H_1'}_{h_2'h_2}\left[\frac{d^2\mathcal{D}}{d\cos\Theta\,d\phi}\right]_{H_1'H_1} \quad (4,1)$$

where $h_i(h_i')$ and $H(H')$ are indices labeling the helicity states of quark and nucleon, and $H_1(H_1')$ labeling the helicity state of resonance the $(\sigma,\ \rho)$. See Fig. 4-1. In order to incorporate the final state interaction, we have separated the $q \to \pi^+\pi^-$ fragmentation process into two steps. First, the quark fragments into the resonance $(\sigma,\ \rho)$, then the resonance decays into two pions, as shown at the top part of the Fig. 4-1.

We first discuss two-meson fragmentation, first examined in the second paper of Ref. [54]. Here we introduce only those pieces necessary to describe *s-p* interference in $\pi^+\pi^-(K\overline{K})$ production. A full account of these fragmentation functions will be given in Ref. [58]. A two-meson fragmentation function can be defined by a natural

generalization of the single particle case. Using the light-cone formalism of Collins and Soper [59], the following replacement suffices,

$$|hX\rangle_{\text{out out}}\langle hX| \;\rightarrow\; |\pi^+\pi^-X\rangle_{\text{out out}}\langle\pi^+\pi^-X|. \tag{4.2}$$

The resulting two meson fragmentation function depends on the momentum fraction of each pion, z_1, z_2, the $\pi\pi$ invariant mass, m, and the angles Θ and ϕ. The subscript "out" places outgoing wave boundary conditions on the $\pi\pi X$ state. Two types of final state interactions can generate a non-trivial phase: i) those between the two pions, and ii) those between the pions and the hadronic state X. We ignore the latter because we expect the phase to average to zero when the sum on X is performed — $|\pi^+\pi^-X\rangle_{\text{out}} \rightarrow |(\pi^+\pi^-)_{\text{out}}X\rangle$. Furthermore, if the two-pion system is well approximated by a single resonance, then the resonance phase cancels in the product $|(\pi^+\pi^-)_{\text{out}}X\rangle\ \langle(\pi^+\pi^-)_{\text{out}}X|$. This leaves only the interference between two partial waves as a potential source of an asymmetry. The final state phase of the two-pion system is determined by the $\pi\pi$ $\mathcal{T}$-matrix [60]. We separate out the phase for later consideration and analyze the (real) ρ-σ interference fragmentation function as if the two particles were stable.

The s-p interference fragmentation function describes the emission of a $\rho(\sigma)$ with helicity H_1 from a quark of helicity h_2, followed by absorption of $\sigma(\rho)$, with helicity H_1' forming a quark of helicity h_2'. Conservation of angular momentum along the $\hat{e}_3$ axis requires

$$H_1 + h_2' = H_1' + h_2\ . \tag{4.3}$$

Parity and time reversal restrict the number of independent components of $\hat{\mathcal{M}}$:

$$\hat{\mathcal{M}}^{sp(ps)}_{H_1'H_1,h_2h_2'} \;=\; \hat{\mathcal{M}}^{sp(ps)}_{-H_1'-H_1,-h_2-h_2'} \quad \text{(parity)}\ , \tag{4.4}$$

$$\hat{\mathcal{M}}^{sp}_{H_1'H_1,h_2h_2'} \;=\; \hat{\mathcal{M}}^{ps}_{H_1H_1',h_2'h_2} \quad (\text{T}-\text{reversal})\ . \tag{4.5}$$

Note that Eq. (4.5) holds only after the T-reversal violating final state interaction between two pions is separated out. After these symmetry restrictions, only two

independent components remain,

$$\hat{\mathcal{M}}^{sp}_{00,++} = \hat{\mathcal{M}}^{ps}_{00,++} = \hat{\mathcal{M}}^{sp}_{00,--} = \hat{\mathcal{M}}^{ps}_{00,--} \propto \hat{q}_I \ , \tag{4.6}$$

$$\hat{\mathcal{M}}^{sp}_{01,+-} = \hat{\mathcal{M}}^{ps}_{10,-+} = \hat{\mathcal{M}}^{sp}_{0-1,-+} = \hat{\mathcal{M}}^{ps}_{-10,+-} \propto \delta\hat{q}_I \ , \tag{4.7}$$

and they can be identified with two novel interference fragmentation functions, $\hat{q}_I$, $\delta\hat{q}_I$, where the subscript I stands for interference. Here, to preserve clarity, the flavor, Q^2, and z have been suppressed. The helicity $\pm\frac{1}{2}$ states of quarks are denoted $\pm$, respectively. Hermiticity and time reversal invariance guarantee $\hat{q}_I$ and $\delta\hat{q}_I$ are real.

From Eq. (4.7) it is clear that the interference fragmentation function, $\delta\hat{q}_I$, is associated with quark helicity flip and is therefore chiral-odd. It is this feature that enables us to access the chiral-odd quark transversity distribution in DIS.

Encoding this information into a double density matrix notation, we define

$$\begin{aligned}\frac{d^2\hat{\mathcal{M}}}{dz\,dm^2} = \quad & \Delta_0(m^2)\left\{I\otimes\bar{\eta}_0\,\hat{q}_I(z) + (\sigma_+\otimes\bar{\eta}_- + \sigma_-\otimes\bar{\eta}_+)\,\delta\hat{q}_I(z)\right\}\Delta_1^*(m^2) \\ & + \Delta_1(m^2)\left\{I\otimes\eta_0\,\hat{q}_I(z) + (\sigma_-\otimes\eta_+ + \sigma_+\otimes\eta_-)\,\delta\hat{q}_I(z)\right\}\Delta_0^*(m^2)\end{aligned} \tag{4.8}$$

where $\sigma_\pm \equiv (\sigma_1 \pm i\sigma_2)/2$ with $\{\sigma_i\}$ the usual Pauli matrices. The η's are 4×4 matrices in (σ,ρ) helicity space with nonzero elements only in the first column, and the $\bar{\eta}$'s are the transpose matrices ($\bar{\eta}_0 = \eta_0^T, \bar{\eta}_+ = \eta_-^T, \bar{\eta}_- = \eta_+^T$), with the first rows $(0,0,1,0)$, $(0,0,0,1)$, and $(0,1,0,0)$ for $\bar{\eta}_0$, $\bar{\eta}_+$, and $\bar{\eta}_-$, respectively. The explicit definition of the fragmentation functions will be given in Ref. [58].

The final state interactions between the two pions are included explicitly in

$$\Delta_0(m^2) = -i\sin\delta_0 e^{i\delta_0} \ , \qquad \Delta_1(m^2) = -i\sin\delta_1 e^{i\delta_1} \ , \tag{4.9}$$

where δ_0 and δ_1 are the strong interaction $\pi\pi$ phase shifts. Here we have suppressed the m^2 dependence of the phase shifts for simplicity. The decay process, $(\sigma,\rho)\to\pi\pi$, can be easily calculated and encoded into the helicity matrix formalism. The result

for the interference part is

$$\frac{d^2\mathcal{D}}{d\cos\Theta\, d\phi} = \frac{\sqrt{6}}{8\pi^2 m}\sin\Theta\left[ie^{-i\phi}\left(\eta_- - \bar{\eta}_-\right) + ie^{i\phi}\left(\eta_+ - \bar{\eta}_+\right) - \sqrt{2}\cot\Theta\left(\bar{\eta}_0 + \eta_0\right)\right] . \tag{4.10}$$

Here we have adopted the customary conventions for the ρ polarization vectors, $\vec{\epsilon}_\pm = \mp(\hat{e}_1 \pm i\hat{e}_2)/\sqrt{2}$ and $\vec{\epsilon}_0 = \hat{e}_3$ in its rest frame with e's the unit vectors.

In the double density matrix notation, the quark distribution function $\mathcal{F}$ can be expressed as [6]

$$\mathcal{F} = \frac{1}{2}q(x)\; I\otimes I + \frac{1}{2}\Delta q(x)\;\sigma_3\otimes\sigma_3 + \frac{1}{2}\delta q(x)\;\left(\sigma_+\otimes\sigma_- + \sigma_-\otimes\sigma_+\right) , \tag{4.11}$$

where the first matrix in the direct product is in the nucleon helicity space and the second in the quark helicity space. Here q, Δq, and δq are the spin average, helicity difference, and transversity distribution functions, respectively, and their dependence on Q^2 has been suppressed.

The hard partonic process of interest here is essentially the forward virtual Compton scattering as shown in the middle of Fig. 4-1. For an *unpolarized* electron beam, the resulting cross section is [6]

$$\begin{aligned}\frac{d^2\sigma(eq\to e'q')}{dx\,dy} = \quad & \frac{e^4 e_q^2}{8\pi Q^2}\left[\frac{1+(1-y)^2}{2y}\left(I\otimes I + \sigma_3\otimes\sigma_3\right)\right. \\ & \left. + \frac{2(1-y)}{y}\left(\sigma_+\otimes\sigma_- + \sigma_-\otimes\sigma_+\right)\right] ,\end{aligned} \tag{4.12}$$

in the collinear approximation. Here e_q is the charge fraction carried by a quark. We have integrated out the azimuthal angle of the scattering plane.

Combining all the ingredients together, and integrating over Θ to eliminate the $\hat{q}_I$ dependence, we obtain the transversity dependent part of the cross section for the production of two pions (kaons) in the current fragmentation region for unpolarized

electrons incident on a transversely polarized nucleon as follows

$$\frac{d^5\sigma_\perp}{dx\,dy\,dz\,dm^2\,d\phi} = -\frac{\pi}{2}\frac{e^4}{32\pi^3 Q^2 m}\frac{1-y}{y}\sqrt{6}\cos\phi \times \sin\delta_0 \sin\delta_1 \sin(\delta_0-\delta_1)\sum_a e_a^2 \delta q_a(x)\,\delta\hat{q}_I^a(z)\ . \quad (4.13)$$

Here the sum over a covers all quark and antiquark flavors.

An asymmetry is obtained by dividing out the polarization independent cross section,

$$\mathcal{A}_{\perp\top} \equiv \frac{d\sigma_\perp - d\sigma_\top}{d\sigma_\perp + d\sigma_\top} = -\frac{\pi}{4}\frac{\sqrt{6}(1-y)}{1+(1-y)^2}\cos\phi\ \sin\delta_0\sin\delta_1\sin(\delta_0-\delta_1) \times \frac{\sum_a e_a^2\delta q_a(x)\,\delta\hat{q}_I^a(z)}{\sum_a e_a^2 q_a(x)\left[\sin^2\delta_0\hat{q}_0^a(z)+\sin^2\delta_1\hat{q}_1^a(z)\right]}\ , \quad (4.14)$$

where $\hat{q}_0$ and $\hat{q}_1$ are spin-average fragmentation functions for the σ and ρ resonances, respectively. This asymmetry can be measured either by flipping the target transverse spin or by binning events according to the sign of the crucial azimuthal angle ϕ. Note that this asymmetry only requires a transversely polarized nucleon target, but not a polarized electron beam.

The flavor content of the asymmetry $\mathcal{A}_{\perp\top}$ can be revealed by using isospin symmetry and charge conjugation restrictions. For $\pi^+\pi^-$ production, isospin symmetry gives $\delta\hat{u}_I = -\delta\hat{d}_I$ and $\delta\hat{s}_I = 0$. Charge conjugation implies $\delta\hat{q}_I^a = -\delta\hat{\bar{q}}_I^a$. Thus there is only one independent interference fragmentation function for $\pi\pi$ production, and it may be factored out of the asymmetry, $\sum_a e_a^2\delta q_a\delta\hat{q}_I^a = [4/9(\delta u-\delta\bar{u})-1/9(\delta d-\delta\bar{d})]\delta\hat{u}_I$. For the $K\overline{K}$ system, the isospin symmetry requires $\delta\hat{u}_I = \delta\hat{d}_I$, and $\delta\hat{s}_I \neq 0$, implying $\sum_a e_a^2\delta q_a\delta\hat{q}_I^a = [4/9(\delta u-\delta\bar{u})+1/9(\delta d-\delta\bar{d})]\delta\hat{u}_I + 1/9(\delta s-\delta\bar{s})\delta\hat{s}_I$. Similar application of isospin symmetry and charge conjugation to the ρ and σ fragmentation functions that appear in the denominator of Eq. (4.14) leads to a reduction in the number of independent functions: $\hat{u}_i = \hat{d}_i = \hat{\bar{u}}_i = \hat{\bar{d}}_i$ and $\hat{s}_i = \hat{\bar{s}}_i$ for $i = \{0,1\}$. We also note that application of the Schwartz inequality puts an upper bound on the interference fragmentation function, $\delta\hat{q}_I^2 \leq 4\hat{q}_0\hat{q}_1/3$ for each flavor.

Finally, a few comments can be made about our results. First, the final state phase generated by the *s-p* interference is crucial to this analysis. If the data are not kept differential in enough kinematic variables, the effect will almost certainly average to zero. We are particularly concerned about the two-meson invariant mass, m, where we can see explicitly that the interference averages to zero over the ρ as shown in Fig. 4-2. Second, the transversity distribution is multiplied by the fragmentation function $\delta\hat{q}_I$. Note that the transversity distribution *always* appears in a product of two soft QCD functions due to its chiral-odd nature. In order to disentangle the transversity distribution from the asymmetry, one may invoke the process $e^+e^- \to (\pi^+\pi^- X)(\pi^+\pi^- X)$ to measure $\delta\hat{q}_I$, or use QCD inspired models to estimate it [58].

To summarize, we have introduced twist-two interference quark fragmentation functions in helicity density matrix formalism and shown how the nucleon's transversity distribution can be probed through the final state interaction between two mesons ($\pi^+\pi^-$ or $K\overline{K}$) produced in the current fragmentation region in deep inelastic scattering on a transversely polarized nucleon. The technique developed in this chapter can also be applied to other processes. Straightforward applications include the longitudinally polarized nucleon, and $e^+e^- \to (\pi^+\pi^- X)(\pi^+\pi^- X)$. A somewhat more complicated extension can be made to two-meson production in single polarized nucleon-nucleon collisions — $p\vec{p}_\perp \to \pi^+\pi^- X$, *etc.* These applications will be presented in the following chapters.

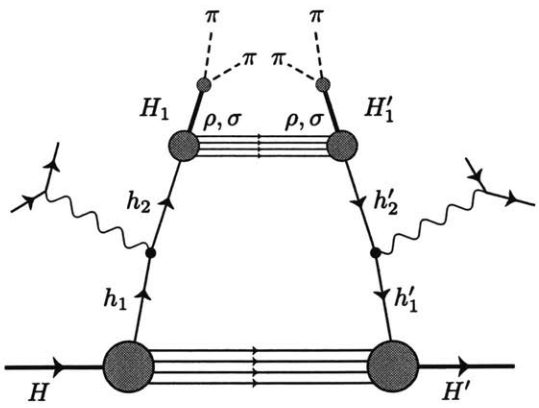

Figure 4-1: Hard scattering diagram for $\pi^+\pi^-(K\overline{K})$ production in the current fragmentation region of electron scattering from a target nucleon. In perturbative QCD the diagram (from bottom to top) factors into the products of distribution function, hard scattering, fragmentation function, and final state interaction. Helicity density matrix labels are shown explicitly.

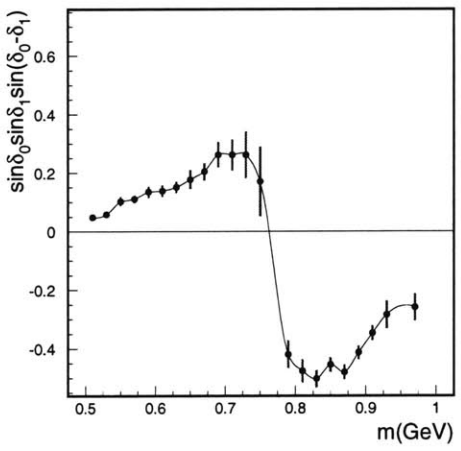

Figure 4-2: The factor, $\sin\delta_0 \sin\delta_1 \sin(\delta_0 - \delta_1)$, as a function of the invariant mass m of two-pion system. The data on $\pi\pi$ phase shifts are taken from Ref. [61].

Chapter 5

Probing the Nucleon's Transversity Via Two-Meson Production in Polarized Nucleon-Nucleon Collisions

In chapter 4, we have studied the semi-inclusive production of two mesons (*e.g.* $\pi^+\pi^-$, πK, or $K\overline{K}$) in the current fragmentation region in DIS on a transversely polarized nucleon. We have shown that the interference effect between the $s-$ and $p-$wave of the two-meson system around the ρ (for pions), K^* (for πK), or ϕ (for kaons) provides a single spin asymmetry which may be sensitive to the quark transversity distribution in the nucleon. Such interference allows the quark's polarization information to be carried through the quantity $\vec{k}_+ \times \vec{k}_- \cdot \vec{S}_\perp$, where $\vec{k}_+$, $\vec{k}_-$, and $\vec{S}_\perp$ are the three-momenta of π^+ (K), π^- ($\overline{K}$), and the nucleon's transverse spin, respectively. This effect appears at the leading twist level, and the production rates for pions and kaons are large in DIS. However, it would vanish by T-invariance in the absence of final state interactions, or by C-invariance if the two-meson state were an eigenstate of C-parity. Hence there is no effect in the regions of the two-meson mass dominated by a single resonance. However, both suppressions are evaded in the ρ ($\pi^+\pi^-$), K^*

(πK), and ϕ ($K\overline{K}$) mass regions where both $s-$ and $p-$wave production channels are active.

In this chapter, we extend our study to discuss the possibility of probing the quark transversity distribution in the nucleon via two-meson semi-inclusive production in transversely polarized nucleon-nucleon collisions. Various processes in transversely polarized nucleon-nucleon collisions have been suggested to measure the nucleon's transversity distribution since it was first introduced about two decades ago[44], among which are transversely polarized Drell-Yan [44] and two-jet production[52, 53]. However, the Drell-Yan cross section is small and requires an antiquark transversity distribution, which is likely to be quite small. The asymmetry obtained in two-jet production is rather small due to the lack of a gluon contribution[52, 53]. On the other hand, in the process described here, the gluon-quark scattering dominates and only one beam need be transversely polarized. Unless the novel interference fragmentation function is anomalously small, this will provide a feasible way to probe the nucleon's transversity distribution. The results of our analysis are summarized by Eq. (4.14) where we present the asymmetry for $\pi^+\pi^-(\pi K, K\overline{K})$ production in transversely polarized nucleon-nucleon collisions.

We consider the semi-inclusive nucleon-nucleon collision process with two-pion final states being detected: $N\vec{N}_\perp \to \pi^+\pi^- X$. (The analysis to follow applies as well to πK or $K\overline{K}$ production.) One of the nucleon beams is transversely polarized with polarization vector S_μ, and momentum P_μ^A. The other is unpolarized, with momentum denoted by P_μ^B. The experimentally observable invariant variables are defined as $s \equiv (P_A + P_B)^2$, $t \equiv (P_h - P_A)^2$, $u \equiv (P_h - P_B)^2$, and the invariants for the underlying partonic processes are $\hat{s} \equiv (p_a + p_b)^2$, $\hat{t} \equiv (p_c - p_a)^2$, $\hat{u} \equiv (p_c - p_b)^2$, where P_h is the total momentum of the two-pion system, p_a, p_b, p_c, p_d are the momenta for the underlying partonic scattering processes (see Fig. 4-1). The longitudinal momentum fractions x_a, x_b and z are given by $p_a = x_a P_A$, $p_b = x_b P_B$ and $P_h = z p_c$. The $\sigma[(\pi\pi)_{l=0}^{I=0}]$ and $\rho[(\pi\pi)_{l=1}^{I=1}]$ resonances are produced with momentum P_h. We recognize that the $\pi\pi$ s-wave is not resonant in the vicinity of the ρ and our analysis does not depend on a resonance approximation. For simplicity we refer to

the non-resonant s-wave as the "σ".

The invariant squared mass of the two-pion system is $m^2 = (k_+ + k_-)^2$, with k_+ and k_- the momentum of π^+ and π^-, respectively. The decay polar angle in the rest frame of the two-meson system is denoted by Θ, and the azimuthal angle ϕ is defined as the angle of the normal of two-pion plane with respect to the polarization vector $\vec{S}_\perp$ of the nucleon, $\cos\phi = \vec{k}_+ \times \vec{k}_- \cdot \vec{S}_\perp / |\vec{k}_+ \times \vec{k}_-||\vec{S}_\perp|$. This is the analog of the "Collins angle" defined by the $\pi^+\pi^-$ system [54].

Since we are only interested in a result at the leading twist, we follow the helicity density matrix formalism developed in Refs. [37, 6], in which all spin dependence is summarized in a *double* helicity density matrix. We factor the process at hand into basic ingredients (See Fig. 4-1): the $N \to q$ (or $N \to g$) distribution function, the hard partonic $q_a q_b \to q_c q_d$ cross section, the $q \to (\sigma, \rho)$ fragmentation, and the decay $(\sigma, \rho) \to \pi^+\pi^-$, all as density matrices in helicity basis:

$$\left[\frac{d^7\sigma(N\vec{N}_\perp \to \pi^+\pi^- X)}{dx_a\, dx_b\, d\hat{t}\, dz\, dm^2\, d\cos\Theta\, d\phi}\right]_{H'H}$$

$$= \left[\mathcal{F}(x_a) \otimes \frac{d^3\sigma(q_a q_b \to q_c q_d)}{dx_a\, dx_b\, d\hat{t}} \otimes \frac{d^2\hat{\mathcal{M}}}{dz\, dm^2} \otimes \frac{d^2\mathcal{D}}{d\cos\Theta\, d\phi} \otimes \mathcal{F}(x_b)\right]_{H'H} \quad (5.1)$$

where $H(H')$ are indices labeling the helicity states of the polarized nucleon. In order to incorporate the final state interaction, we have separated the $q \to \pi^+\pi^-$ fragmentation process into two steps. First, the quark fragments into the resonance (σ, ρ) , then the resonance decays into two pions, as shown in the middle of the Fig. 4-1.

The $s-p$ interference fragmentation functions describe the emission of a $\rho(\sigma)$ from a parton, followed by absorption of $\sigma(\rho)$ forming a parton. Imposing various symmetry (helicity, parity and time-reversal) restrictions, the interference fragmentation can be cast into a double density matrix notation[35]

$$\begin{aligned}\frac{d^2\hat{\mathcal{M}}}{dz\, dm^2} = \quad & \Delta_0(m^2)\left\{I \otimes \bar{\eta}_0\, \hat{q}_I(z) + (\sigma_+ \otimes \bar{\eta}_- + \sigma_- \otimes \bar{\eta}_+)\, \delta\hat{q}_I(z)\right\} \Delta_1^*(m^2) \\ & + \Delta_1(m^2)\left\{I \otimes \eta_0\, \hat{q}_I(z) + (\sigma_- \otimes \eta_+ + \sigma_+ \otimes \eta_-)\, \delta\hat{q}_I(z)\right\} \Delta_0^*(m^2) \quad (5.2)\end{aligned}$$

where $\sigma_\pm \equiv (\sigma_1 \pm i\sigma_2)/2$ with $\{\sigma_i\}$ the usual Pauli matrices. The η's are 4×4 matrices in (σ,ρ) helicity space with nonzero elements only in the first column, and the $\bar{\eta}$'s are the transpose matrices ($\bar{\eta}_0 = \eta_0^T, \bar{\eta}_+ = \eta_-^T, \bar{\eta}_- = \eta_+^T$), with the first rows $(0,0,1,0)$, $(0,0,0,1)$, and $(0,1,0,0)$ for $\bar{\eta}_0$, $\bar{\eta}_+$, and $\bar{\eta}_-$, respectively. The explicit definition of the fragmentation functions will be given in Ref. [62].

The final state interactions between the two pions are included explicitly in

$$\Delta_0(m^2) = -i\sin\delta_0 e^{i\delta_0} \ , \qquad \Delta_1(m^2) = -i\sin\delta_1 e^{i\delta_1} \ , \tag{5.3}$$

where δ_0 and δ_1 are the strong interaction $\pi\pi$ phase shifts which can be determined by the $\pi\pi$ $\mathcal{T}$-matrix [60]. Here we have suppressed the m^2 dependence of the phase shifts for simplicity.

The decay process, $(\sigma,\rho) \to \pi^+\pi^-$, can be easily calculated and encoded into the helicity matrix formalism. The result for the interference part is [35]

$$\frac{d^2\mathcal{D}}{d\cos\Theta\, d\phi} = \frac{\sqrt{6}}{8\pi^2 m}\sin\Theta\left[ie^{-i\phi}(\eta_- - \bar{\eta}_-) + ie^{i\phi}(\eta_+ - \bar{\eta}_+) - \sqrt{2}\cot\Theta\,(\bar{\eta}_0 + \eta_0)\right] . \tag{5.4}$$

Here we have adopted the customary conventions for the ρ polarization vectors, $\vec{\epsilon}_\pm = \mp(\hat{e}_1 \pm i\hat{e}_2)/\sqrt{2}$ and $\vec{\epsilon}_0 = \hat{e}_3$ in its rest frame with $\hat{e}_j$'s the unit vectors.

In the double density matrix notation, the quark distribution function $\mathcal{F}_q(x)$ in the nucleon can be expressed as [6]

$$\mathcal{F}_q(x) = \frac{1}{2}q(x)\ I\otimes I + \frac{1}{2}\Delta q(x)\ \sigma_3\otimes\sigma_3 + \frac{1}{2}\delta q(x)\ (\sigma_+\otimes\sigma_- + \sigma_-\otimes\sigma_+) \ , \tag{5.5}$$

where the first matrix in the direct product is in the nucleon helicity space and the second in the quark helicity space. Here $q(x)$, $\Delta q(x)$, and $\delta q(x)$ are the spin average, helicity difference, and transversity distribution functions, respectively, and their dependences on Q^2 have been suppressed.

The gluon distribution function $\mathcal{F}_g(x)$ in the nucleon can be written as

$$\mathcal{F}_g(x) = \frac{1}{3}G(x)\ I\otimes I_g + \frac{1}{2}\Delta G(x)\ \sigma_3\otimes S_g^3 \ , \tag{5.6}$$

where I_g and S_g^3 are 3×3 matrices in gluon helicity space with nonzero elements only on the diagonal: diag(I_g)=$\{1,1,1\}$ and diag(S_g^3)=$\{1,0,-1\}$. Here $G(x)$ and $\Delta G(x)$ are the spin average and helicity difference gluon distributions in the nucleon, respectively, and, just like in Eq. (5.5), their dependences on Q^2 have been suppressed. Note that there is no gluon transversity distribution $\delta G(x)$ in the nucleon at the leading twist due to helicity conservation. This is one of the reasons why transverse asymmetries in two-jet production are typically small, as pointed out by Ji[52], Jaffe and Saito[53].

Several hard partonic processes contribute here, as shown in the middle of Fig. 5-1. The cross sections can be written as follows (here we list only the relevant parts, i.e. spin-average and transversity-dependent ones),

$$\frac{d^3\sigma(q_a q_b \to q_c q_d)}{dx_a\, dx_b d\hat{t}} = \frac{\pi\alpha_s^2}{2\hat{s}^2} I_b \otimes \left[\hat{\bar{\sigma}}_{ab}^{cd} I_a \otimes I_c + 4\delta\hat{\sigma}_{ab}^{cd}\left(\sigma_a^+ \otimes \sigma_c^- + \sigma_c^- \otimes \sigma_a^+\right)\right] , \quad (5.7)$$

where subscripts a, b, c means that the helicity matrices above are in a, b, c parton helicity spaces, respectively (See Fig. 5-1). $\hat{\bar{\sigma}}_{ab}^{cd}$ and $\delta\hat{\sigma}_{ab}^{cd}$ are the spin-average and transversity-dependent cross sections for the underlying partonic processes $q_a q_b \to q_c q_d$, respectively, which are shown in the Table I.

Combining all the above ingredients together, and integrating over Θ to eliminate the $\hat{q}_I$ dependence, we obtain a single spin asymmetry as follows,

$$\begin{aligned} \mathcal{A}_{\perp\top} \equiv \frac{d\sigma_\perp - d\sigma_\top}{d\sigma_\perp + d\sigma_\top} = -\frac{\sqrt{6}\pi}{4} \sin\delta_0 \sin\delta_1 \sin(\delta_0 - \delta_1) \cos\phi \otimes \\ \frac{[\delta q(x_a) \otimes G(x_b) \otimes \delta\hat{q}_I(z)]\delta\hat{\sigma}_{qg}^{qg} + [\delta\bar{q}(x_a) \otimes G(x_b) \otimes \delta\hat{\bar{q}}_I(z)]\delta\hat{\sigma}_{\bar{q}g}^{\bar{q}g} + \ldots}{\{[G(x_a) \otimes G(x_b)]\hat{\bar{\sigma}}_{gg}^{q\bar{q}} + [q(x_a) \otimes G(x_b)]\hat{\bar{\sigma}}_{qg}^{qg} + \ldots\} \otimes [\sin^2\delta_0 \hat{q}_0(z) + \sin^2\delta_1 \hat{q}_1(z)]} \end{aligned} \quad (5.8)$$

where $\hat{q}_0(z)$ and $\hat{q}_1(z)$ are spin-average fragmentation functions for the σ and ρ resonances, respectively, and the summation over flavor is suppressed for simplicity. The terms denoted by ... include quark quark and quark antiquark scattering contributions. This asymmetry can be measured either by flipping the target transverse spin

or by binning events according to the sign of the crucial azimuthal angle ϕ (See Fig. 5-2). The "figure of merit" for this asymmetry, $\sin\delta_0 \sin\delta_1 \sin(\delta_0 - \delta_1)$, is shown in Fig. 5-3.

The flavor content of the asymmetry $\mathcal{A}_{\perp\top}$ can be revealed by using isospin symmetry and charge conjugation restrictions. For $\pi^+\pi^-$ production, isospin symmetry gives $\delta\hat{u}_I = -\delta\hat{d}_I$ and $\delta\hat{s}_I = 0$. Charge conjugation implies $\delta\hat{q}^a_I = -\delta\hat{\bar{q}}^a_I$. Thus there is only one independent interference fragmentation function for $\pi^+\pi^-$ production, and it may be factored out of the asymmetry, e.g. $\sum_a \delta q_a \delta\hat{q}^a_I = [(\delta u - \delta\bar{u}) - (\delta d - \delta\bar{d})]\delta\hat{u}_I$. Similar application of isospin symmetry and charge conjugation to the ρ and σ fragmentation functions that appear in the denominator of Eq. (5.8) leads to a reduction in the number of independent functions: $\hat{u}_i = \hat{d}_i = \hat{\bar{u}}_i = \hat{\bar{d}}_i$ and $\hat{s}_i = \hat{\bar{s}}_i$ for $i = \{0, 1\}$. For other systems the situation is more complicated due to the relaxation of the Bose symmetry restriction. For example, for the $K\overline{K}$ system, $\delta\hat{q}^a_I = -\delta\hat{\bar{q}}^a_I$ still holds, but $\delta\hat{u}_I$, $\delta\hat{d}_I$, and $\delta\hat{s}_I$, are in general independent. We also note that application of the Schwartz inequality puts an upper bound on the interference fragmentation function, $\delta\hat{q}^2_I \leq 4\hat{q}_0\hat{q}_1/3$ for each flavor.

The size of the asymmetry $\mathcal{A}_{\perp\top}$ critically depends upon the ratio of the $s-p$ interference fragmentation function and ρ and σ fragmentation functions, which is unknown at present. In order to estimate the magnitude of $\mathcal{A}_{\perp\top}$, we saturate the Schwartz inequality and replace the interference fragmentation with its upper bound, i.e. $\delta\hat{q}^2_I = 4\hat{q}_0\hat{q}_1/3$ for each flavor. Meanwhile, we assume the σ and ρ fragmentation functions are equal to each other. Thus, the fragmentation function dependences cancel out in $\mathcal{A}_{\perp\top}$. We also assume that the transversity $\delta q(x, Q^2)$ saturates the Soffer inequality[49]: $2|\delta q(x, Q^2)| = q(x, Q^2) + \Delta q(x, Q^2)$. We use the polarized structure functions obtained by Gehrmann and Stirling through next-to-leading order analysis of experimental data[63]. We also go to the region $m = 0.83$GeV, around which the phase factor $|\sin\delta_0 \sin\delta_1 \sin(\delta_0 - \delta_1)|$ is large (See Fig. 5-3), and let $\cos\phi = 1$. The asymmetry as function of p_T^{jet} at $\sqrt{s} = 500$GeV and $\sqrt{s} = 200$GeV for pseudo-rapidity $\eta = 0.0$ and $\eta = 0.35$ is shown in Fig. 5-4, where p_T^{jet} is the transverse momentum of the jet. The size of asymmetry is about $12 - 15\%$ at $p_T^{\text{jet}} = 120$GeV for $\sqrt{s} = 500$GeV

and about $17 - 20\%$ at $p_T^{\text{jet}} = 90\text{GeV}$ for $\sqrt{s} = 200\text{GeV}$, which would be measurable at RHIC.

A few comments can be made about our numerical results. Firstly, under the above approximations, the asymmetry is independent of z. Of course, the experiment may not be able to determine p_T^{jet} — the transverse momentum of the jet, so direct comparison between our asymmetry and experimental data will require event simulation. Secondly, because we don't know the sign of the unknown quantities yet, we can not determine the sign of the asymmetry, the asymmetry shown in Fig. 5-4 should only be taken as its magnitude. Finally, in order to estimate the asymmetry, we have made very optimistic assumptions about the novel interference fragmentation functions and transversity distribution functions, so our estimates here should be regarded as "the high side".

To summarize, we have studied the possibility of probing the quark transversity distribution in the nucleon via two-meson semi-inclusive production of (only one beam) transversely polarized nucleon-nucleon collisions. We obtained a single spin asymmetry that is sensitive to the quark transversity and estimated its magnitude.

Partonic process $ab \to cd$	Spin Average Cross Section$-\hat{\bar{\sigma}}_{ab}^{cd}$	Transversity Dependent Cross Section$-\delta\hat{\sigma}_{ab}^{cd}$
$qg \to qg$	$\frac{\hat{s}^2+\hat{u}^2}{\hat{t}^2} - \frac{4}{9}\frac{\hat{s}^2+\hat{u}^2}{\hat{s}\hat{u}}$	$\frac{\hat{s}\hat{u}}{\hat{t}^2} - \frac{4}{9}$
$\bar{q}g \to \bar{q}g$	$\frac{\hat{s}^2+\hat{u}^2}{\hat{t}^2} - \frac{4}{9}\frac{\hat{s}^2+\hat{u}^2}{\hat{s}\hat{u}}$	$\frac{\hat{s}\hat{u}}{\hat{t}^2} - \frac{4}{9}$
$qq \to qq$	$\frac{4}{9}\left(\frac{\hat{s}^2+\hat{u}^2}{\hat{t}^2} + \frac{\hat{s}^2+\hat{t}^2}{\hat{u}^2}\right) - \frac{8}{27}\frac{\hat{s}^2}{\hat{u}\hat{t}}$	$\frac{4}{27}\frac{\hat{s}}{\hat{t}} - \frac{4}{9}\frac{\hat{s}\hat{u}}{\hat{t}^2}$
$qq' \to qq'$	$\frac{4}{9}\frac{\hat{s}^2+\hat{u}^2}{\hat{t}^2}$	$-\frac{4}{9}\frac{\hat{s}\hat{u}}{\hat{t}^2}$
$q\bar{q} \to q\bar{q}$	$\frac{4}{9}\left(\frac{\hat{s}^2+\hat{u}^2}{\hat{t}^2} + \frac{\hat{u}^2+\hat{t}^2}{\hat{s}^2}\right) - \frac{8}{27}\frac{\hat{u}^2}{\hat{s}\hat{t}}$	$\frac{8}{27}\frac{\hat{u}}{\hat{t}} - \frac{4}{9}\frac{\hat{s}\hat{u}}{\hat{t}^2}$
$q\bar{q}' \to q\bar{q}'$	$\frac{4}{9}\frac{\hat{s}^2+\hat{u}^2}{\hat{t}^2}$	$-\frac{4}{9}\frac{\hat{s}\hat{u}}{\hat{t}^2}$
$gg \to q\bar{q}$	$\frac{1}{6}\frac{\hat{t}^2+\hat{u}^2}{\hat{t}\hat{u}} - \frac{3}{8}\frac{\hat{t}^2+\hat{u}^2}{\hat{s}^2}$	$- - -$

Table 5.1: Partonic cross sections for $q_a q_b \to q_c q_d$ (only spin-average and transversity-dependent parts are shown here).

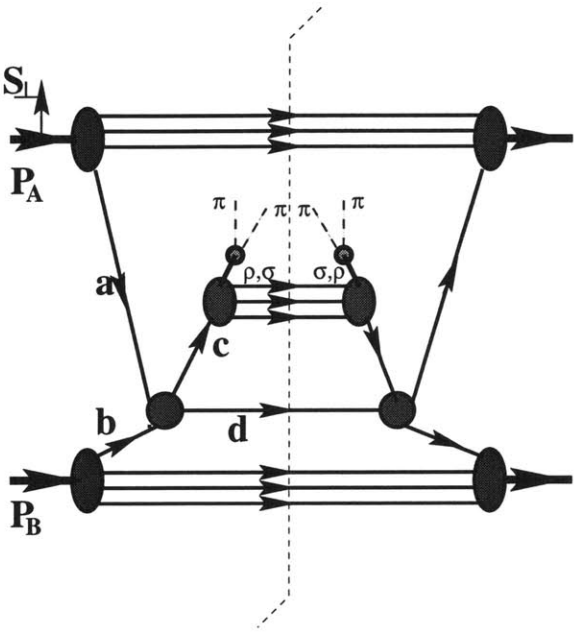

Figure 5-1: Hard scattering diagram for two-meson semi-inclusive production in nucleon-nucleon collision.

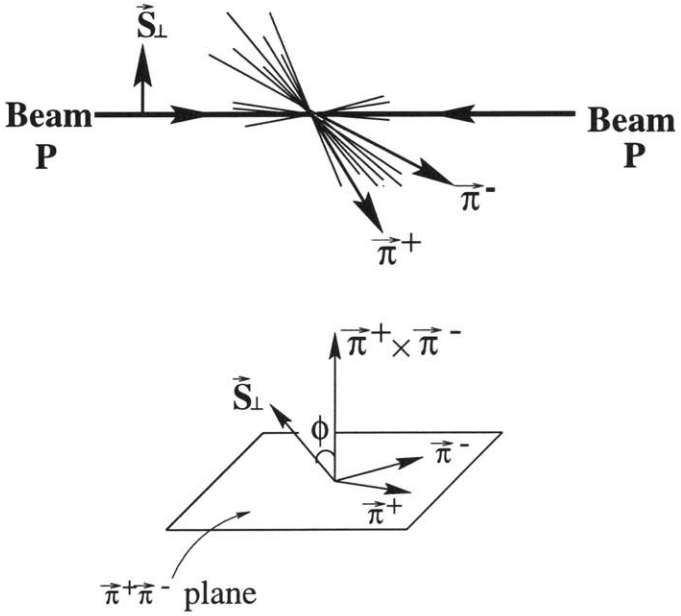

Figure 5-2: Illustration of the *pp* collision at the center-of-mass frame and the so-called "Collins angle" ϕ.

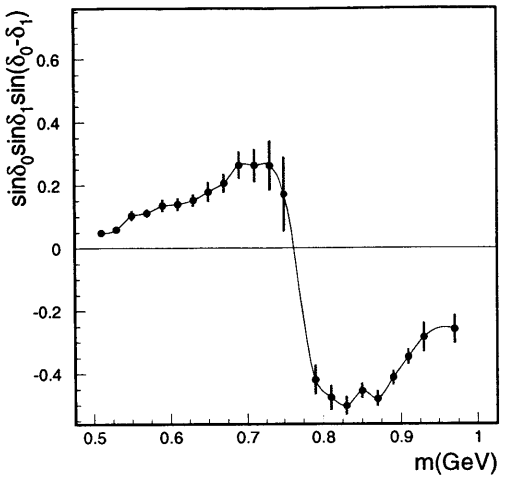

Figure 5-3: The factor, $\sin\delta_0 \sin\delta_1 \sin(\delta_0 - \delta_1)$, as a function of the invariant mass m of two-pion system. The data on $\pi\pi$ phase shifts are taken from Ref. [61].

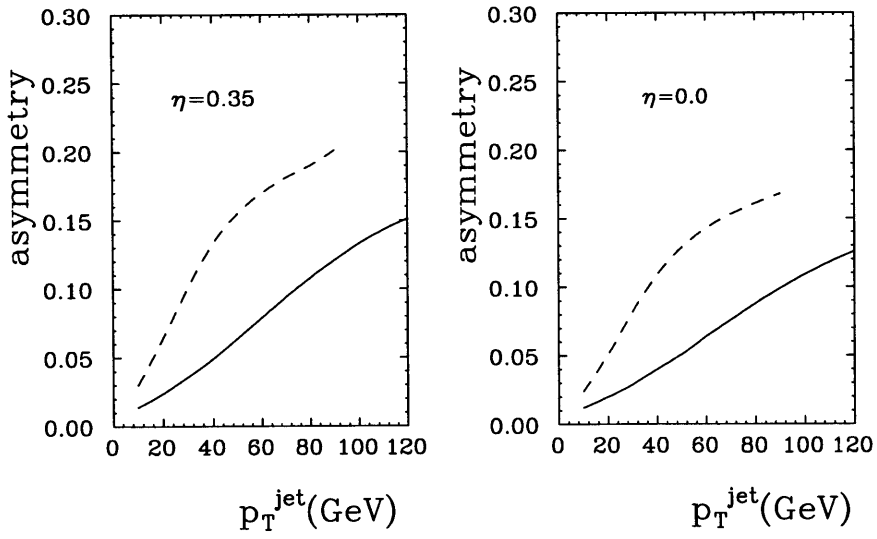

Figure 5-4: The single spin symmetry as function of p_T^{jet} for two-pion production in pp collision at $\sqrt{s}$ =500 GeV(solid) and $\sqrt{s}$ =200 GeV(dashes) (pseudo-rapidity $\eta = 0.0$ and $\eta = 0.35$).

Chapter 6

Interference Fragmentation Functions and Valence Quark Spin Distributions in the Nucleon

In this chapter, we extend our study on the interference fragmentation functions to the case of a longitudinally polarized electron beam scattering off a longitudinally polarized nucleon target. We show that the interference between the s- and p-wave of the two-pion system around the ρ can provide an asymmetry [Eq. (4.14)] which is sensitive to the valence quark spin distribution in the nucleon. Note that the asymmetry would vanish by C-invariance if the two pions were in a charge conjugation eigenstate. Hence there is no effect in regions of the $\pi\pi$ mass dominated by a single resonance. Significant effects are possible, however, in the ρ mass region where the s- and p-wave production channels are both active and provide exactly the charge conjugation mixing necessary.

The asymmetry we obtain throws pions of one charge forward along the fragmentation axis relative to pions of the other charge. If one integrated over the other kinematic variables, whatever result persisted would appear as a difference between the π^+ and π^- fragmentation functions correlated with the valence quark spin distributions. This effect in single pion fragmentation was proposed and studied some years ago by Frankfurt *et al.* [65] and Close and Milner [66]. The asymmetry we

describe is therefore one particular contribution to this more general effect, with the advantage that it can be characterized in terms of $\pi\pi$ phase shifts and two particle fragmentation functions that appear in other hard processes.

Consider the semi-inclusive deep inelastic scattering process: $\vec{e}\vec{N} \to e'\pi^+\pi^- X$. We define the kinematics as follows. The four-momenta of the initial and final electron are $k = (E, \vec{k})$ and $k' = (E', \vec{k}')$, and the nucleon's momentum is P_μ. The momentum of the virtual photon is $q = k - k'$, and $Q^2 = -q^2 = -4EE' \sin^2 \theta/2$, where θ is the electron scattering angle. The standard variables in DIS, $x = Q^2/2P \cdot q$ and $y = P \cdot q/P \cdot k$, are adopted. We work at low $\pi\pi$ invariant mass, where only the s- and p-waves are significant. The $\sigma[(\pi\pi)^{I=0}_{l=0}]$ and $\rho[(\pi\pi)^{I=1}_{l=1}]$ resonances are produced in the current fragmentation region with momentum P_h and momentum fraction $z = P_h \cdot q/q^2$.[1] The invariant squared mass of the two-pion system is $m^2 = (k_+ + k_-)^2$, with k_+ and k_- the four-momentum of π^+ and π^-, respectively. The decay polar angle in the rest frame of the two-pion system is denoted by Θ. Note that the azimuthal angle ϕ of the two-pion system does not figure in present analysis and can be integrated out.

Following Ref. [35], we use a collinear approximation, *i.e.*, $\theta \approx 0$ for simplicity, and work only to the leading twist (the complete analysis will be published elsewhere[58]). Invoking the helicity density matrix formalism developed in Refs. [37, 6], we factor the process into various basic ingredients expressed as helicity density matrices:

$$\left[\frac{d^5\sigma}{dx\,dy\,dz\,dm^2\,d\cos\Theta}\right]_{H'H} = \mathcal{F}^{h_1 h_1'}_{H'H}\left[\frac{d^2\sigma(eq \to e'q')}{dx\,dy}\right]^{h_2 h_2'}_{h_1' h_1}\left[\frac{d^2\hat{\mathcal{M}}}{dz\,dm^2}\right]^{H_1 H_1'}_{h_2' h_2}\left[\frac{d\mathcal{D}}{d\cos\Theta}\right]_{H_1' H_1}, \quad (6.1)$$

where $h_i(h_i')$ and $H(H')$ are indices labeling the helicity states of quark and nucleon, and $H_1(H_1')$ labeling the helicity state of the resonance (σ, ρ). Physically, the four

[1] We recognize that the $\pi\pi$ s-wave is not resonant in the vicinity of the ρ and our analysis does not depend on a resonance approximation. For simplicity we refer to the non-resonant s-wave as the "σ".

factors on the right-hand side of Eq. (6.1) represent the $N \to q$ distribution function, the hard partonic $eq \to e'q'$ cross section, the $q \to (\sigma, \rho)$ fragmentation, and the decay $(\sigma, \rho) \to \pi\pi$, respectively. In order to incorporate the final state interaction, we have separated the $q \to \pi^+\pi^-$ fragmentation process into two steps. First, the quark fragments into the resonance (σ, ρ), then the resonance decays into two pions (see Figure 1 of Ref. [35]).

The *s-p* interference fragmentation function describes the emission of a $\rho(\sigma)$ with helicity H_1 from a quark of helicity h_2, followed by absorption of $\sigma(\rho)$, with helicity H_1' forming a quark of helicity h_2'. Imposing various symmetry restrictions, the interference fragmentation can be cast into a double density matrix [35]

$$\begin{aligned}\frac{d^2\hat{\mathcal{M}}}{dz\,dm^2} &= \Delta_0(m^2)\left\{I \otimes \bar{\eta}_0\,\hat{q}_I(z,m^2) + (\sigma_+ \otimes \bar{\eta}_- + \sigma_- \otimes \bar{\eta}_+)\,\delta\hat{q}_I(z,m^2)\right\}\Delta_1^*(m^2) \\ &\quad +\Delta_1(m^2)\left\{I \otimes \eta_0\,\hat{q}_I(z,m^2) + (\sigma_- \otimes \eta_+ + \sigma_+ \otimes \eta_-)\,\delta\hat{q}_I(z,m^2)\right\}\Delta_0^*(m^2)\ ,\end{aligned} \tag{6.2}$$

where $\sigma_\pm \equiv (\sigma_1 \pm i\sigma_2)/2$ with $\{\sigma_i\}$ the usual Pauli matrices. The η's are 4×4 matrices in (σ, ρ) helicity space with nonzero elements only in the first column, and the $\bar{\eta}$'s are the transpose matrices ($\bar{\eta}_0 = \eta_0^T, \bar{\eta}_+ = \eta_-^T, \bar{\eta}_- = \eta_+^T$), with the first rows $(0,0,1,0)$, $(0,0,0,1)$, and $(0,1,0,0)$ for $\bar{\eta}_0$, $\bar{\eta}_+$, and $\bar{\eta}_-$, respectively. The final state interactions between the two pions are included explicitly in $\Delta_0(m^2) = -i\sin\delta_0 e^{i\delta_0}$ and $\Delta_1(m^2) = -i\sin\delta_1 e^{i\delta_1}$, with δ_0 and δ_1 the strong interaction $\pi\pi$ phase shifts. Here we have suppressed the m^2 dependence of the phase shifts. Note that $\hat{q}_I$ and $\delta\hat{q}_I$ depend on both m^2 and z. We expect that the principal m^2 dependence will enter through the final state factors Δ_0 and Δ_1. To preserve clarity, the Q^2 dependence of the fragmentation functions has been suppressed. Henceforth we suppress the m^2 dependence as well.

The decay density matrix, quark distribution function, and hard scattering cross section have been given explicitly in Ref. [35]. For completeness we quote the results relevant to the present analysis. The interference part of the decay density matrix

(after integration over the azimuthal angle ϕ) is

$$\frac{d\mathcal{D}}{d\cos\Theta} = -\frac{\sqrt{3}}{2\pi m}\cos\Theta\,(\bar{\eta}_0 + \eta_0)\ . \tag{6.3}$$

The quark distribution function $\mathcal{F}$ is expressed as [6]

$$\mathcal{F} = \frac{1}{2}q(x)\ I\otimes I + \frac{1}{2}\Delta q(x)\ \sigma_3\otimes\sigma_3 + \frac{1}{2}\delta q(x)\ (\sigma_+\otimes\sigma_- + \sigma_-\otimes\sigma_+)\ , \tag{6.4}$$

where the first matrix in the direct product is in the nucleon helicity space and the second in the quark helicity space. Here $q(x)$, $\Delta q(x)$, and $\delta q(x)$ are the spin average, spin, and transversity distribution functions, respectively, and their dependence on Q^2 has been suppressed. Finally, for a longitudinally polarized electron beam, the hard scattering cross section is given by [6]

$$\begin{aligned}\frac{d^2\sigma_\pm(eq\to e'q')}{dx\,dy} &= \frac{e^4e_q^2}{8\pi Q^2}\Bigg[\frac{1+(1-y)^2}{2y}\,(I\otimes I+\sigma_3\otimes\sigma_3)\\ &\quad +\frac{2(1-y)}{y}\,(\sigma_+\otimes\sigma_- + \sigma_-\otimes\sigma_+) \pm \frac{2-y}{2}\,(\sigma_3\otimes I + I\otimes\sigma_3)\Bigg]\ ,\end{aligned} \tag{6.5}$$

in the collinear approximation, where the $\pm$ sign refers to the initial electron helicity. Here e_q is the charge fraction carried by a quark, and we have integrated out the azimuthal angle of the scattering plane.

The cross section can be obtained by putting all the ingredients together. To facilitate our discussions, we define forward and backward cross sections, $d\sigma^{\rm F}$ and $d\sigma^{\rm B}$, where the Θ dependence has been integrated over the forward ($0 \le \Theta \le \pi/2$) and backward ($\pi/2 \le \Theta \le \pi$) hemisphere in the two-pion rest frame, respectively. For a longitudinally polarized nucleon target with a longitudinally polarized electron

beam, we then obtain the following double asymmetry

$$\begin{aligned}
\mathcal{A}_{\Uparrow\Downarrow}^{\mathrm{FB}} &\equiv \frac{\left(d\sigma_{\uparrow\Uparrow}^{\mathrm{F}} - d\sigma_{\uparrow\Uparrow}^{\mathrm{B}}\right) - \left(d\sigma_{\uparrow\Downarrow}^{\mathrm{F}} - d\sigma_{\uparrow\Downarrow}^{\mathrm{B}}\right)}{\left(d\sigma_{\uparrow\Uparrow}^{\mathrm{F}} + d\sigma_{\uparrow\Uparrow}^{\mathrm{B}}\right) + \left(d\sigma_{\uparrow\Downarrow}^{\mathrm{F}} + d\sigma_{\uparrow\Downarrow}^{\mathrm{B}}\right)} \\
&= -\frac{\sqrt{3}\, y(2-y)}{1+(1-y)^2}\, \sin\delta_0 \sin\delta_1 \cos\left(\delta_0 - \delta_1\right) \\
&\quad \times \frac{\sum_a e_a^2 \Delta q_a(x)\, \hat{q}_I^a(z)}{\sum_a e_a^2 q_a(x) \left[\sin^2\delta_0 \hat{q}_0^a(z) + \sin^2\delta_1 \hat{q}_1^a(z)\right]}\,, \qquad (6.6)
\end{aligned}$$

where $\hat{q}_0$ and $\hat{q}_1$ are spin-average fragmentation functions for the σ and ρ resonances, respectively. The arrows $\Uparrow$ and $\Downarrow$ ($\uparrow$ and $\downarrow$) indicate the nucleon's (electron's) polarization along and opposite to the beam direction. Note that in Eq. (6.6) the electron's polarization is fixed and the asymmetry requires flipping the nucleon's polarization. This result also holds when the electron and nucleon polarizations are exchanged.

The flavor structure of the asymmetry $\mathcal{A}_{\Uparrow\Downarrow}^{\mathrm{FB}}$ is quite simple. Isospin symmetry gives $\hat{u}_I = -\hat{d}_I$ and $\hat{s}_I = 0$, and charge conjugation requires $\hat{q}_I^a = -\hat{\bar{q}}_I^a$. This implies $\sum_a e_a^2\, \Delta q_a\, \hat{q}_I^a = [4/9\, \Delta u_v - 1/9\, \Delta d_v]\, \hat{u}_I$, where $\Delta q_v \equiv \Delta q - \Delta\bar{q}$. Therefore $\mathcal{A}_{\Uparrow\Downarrow}^{\mathrm{FB}}$ is sensitive to the valence quark spin distribution. Note that the interference between the two partial waves makes the interference fragmentation function $\hat{q}_I^a(z)$ charge conjugation odd and accesses the valence quark spin distribution. The role of final state interactions is quite different here than in Ref. [35]. Here the effect persists as long as two partial waves of opposite C-parity are active, whether or not they are out of phase. This is evidenced in Eq. (6.6) by the factor $\cos(\delta_0 - \delta_1)$. Note that if either δ_0 or δ_1 goes to zero and thus only one partial wave is active, the asymmetry vanishes as required by charge conjugation. In Fig. 6-1 we have plotted the factor, $\sin\delta_0 \sin\delta_1 \cos(\delta_0 - \delta_1)$, as a function of the two-pion invariant mass m. It is positive over the ρ region and hence the effect does not average to zero over this region. This differs from the case of the transversity asymmetry derived in Ref. [35], where the interference averages to zero over the ρ region due to a factor $\sin(\delta_0 - \delta_1)$. We also see from Fig. 6-1 that the interference peaks near the ρ mass, indicating that an optimal signal would be in the vicinity of $m \sim m_\rho$. It is unclear at this stage whether the

effect would survive averaging over the z dependence of the interference fragmentation function.

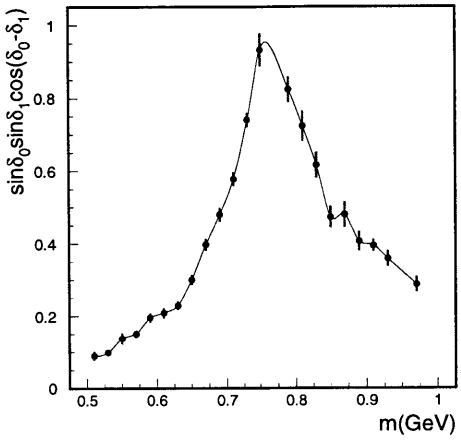

Figure 6-1: The factor, $\sin\delta_0 \sin\delta_1 \cos(\delta_0 - \delta_1)$, as a function of the invariant mass m of two-pion system. The data on $\pi\pi$ phase shifts are taken from Ref. [61].

A similar forward-backward asymmetry appears in the unpolarized process

$$\mathcal{A}^{\rm FB} \equiv \frac{d\sigma^{\rm F} - d\sigma^{\rm B}}{d\sigma^{\rm F} + d\sigma^{\rm B}} = -\sqrt{3}\ \sin\delta_0 \sin\delta_1 \cos\left(\delta_0 - \delta_1\right) \times \frac{\sum_a e_a^2 q_a(x)\, \hat{q}_I^a(z)}{\sum_a e_a^2 q_a(x) \left[\sin^2\delta_0 \hat{q}_0^a(z) + \sin^2\delta_1 \hat{q}_1^a(z)\right]} \,. \qquad (6.7)$$

Isospin symmetry and charge conjugation again dictate that $\sum_a e_a^2\, q_a\, \hat{q}_I^a = [4/9\, u_v - 1/9\, d_v]\, \hat{u}_I$ for $\pi^+\pi^-$ system, where $q_v \equiv q - \bar{q}$. Given that the valence quark distributions u_v and d_v are known experimentally, this asymmetry can be used to determine the interference fragmentation function $\hat{q}_I^a(z)$ and hence isolate the valence quark spin distribution from $\mathcal{A}_{\Uparrow\Downarrow}^{\rm FB}$. This point becomes more transparent when $\mathcal{A}_{\Uparrow\Downarrow}^{\rm FB}$ is combined with $\mathcal{A}^{\rm FB}$. In this case, one can find an asymmetry *independent* of the interference

fragmentation functions:

$$\frac{\left(d\sigma^{\rm F}_{\uparrow\Uparrow} - d\sigma^{\rm B}_{\uparrow\Uparrow}\right) - \left(d\sigma^{\rm F}_{\uparrow\Downarrow} - d\sigma^{\rm B}_{\uparrow\Downarrow}\right)}{\left(d\sigma^{\rm F}_{\uparrow\Uparrow} - d\sigma^{\rm B}_{\uparrow\Uparrow}\right) + \left(d\sigma^{\rm F}_{\uparrow\Downarrow} - d\sigma^{\rm B}_{\uparrow\Downarrow}\right)} = \frac{y(2-y)}{1+(1-y)^2}\ \frac{4\Delta u_v - \Delta d_v}{4u_v - d_v}\ . \qquad (6.8)$$

So, one may use $\pi^+\pi^-$ production on both nucleon and deuteron targets to measure Δu_v and Δd_v. Although the results in Eq. (6.8) are independent of z, one should keep the cross section differential in z to avoid possibly washing out the effect.

Refs. [65, 66] explain how to use single meson (pion or kaon) production in deep inelastic scattering to measure the valence quark spin distribution in the nucleon. It is clear from Eq. (6.8) that our asymmetry is a particular contribution to the ones described in Refs. [65, 66]. Ours is perhaps more under control since it is differential in m^2 and expressed in terms of $\pi\pi$ phase shifts. The single particle asymmetry makes use of a larger data set. These independent ways of measuring the valence quark spin distributions should both be pursued. In addition, the asymmetries we have studied are sensitive to two particle interference fragmentation functions which may be interesting quantities in their own right. These measurements may be carried out in facilities such as HERMES at HERA and COMPASS at CERN, both of which have sensitivity to the hadronic final state in electron scattering.

To summarize, we have discussed the applications of the twist-two interference quark fragmentation functions introduced previously to the case of longitudinally polarized electron beam and longitudinally polarized nucleon target. We obtain two asymmetries: one provides a probe of the valence quark spin distribution, and the other can be used to extract the interference fragmentation functions.

Chapter 7

Conclusions

In this thesis, we have developed a new formalism to deal with the polarized processes in quantum chromodynamics(QCD)—Helicity Density Matrix Formalism. We applied it to propose new ways to measure nucleon's transversity, one of the least known quark distributions inside the nucleon. The processes of interest are the two pion semi-inclusive productions in the transversely polarized deep inelastic scattering(DIS) and nucleon nucleon collisions. A set of novel quark interference fragmentation functions are introduced in the framework of the helicity density matrix formalism and used to probe the nucleon's transversity distributions. The single spin asymmetry obtained in the transversely polarized PP collision is estimated to be about 10% under assumptions for the unknown interference fragmentation and transversity distribution, which would be accessible at RHIC energy scale($\sqrt{s} = 500\text{GeV}$). It is also used to probe the valence quark distribution inside the nucleon. The advantages of this method over others are that the effect is leading twist, hence there is no $1/Q$ suppression; the meson pairs are copiously produced in the quark fragmentation; the final state interaction phase can be measured in meson-meson scattering; the final state interaction phase remains fixed even after the summation on the X states is performed; it can be performed in different experiments, e.g. RHIC, HERMES or COMPASS.

.1 Notations and Conventions

.1.1 Natural Units

As generally used in elementary particle physics, we use the natural units in this thesis. The natural unit is such a system in which we write

$$c = \hbar = 1 \ , \tag{1}$$

where c is the speed of the light, $\hbar$ is the Planck's constant.

Since $[c]$ = distance/time and $[\hbar] \sim$ enegy $\cdot$ time, there is only one single arbitrary unit remaining, which is usually chosen to be the unit of energy in elementary particle physics. The frequently used unit of energy are KeV $= 10^3$eV, MeV $= 10^3$KeV, GeV $= 10^3$MeV . Other units such as length and time can be translated to energy by the experimental values of some physical constants[41]

$$\begin{aligned} c &= 299792458 \quad \text{m s}^{-1} \\ \hbar &= 6.5821220(20) \times 10^{-22} \quad \text{MeV s} \\ \hbar c &= 197.327053(59) \quad \text{MeV fm} \ . \end{aligned} \tag{2}$$

.1.2 Metric

The metric tensor $g_{\mu\nu}$ is defined by

$$g_{\mu\nu} = g^{\mu\nu} = \begin{pmatrix} 1 & 0 & 0 & 0 \\ 0 & -1 & 0 & 0 \\ 0 & 0 & -1 & 0 \\ 0 & 0 & 0 & -1 \end{pmatrix} \ . \tag{3}$$

Note that in this thesis the Greek letters represent the Lorentz indices(from 0 to 3), while the Latin letters represent the space indices(from 1 to 3).

A contravariant four-vector is denoted by

$$V^{\mu} = (V^0, V^1, V^2, V^3) \ , \tag{4}$$

which can be transformed into a covariant vector using the metric tensor $g_{\mu\nu}$ as follows

$$V_{\mu\nu} \equiv (V_0, V_1, V_2, V_3) = g_{\mu\nu} V^{\nu} = (V^0, -V^1, -V^2, -V^3) \ . \tag{5}$$

Summation over repeated Lorentz indices is assumed unless explicitly stated,

$$V^{\mu} W_{\mu} = V_{\mu} W^{\mu} = g_{\mu\nu} V^{\mu} W^{\nu} = g^{\mu\nu} V_{\mu} V_{\nu} = V^0 W^0 - V^1 W^1 - V^2 W^2 - V^3 W^3 \ . \tag{6}$$

A boldface letter denotes a three-vector,

$$\mathbf{V} = (V^1, V^2, V^3) = (V_x, V_y, V_z) \ . \tag{7}$$

The gradient operator is defined by

$$\begin{aligned} \partial_{\mu} &\equiv \frac{\partial}{\partial x^{\mu}} = (\partial_0, \partial_1, \partial_2, \partial_3) = (\frac{\partial}{\partial t}, \frac{\partial}{\partial x}, \frac{\partial}{\partial y}, \frac{\partial}{\partial z}), \\ \partial^{\mu} &\equiv \frac{\partial}{\partial x_{\mu}} = (\partial^0, \partial^1, \partial^2, \partial^3) = (\frac{\partial}{\partial t}, -\frac{\partial}{\partial x}, -\frac{\partial}{\partial y}, -\frac{\partial}{\partial z}) \ . \end{aligned} \tag{8}$$

The four-momentum operator is

$$p^{\mu} \equiv i\partial^{\mu} = (i\partial^0, -i\nabla) \ , \tag{9}$$

where $\nabla \equiv (\nabla_x, \nabla_y, \nabla_z) = (\partial_1, \partial_2, \partial_3) = (\frac{\partial}{\partial x}, \frac{\partial}{\partial y}, \frac{\partial}{\partial z})$.

.1.3 Some special tensors

Four-dimensional totally antisymmetric Levi-Civita tensor $\epsilon^{\mu\nu\rho\sigma}$

The four-dimensional totally antisymmetric Levi-Civita tensor $\epsilon^{\mu\nu\rho\sigma}$ is defined by

$$\epsilon^{\mu\nu\rho\sigma} = \begin{cases} +1 & \text{if } \{\mu,\nu,\rho,\sigma\} \text{ is an even permutation of } \{0,1,2,3\} \\ -1 & \text{if } \{\mu,\nu,\rho,\sigma\} \text{ is an odd permutation of } \{0,1,2,3\} \\ 0 & \text{otherwise} \end{cases} \tag{10}$$

Useful identities:

$$\begin{aligned} \epsilon_{\mu\nu\rho\sigma} &= -\epsilon^{\mu\nu\rho\sigma} \\ \epsilon^{\mu\nu\rho\sigma}\epsilon^{\mu'\nu'\rho'\sigma'} &= -\det(g^{\alpha\alpha'}) \quad \text{where } \alpha = \mu,\nu,\rho,\sigma, \text{ and } \alpha' = \mu',\nu',\rho',\sigma' \\ \epsilon^{\mu\nu\rho\sigma}\epsilon_{\mu}{}^{\nu'\rho'\sigma'} &= -\det(g^{\alpha\alpha'}) \quad \text{where } \alpha = \nu,\rho,\sigma, \text{ and } \alpha' = \nu',\rho',\sigma' \\ \epsilon^{\mu\nu\rho\sigma}\epsilon_{\mu\nu}{}^{\rho'\sigma'} &= -2\det(g^{\alpha\alpha'}) \quad \text{where } \alpha = \rho,\sigma, \text{ and } \alpha' = \rho',\sigma' \\ \epsilon^{\mu\nu\rho\sigma}\epsilon_{\mu\nu\rho}{}^{\sigma'} &= -6g^{\sigma\sigma'} \\ \epsilon^{\mu\nu\rho\sigma}\epsilon_{\mu\nu\rho\sigma} &= -24\,, \end{aligned} \tag{11}$$

where det means the determinant of a matrix, e.g. for $\alpha = \rho,\sigma$ and $\alpha = \rho',\sigma'$

$$\det(g^{\alpha\alpha'}) = \begin{vmatrix} g^{\rho\rho'} & g^{\rho\sigma'} \\ g^{\rho'\sigma} & g^{\sigma\sigma'} \end{vmatrix} = g^{\rho\rho'}g^{\sigma\sigma'} - g^{\rho\sigma'}g^{\rho'\sigma}\,. \tag{12}$$

Three-dimensional totally antisymmetric tensor ϵ^{ijk}

The definition of ϵ^{ijk} is very similar to $\epsilon^{\mu\nu\rho\sigma}$,

$$\epsilon^{ijk} = \begin{cases} +1 & \text{if } \{ijk\} \text{ is an even permutation of } \{123\} \\ -1 & \text{if } \{ijk\} \text{ is an odd permutation of } \{123\} \\ 0 & \text{otherwise} \end{cases} \tag{13}$$

Useful identities:

$$\begin{aligned}
\epsilon_{ijk}\epsilon_{lmn} &= \delta_{il}(\delta_{jm}\delta_{kn} - \delta_{jn}\delta_{km}) - \delta_{im}(\delta_{jl}\delta_{kn} - \delta_{jn}\delta_{kl}) - \delta_{in}(\delta_{jm}\delta_{kl} - \delta_{jl}\delta_{km}) \\
\epsilon_{ijk}\epsilon_{lmk} &= \delta_{il}\delta_{jm} - \delta_{im}\delta_{jl} \\
\epsilon_{ijk}\epsilon_{ljk} &= 2\delta_{il} \\
\epsilon_{ijk}\epsilon_{ijk} &= 6 \ . \qquad (14)
\end{aligned}$$

Kronecker delta

$$\delta_{ij} = \begin{cases} 1 & \text{if } i = j \\ 0 & \text{otherwise} \end{cases} \qquad (15)$$

$$\delta_i^i = 3 \ . \qquad (16)$$

.2 Dirac Matrices and Spinors

.2.1 Dirac Algebra

Dirac matrices

The Dirac γ matrices satisfy the following anticommutation relations

$$\{\gamma_\mu, \gamma_\nu\} = \gamma_\mu\gamma_\nu + \gamma_\nu\gamma_\mu = 2g_{\mu\nu} \ . \tag{17}$$

γ^0 is hermitian, whereas γ^i antihermitian,

$$\gamma^{\mu\dagger} = \gamma^0\gamma^\mu\gamma^0 \ . \tag{18}$$

A matrix, which anticommutes with γ^μ, γ_5 is defined by

$$\gamma_5 = \gamma^5 = i\gamma^0\gamma^1\gamma^2\gamma^3 = -\frac{i}{4!}\epsilon_{\mu\nu\rho\sigma}\gamma^\mu\gamma^\nu\gamma^\rho\gamma^\sigma = \gamma_5^\dagger \tag{19}$$

$$\begin{aligned} \gamma_5^2 &= I \\ \{\gamma_5, \gamma^\mu\} &= 0 \end{aligned} \tag{20}$$

A useful tensor $\sigma^{\mu\nu}$ is defined as

$$\sigma^{\mu\nu} = \frac{i}{2}\left[\gamma^\mu, \gamma^\nu\right] \ . \tag{21}$$

Useful Identities

$$\gamma_\mu\gamma^\mu = 4 \tag{22}$$

$$\gamma_\mu\gamma^\alpha\gamma^\mu = -2\gamma^\alpha \tag{23}$$

$$\gamma_\mu\gamma^\alpha\gamma^\beta\gamma^\mu = 4g^{\alpha\beta} \tag{24}$$

$$\gamma_\mu\gamma^\alpha\gamma^\beta\gamma^\lambda\gamma^\mu = -2\gamma^\lambda\gamma^\beta\gamma^\alpha \tag{25}$$

$$\gamma_\mu\gamma^\alpha\gamma^\beta\gamma^\lambda\gamma^\sigma\gamma^\mu = 2(\gamma^\sigma\gamma^\alpha\gamma^\beta\gamma^\lambda + \gamma^\lambda\gamma^\beta\gamma^\alpha\gamma^\sigma) \quad (26)$$

$$\gamma_5\sigma^{\mu\nu} = \frac{i}{2}\epsilon^{\mu\nu\rho\sigma}\sigma_{\rho\sigma} \quad (27)$$

$$i\gamma^\mu\epsilon_{\mu\alpha\beta\gamma} = (\gamma_\alpha\gamma_\beta\gamma_\gamma - \gamma_\alpha g_{\beta\gamma} + \gamma_\beta g_{\alpha\gamma} - \gamma_\gamma g_{\alpha\beta})\gamma_5 \ , \quad (28)$$

Traces

$$\mathrm{Tr}\gamma^\mu = 0 \quad (29)$$

$$\mathrm{Tr}\gamma_5 = 0 \quad (30)$$

$$\mathrm{Tr}\sigma^{\mu\nu} = 0 \quad (31)$$

$$\mathrm{Tr}\gamma^\mu\gamma^\nu\gamma^5 = 0 \quad (32)$$

$$\mathrm{Tr}\gamma^\mu\gamma^\nu = 4g^{\mu\nu} \quad (33)$$

$$\mathrm{Tr}(\text{odd\# of } \gamma's) = 0 \quad (34)$$

$$\mathrm{Tr}\gamma^\mu\gamma^\nu\gamma^\rho\gamma^\sigma = 4(g^{\mu\nu}g^{\rho\sigma} - g^{\mu\rho}g^{\nu\sigma} + g^{\mu\sigma}g^{\nu\rho}) \quad (35)$$

$$\mathrm{Tr}\gamma_5\gamma^\mu\gamma^\nu\gamma^\rho\gamma^\sigma = -4i\epsilon^{\mu\nu\rho\sigma} = 4i\epsilon_{\mu\nu\rho\sigma} \quad (36)$$

.2.2 Two Representations for Dirac Matrices

Dirac representation

$$\gamma^0 = \rho^3 \otimes I = \begin{pmatrix} I & 0 \\ 0 & -I \end{pmatrix}$$

$$\gamma^i = i\rho^2 \otimes \sigma^i = \begin{pmatrix} 0 & \sigma^i \\ -\sigma^i & 0 \end{pmatrix}$$

$$\gamma^5 = \rho^1 \otimes I = \begin{pmatrix} 0 & I \\ I & 0 \end{pmatrix} \ , \quad (37)$$

where ρ^i and σ^i are two copies of Pauli matrices,

$$\rho^1 = \sigma^1 = \begin{pmatrix} 0 & 1 \\ 1 & 0 \end{pmatrix}, \quad \rho^2 = \sigma^2 = \begin{pmatrix} 0 & -i \\ i & 0 \end{pmatrix}, \quad \rho^3 = \sigma^3 = \begin{pmatrix} 1 & 0 \\ 0 & -1 \end{pmatrix}, \tag{38}$$

and I is the unit matrix in 2×2 space

$$I = \begin{pmatrix} 1 & 0 \\ 0 & 1 \end{pmatrix}. \tag{39}$$

Chiral representation

$$\begin{aligned} \gamma^0 &= -\rho^1 \otimes I = \begin{pmatrix} 0 & -I \\ -I & 0 \end{pmatrix} \\ \gamma^i &= i\rho^2 \otimes \sigma^i = \begin{pmatrix} 0 & \sigma^i \\ -\sigma^i & 0 \end{pmatrix} \\ \gamma^5 &= \rho^3 \otimes I = \begin{pmatrix} I & 0 \\ 0 & -I \end{pmatrix}, \end{aligned} \tag{40}$$

.2.3 Dirac Spinors

Dirac equations

The Dirac spinor $u(ps)$ describing a free fermion with mass m and spin s satisfies the Dirac equation

$$(\not{p} - m)u(ps) = 0\ , \tag{41}$$

and its adjoint $\bar{u}(ps) \equiv u^\dagger(ps)\gamma^0$ satisfies

$$\bar{u}(ps)(\not{p} - m) = 0\ , \tag{42}$$

where $p^2 = m^2$, $s^2 = -m^2$ and $s \cdot p = 0$.

The antifermion satisfies

$$\begin{aligned} (\not{p} - m)v(ps) &= 0 \,, \\ \bar{v}(ps)(\not{p} - m) &= 0 \,, \end{aligned} \tag{43}$$

where $\bar{v}(ps) \equiv v^\dagger(ps)\gamma^0$.

Normalization

$$\begin{aligned} \bar{u}(pr)u(ps) &= 2m\delta_{rs} \,, \\ \bar{v}(pr)v(ps) &= -2m\delta_{rs} \,, \\ \bar{u}(pr)\gamma^\mu u(ps) &= 2p^\mu\delta_{rs} \,, \\ \bar{v}(pr)\gamma^\mu v(ps) &= 2p^\mu\delta_{rs} \,. \end{aligned} \tag{44}$$

Projection operators

$$\begin{aligned} \Lambda_+(p) &\equiv \sum_s u(ps)\bar{u}(ps) = \not{p} + m \,, \\ \Lambda_-(p) &\equiv \sum_s v(ps)\bar{v}(ps) = \not{p} - m \,, \\ P(ps) &\equiv u(ps)\bar{u}(ps) = \frac{(\not{p} + m)}{2}(1 + \gamma_5\not{s}) \,. \end{aligned} \tag{45}$$

$$\begin{aligned} (1 \pm \gamma_5)u(p)\bar{u}(p)(1 \mp \gamma_5) &= (1 \pm \gamma_5)\left(\sum_{pol} u(p)\bar{u}(p)\right)(1 \mp \gamma_5) \\ &= 2(1 \pm \gamma_5)\not{p} \,. \end{aligned} \tag{46}$$

.2.4 Helicity and Chirality for Massless Fermions

Helicity

The helicity λ for a moving particle is defined as its polarization projection along its momentum direction. It is defined as the eigenstates of the following helicity operator

$$\hat{H} = \frac{\vec{\Sigma} \cdot \vec{p}}{|\vec{p}|} , \tag{47}$$

where $\vec{\Sigma}$ is spin operator as defined by

$$\Sigma^i = \frac{1}{2}\epsilon_{ijk}\sigma^{jk} = \gamma_5\gamma^0\gamma^i , \tag{48}$$

and $|\vec{p}|$ is the module of the particle's three momentum $\vec{p}$.

$$\frac{\vec{\Sigma} \cdot \vec{p}}{|\vec{p}|}u(p\lambda) = \lambda u(p\lambda) . \tag{49}$$

Chirality

Chirality of a massless fermion is defined as the eigenvalue of the chirality operator γ^5,

$$\gamma^5 u(ps) = \pm u(ps) . \tag{50}$$

Chirality = Helicity for Massless Fermions

The Dirac equation for massless fermions is

$$\not{p}u(ps) = 0 . \tag{51}$$

Multiplying it by $\gamma^5\gamma^0 = -i\gamma^1\gamma^2\gamma^3$ yields

$$\frac{\vec{\Sigma} \cdot \vec{p}}{|\vec{p}|}u(ps) = \gamma^5 u(ps) , \tag{52}$$

where we have used the fact that $|\vec{p}| = p^0$ for the massless fermions.

Therefore it can be concluded that a massless fermion's chirality is equal to its helicity(it is opposite for an antifermion).

The Dirac spinors in chiral representation

An explicit form of the spinor in chrial representation for a massless fermion is

$$u_+(k) = v_-(k) = \begin{pmatrix} \sqrt{k_+} \\ \sqrt{k_-}e^{i\phi_k} \\ 0 \\ 0 \end{pmatrix}, \quad u_-(k) = v_+(k) = \begin{pmatrix} 0 \\ 0 \\ -\sqrt{k_-}e^{-i\phi_k} \\ \sqrt{k_+} \end{pmatrix} \tag{53}$$

for any light-like vector k_μ, where

$$k_\pm = k_0 \pm k_z, \qquad k_\perp = k_x + ik_y = |k_\perp|e^{i\phi_k} \ , \tag{54}$$

and the antiquark helicity states are chosen to be

$$v(k\lambda) = C\bar{u}(k\lambda)^T \ , \tag{55}$$

where $C = i\gamma^2\gamma^0$ is the charge conjugate matrix, and T means taking the transpose of a matrix.

.3 Color SU(3)

The 3×3 SU(3) traceless color matrices T^a satisfy

$$[T^a, T^b] = if^{abc}T^c \ , \tag{56}$$

where $a = 1, ..., 8$ is color index, f^{abc} are the antisymmetric $SU(3)$ structure constant with non-zero values given by

a	b	c	f^{abc}
1	2	3	1
1	4	7	$\frac{1}{2}$
1	5	6	$-\frac{1}{2}$
2	4	6	$\frac{1}{2}$
2	5	7	$\frac{1}{2}$
3	4	5	$\frac{1}{2}$
3	6	7	$-\frac{1}{2}$
4	5	8	$\frac{\sqrt{3}}{2}$
6	7	8	$\frac{\sqrt{3}}{2}$

A convenient representation for T^a is Gell-Mann representation

$$\begin{aligned}
T^1 &= \tfrac{1}{2}\begin{pmatrix} 0 & 1 & 0 \\ 1 & 0 & 0 \\ 0 & 0 & 0 \end{pmatrix}, \quad T^2 = \tfrac{1}{2}\begin{pmatrix} 0 & -i & 0 \\ i & 0 & 0 \\ 0 & 0 & 0 \end{pmatrix} \\
T^3 &= \tfrac{1}{2}\begin{pmatrix} 1 & 0 & 0 \\ 0 & -1 & 0 \\ 0 & 0 & 0 \end{pmatrix}, \quad T^4 = \tfrac{1}{2}\begin{pmatrix} 0 & 0 & 1 \\ 0 & 0 & 0 \\ 1 & 0 & 0 \end{pmatrix} \\
T^5 &= \tfrac{1}{2}\begin{pmatrix} 0 & 0 & -i \\ 0 & 0 & 0 \\ i & 0 & 0 \end{pmatrix}, \quad T^6 = \tfrac{1}{2}\begin{pmatrix} 0 & 0 & 0 \\ 0 & 0 & 1 \\ 0 & 1 & 0 \end{pmatrix} \\
T^7 &= \tfrac{1}{2}\begin{pmatrix} 0 & 0 & 0 \\ 0 & 0 & -i \\ 0 & i & 0 \end{pmatrix}, \quad T^8 = \tfrac{1}{2\sqrt{3}}\begin{pmatrix} 1 & 0 & 0 \\ 0 & 1 & 0 \\ 0 & 0 & -2 \end{pmatrix}
\end{aligned} \tag{57}$$

The structure constants d^{abc} are defined as

$$\left\{T^a, T^b\right\} = \frac{1}{3}\delta^{ab} + d^{abc}T^c \ , \tag{58}$$

and T^a satisfy

$$T^aT^b = \frac{1}{2}\left[\frac{1}{3}\delta^{ab} + (d^{abc} + if^{abc})T^c\right] \ . \tag{59}$$

Some useful relations:

$$\begin{aligned}
T^a_{ij}T^a_{kl} &= \frac{1}{2}\left[\delta_{il}\delta_{jk} - \frac{1}{3}\delta_{ij}\delta_{kl}\right] \ , && (60)\\
\mathrm{Tr}(T^a) &= 0 \ , && (61)\\
\mathrm{Tr}(T^aT^b) &= \frac{1}{2}\delta^{ab} \ , && (62)\\
\mathrm{Tr}(T^aT^bT^c) &= \frac{1}{4}(d^{abc} + if^{abc}) \ , && (63)\\
\mathrm{Tr}(T^aT^bT^aT^c) &= -\frac{1}{12}\delta^{bc} \ , && (64)\\
\mathrm{Tr}(T^aT^bT^bT^a) &= \frac{16}{3} \ . && (65)
\end{aligned}$$

The structure constants also satisfy the following Jacobi identities:

$$\begin{aligned}
f^{abe}f^{ecd} + f^{cbe}f^{aed} + f^{dbe}f^{ace} &= 0 \ , && (66)\\
f^{abe}d^{ecd} + f^{cbe}d^{aed} + f^{dbe}f^{ace} &= 0 \ . && (67)
\end{aligned}$$

Three relations derived from the Eq. (60) are very useful to compute the color traces involving a summation over a color index,

$$\begin{aligned}
\mathrm{Tr}(T^a\Gamma_1T^a\Gamma_2) &= \frac{1}{2}\mathrm{Tr}(\Gamma_1)\mathrm{Tr}(\Gamma_2) - \frac{1}{6}\mathrm{Tr}(\Gamma_1\Gamma_2) \ , && (68)\\
\mathrm{Tr}(T^a\Gamma_1)\mathrm{Tr}(T^a\Gamma_2) &= \frac{1}{2}\mathrm{Tr}(\Gamma_1\Gamma_2) - \frac{1}{6}\mathrm{Tr}(\Gamma_1)\mathrm{Tr}(\Gamma_2) \ , && (69)\\
\mathrm{Tr}(T^a\Gamma_1\Gamma_2T^a) &= \frac{4}{3}\mathrm{Tr}(\Gamma_1\Gamma_2) \ , && (70)
\end{aligned}$$

where Γ_1 and Γ_2 are any combinations of the color matrices. For example, it is easy

to obtain

$$\begin{aligned}
\mathrm{Tr}(T^a T^b T^c)\mathrm{Tr}(T^a T^c T^b) &= \frac{1}{2}\mathrm{Tr}(T^b T^c T^c T^b) - \frac{1}{6}\mathrm{Tr}(T^b T^c)\mathrm{Tr}(T^c T^b) \ , \\
&= \frac{2}{3}\mathrm{Tr}(T^c T^c) - \frac{1}{6}\frac{1}{2}\frac{1}{2} \times 8 \ , \\
&= \frac{8}{3} - \frac{1}{3} \ , \\
&= \frac{7}{3} \ . \qquad (71)
\end{aligned}$$

.4 Feynman Rules of QCD

.4.1 External Lines

- quark in initial state $\cdots u(p)$
- quark in final state $\cdots \bar{u}(p)$
- antiquark in initial state $\cdots \bar{v}(p)$
- antiquark in final state $\cdots v(p)$
- gluon in initial state $\cdots \epsilon^{\mu}(\lambda)$

  where $\epsilon^{\mu}(\lambda)$ is the polarization vector for a gluon with helicity λ. It satisfies $\epsilon_{\mu}(\lambda)\epsilon^{\mu}(\lambda') = -\delta_{\lambda\lambda'}$ and $\epsilon \cdot k = 0$ with k_{μ} being the momentum of the gluon.
- gluon in final state $\cdots \epsilon^{*\mu}(\lambda)$
- ghost in initial or antighost in final state $\cdots 1$
- ghost in final or antighost in initial state $\cdots 1$

.4.2 Internal Lines

- quark propagator $\cdots \dfrac{i\delta_{ij}}{\not{p} + i\epsilon}$
- gluon propagator $\cdots i\delta^{ab}\left\{\dfrac{-g_{\mu\nu}}{p^2 + i\epsilon} + \dfrac{(1-\xi)p_{\mu}p_{\nu}}{(p^2+i\epsilon)^2}\right\}$

  gauge parameter $\xi = 1$ is Feynman gauge, $\xi = 0$ is Landau gauge.
- ghost propagator $\cdots \dfrac{-i\delta_{ab}}{p^2 + i\epsilon}$

.4.3 Interaction Vertex Factors

- quark-quark-gluon vertex

$$-ig_s\gamma_{\mu}T^a_{ij} \tag{72}$$

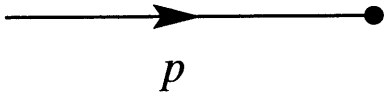

Figure -1: Incoming quark line

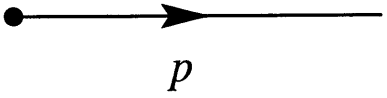

Figure -2: Outgoing quark line

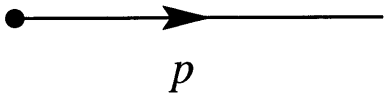

Figure -3: Incoming quark line

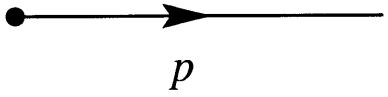

Figure -4: Outgoing quark line

Figure -5: Incoming gluon line

Figure -6: Outgoing gluon line

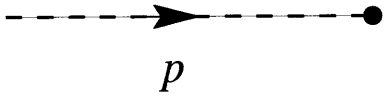

Figure -7: Incoming ghost line

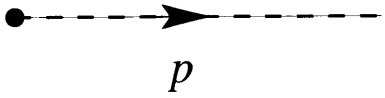

Figure -8: Outgoing quark line

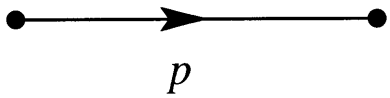

Figure -9: Quark propagator line

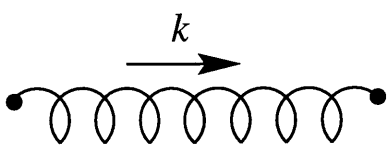

Figure -10: Gluon propagator line

- three-gluon vertex

$$-g_s f_{abc}\left[(p_1-p_2)_\nu g_{\lambda\mu}+(p_2-p_3)_\lambda g_{\mu\nu}+(p_3-p_1)_\mu g_{\nu\lambda}\right] \tag{73}$$

- four-gluon vertex

$$\begin{aligned}
&-ig_s^2 f_{abc}f_{cde}(g_{\lambda\nu}g_{\mu\sigma}-g_{\lambda\sigma}g_{\mu\nu})\\
&-ig_s^2 f_{ace}f_{bde}(g_{\lambda\mu}g_{\nu\sigma}-g_{\lambda\sigma}g_{\mu\nu})\\
&-ig_s^2 f_{ade}f_{cbe}(g_{\lambda\nu}g_{\mu\sigma}-g_{\lambda\mu}g_{\sigma\nu})
\end{aligned} \tag{74}$$

- ghost-ghost-gluon vertex

$$g_s f_{abc} p_\mu \tag{75}$$

.4.4 Loops and Combinbatories

- For each loop with undetermined momentum k, there is a integral $\cdots \int \frac{d^4k}{(2\pi)^4}$.
- For each closed fermion loop, there is an extra factor $\cdots -1$.
- For each closed loop containing n identical bosons, there is a symmetry factor $\cdots \frac{1}{n!}$

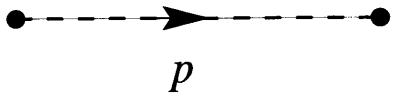

Figure -11: Ghost propagator line

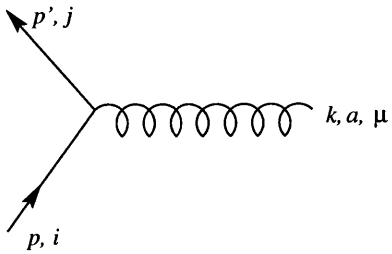

Figure -12: Quark-quark-gluon vertex

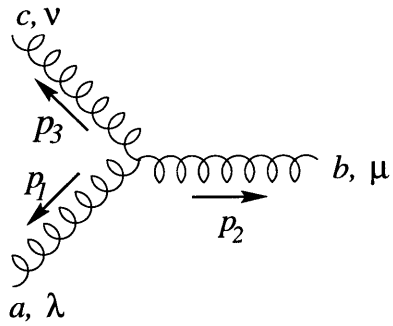

Figure -13: Three-gluon vertex

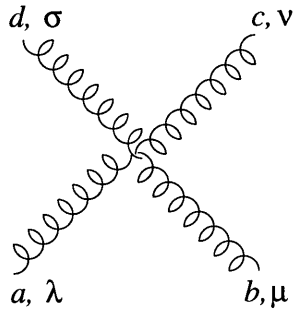

Figure -14: Four-gluon vertex

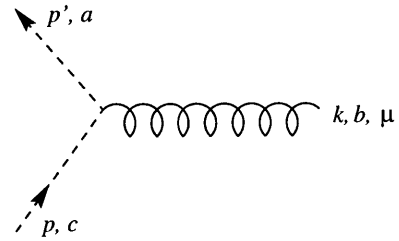

Figure -15: Ghost-ghost-gluon vertex

.5 2-to-2 Differential Cross Sections

.5.1 Invariant Amplitude

The invariant amplitude $\mathcal{M}$ is related to the $\mathcal{S}$ matrix through the relation

$$\mathcal{S}_{\beta\alpha} = \delta_{\beta\alpha} - i\frac{(2\pi)^4}{\sqrt{\prod_i (2E_i)}}\delta^4(p_\beta - p_\alpha)\mathcal{M}_{\beta\alpha} \ , \tag{76}$$

where α and β represent the initial and final states, i runs through both initial and final states.

.5.2 2-to-2 Differential Cross Section

For the process $1 + 2 \rightarrow 3 + 4 + ... + n$, the differential cross section is

$$d\sigma = \frac{(2\pi)^4}{4\sqrt{(p_1 \cdot p_2)^2 - m_1^2 m_2^2}} \prod_{i=3}^{n} \frac{d^3 p_i}{(2\pi)^3 (2E_i)} \delta^4(\sum_{i=3}^{n} p_i - (p_1 + p_2)) |\mathcal{M}_{\beta\alpha}|^2 \ . \tag{77}$$

The 2-to-2 differential cross section in its center-of-mass frame is given by

$$\frac{d\sigma}{d\Omega_{cm}}(s, \theta) = \frac{1}{64\pi^2 s} \frac{p'_{cm}}{p_c m} |\mathcal{M}_{\beta\alpha}|^2 \ , \tag{78}$$

where $d\Omega_{cm} = d\cos\theta_{cm} d\phi_{cm}$. The invariants s, t and u are defined by

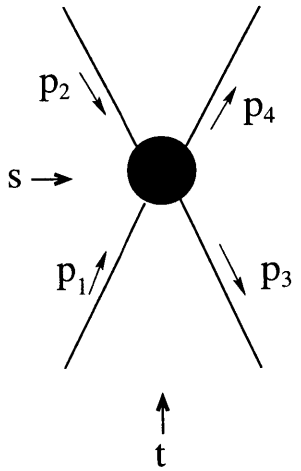

Figure -16: Illustration of a 2-to-2 scattering.

$$s = (p_1 + p_2)^2 = (p_3 + p_4)^2 \ , \tag{79}$$

$$t = (p_1 - p_3)^2 = (p_2 - p_4)^2 \ , \tag{80}$$

$$u = (p_1 - p_4)^2 = (p_2 - p_3)^2 \ . \tag{81}$$

Momentum conservation implies $p_1 + p_2 = p_3 + p_4$.

The initial and final center-of-mass momenta p_{cm} and p'_{cm} are given by

$$p_{cm}^2 = \frac{1}{4s}\left[s - (m_1 + m_2)^2\right]\left[s - (m_1 - m_2)^2\right] \ , \tag{82}$$

$$p'^2_{cm} = \frac{1}{4s}\left[s - (m_3 + m_4)^2\right]\left[s - (m_3 - m_4)^2\right] \ , \tag{83}$$

$$\tag{84}$$

t is the momentum transfer squared and is given by

$$t = t_{min} + 2p_{cm}p'_{cm}(\cos\theta_{cm} - 1) \ , \tag{85}$$

where

$$t_{min} = (E_1^{cm} - E^{cm_3})^2 - (p_{cm} - p'_{cm})^2 \tag{86}$$

with the energies of the particle 1 and 3 in center-of-mass frame

$$E_1^{cm} = \frac{s + m_1^2 - m_2^2}{2\sqrt{s}} \ , \tag{87}$$

$$E_3^{cm} = \frac{s + m_3^2 - m_4^2}{2\sqrt{s}} \ . \tag{88}$$

Therefore, we can have $dt/d\cos\theta_{cm} = 2p_{cm}p'_{cm}$. Substituting it into the cross section, and consider that the amplitude is independent of the azimuthal angle ϕ_{cm}, one can have

$$\frac{d\sigma}{dt}(s,t) = \frac{1}{64\pi^2 s p_{cm}^2}|\mathcal{M}_{\beta\alpha}|^2 \ . \tag{89}$$

.6 Light-Cone Representation of Dirac Matrices

.6.1 Light-cone variables

Light-cone coordinates $(x^+, x^-, \vec{x}_\perp)$ are defined as a linear combinations of the ordinary coordinates (x^0, x^1, x^2, x^3) as below

$$\begin{aligned} x^+ &= \frac{1}{\sqrt{2}}(x^0 + x^3) \\ x^- &= \frac{1}{\sqrt{2}}(x^0 - x^3) \\ \vec{x}_\perp &= (x^1, x^2) \ . \end{aligned} \tag{90}$$

In this representation, the metric $g_{\mu\nu}$ has following form

$$g_{\mu\nu} = \begin{cases} 1 & \text{if } \mu = +, \nu = - \text{ or } \mu = -, \nu = + \\ -1 & \text{if } \mu = \nu = 1 \text{ or } \mu = \nu = 2 \\ 0 & \text{otherwise} \end{cases} \tag{91}$$

such that

$$x \cdot y \equiv g_{\mu\nu} x^\mu y^\nu = x^+ y^- + x^- y^+ - \vec{x}_\perp \cdot \vec{y}_\perp \ . \tag{92}$$

x^+ is to play the role of the time in the light-cone formalism, therefore P^-, the momentum component conjugate to x^+, has the role of the energy. $(P^+, \vec{P}\perp)$ is the three-momentum that specifies the state of a particle in the light-cone formalism.

Two very useful light-like vectors in the light-cone formalism are

$$\begin{aligned} p^\mu &= \frac{\Lambda}{\sqrt{2}}(1, 0, 0, 1) \ , \\ n^\mu &= \frac{1}{\sqrt{2}\Lambda}(1, 0, 0, -1) \ . \end{aligned} \tag{93}$$

with properties

$$\begin{aligned} &p^2 = n^2 = 0 \ , \quad p \cdot n = 1 \ , \\ &p^- = 0 \ , \quad n^+ = 0 \ . \end{aligned} \tag{94}$$

Λ actually selects a specific frame. For example, $\Lambda = M/\sqrt{2}$ selects the hadron rest frame while $\Lambda \to \infty$ selects the infinite momentum frame.

.6.2 Light-Cone Representation of Dirac Matrices

The light-cone representation for the Dirac matrices are ,

$$\begin{aligned} \gamma^0 &= \rho^1 \otimes \sigma^3 = \begin{pmatrix} 0 & \sigma^3 \\ \sigma^3 & 0 \end{pmatrix} \\ \vec{\gamma}^\perp &= 1 \otimes i\vec{\sigma}^\perp = \begin{pmatrix} i\vec{\sigma}^\perp & 0 \\ 0 & i\vec{\sigma}^\perp \end{pmatrix} \\ \gamma^3 &= -i\rho^2 \otimes \sigma^3 = \begin{pmatrix} 0 & -\sigma^3 \\ \sigma^3 & 0 \end{pmatrix} \\ \gamma^5 &= \rho^3 \otimes \sigma^3 = \begin{pmatrix} \sigma^3 & 0 \\ 0 & -\sigma^3 \end{pmatrix}, \end{aligned} \tag{95}$$

(96)

where $\perp = 1 \text{ or } 2$, $\gamma^5 = i\gamma^0\gamma^1\gamma^2\gamma^3$. Here we also write the Dirac matrices in terms of the cross products of two copies of the Pauli matrices: ρ^i and $\sigma^i (i = 1, 2, 3)$. It is easy to check that eq. (96) satisfy the usual algebra, $\{\gamma^\mu, \gamma^\nu\} = 2g^{\mu\nu}$.

A set of projection operators $\mathcal{P}_\pm$ on the upper and lower two component subspaces are defined by,

$$\begin{aligned} \mathcal{P}_\pm &= \frac{1}{2}\gamma^\mp\gamma^\pm = \frac{1}{2}(1 \pm \alpha_3) \\ \gamma^\pm &= \frac{1}{\sqrt{2}}(\gamma^0 \pm \gamma^3), \end{aligned} \tag{97}$$

with the properties:

$$\begin{aligned} \mathcal{P}_-\mathcal{P}_+ &= \mathcal{P}_+\mathcal{P}_- = 0 \\ \mathcal{P}_\pm^2 &= \mathcal{P}_\pm \\ \mathcal{P}_- + \mathcal{P}_+ &= 1 \end{aligned}$$

$$\mathcal{P}_+ = \begin{pmatrix} 1 & 0 \\ 0 & 0 \end{pmatrix} \qquad \mathcal{P}_- = \begin{pmatrix} 0 & 0 \\ 0 & 1 \end{pmatrix} \tag{98}$$

where

$$\alpha_3 = \begin{pmatrix} 1 & 0 \\ 0 & -1 \end{pmatrix} . \tag{99}$$

.6.3 Good and Bad Components of Dirac Field

The "light-cone projections" of the Dirac field, $\psi_+ \equiv \mathcal{P}_+\psi$ and $\psi_- \equiv \mathcal{P}_-\psi$ are known as the "good" and "bad" light-cone components of ψ respectively. To save on subscripts we shall frequently replace $\psi_\pm$ as follows,

$$\psi_+ \Rightarrow \phi \quad \psi_- \Rightarrow \chi \tag{100}$$

Hence

$$\psi = (\mathcal{P}_+ + \mathcal{P}_-)\psi = \phi + \chi \, . \tag{101}$$

The Dirac equation can be projected to two two-component equations using the projection operators $\mathcal{P}_\pm$,

$$\begin{aligned} i\gamma^- D_-\chi &= -\vec{\gamma}^\perp \cdot \vec{D}^\perp \phi + m\phi \\ i\gamma^+ D_+\phi &= -\vec{\gamma}^\perp \cdot \vec{D}^\perp \chi + m\chi, \end{aligned} \tag{102}$$

where $D_\pm = \dfrac{\partial}{\partial\xi^\pm} - igA^\mp$. In the light-cone gauge $A^+ = 0$. ξ^+ is the evolution ("time") parameter, but the first of eq. (102) only involves $\partial/\partial\xi^-$, so it appears that χ is not an independent dynamical field. Instead the Dirac equation constrains χ in terms of ϕ and $\vec{A}_\perp$ at fixed ξ^+,

$$i\gamma^- \frac{\partial}{\partial\xi^-}\chi = -\vec{\gamma}^\perp \cdot \vec{D}^\perp \phi + m\phi \tag{103}$$

Therefore, the *good* components ϕ should be regarded as independent propagating

degrees of freedom; the *bad* components χ are dependent fields – actually quark-gluon composites: $\chi = \mathcal{F}[\phi, \vec{A}_\perp]$. [6] In the helicity basis, where

$$\Sigma^3 \equiv \frac{i}{2}[\gamma^1, \gamma^2] = \begin{pmatrix} \sigma^3 & 0 \\ 0 & \sigma^3 \end{pmatrix}, \tag{104}$$

is diagonalized, both the good and bad components of ψ carry *helicity* labels – the eigenvalues of Σ^3,

$$\psi = \begin{pmatrix} \phi_+ \\ \phi_- \\ \chi_+ \\ \chi_- \end{pmatrix}. \qquad \gamma_5\psi = \begin{pmatrix} +\phi_+ \\ -\phi_- \\ -\chi_+ \\ +\chi_- \end{pmatrix}. \tag{105}$$

Helicity and chirality are identical for the good components of ψ but opposite for the bad components. This will be used to sort out the chirality and helicity selection rules.

Every factor of χ in the light-cone decomposition of a light-cone correlation function contributes and additional unit of twist to the associated distribution function, e.g.

$$\begin{aligned} \phi^\dagger\phi &\leftrightarrow \text{twist 2}\ , \\ \phi^\dagger\chi &\leftrightarrow \text{twist 3}\ , \\ \chi^\dagger\chi &\leftrightarrow \text{twist 4}\ , \end{aligned} \tag{106}$$

.7 Quark Distribution and Fragmentation Functions

We table the quark distribution and fragmentation function for different targets, associated with their relations with the helicity amplitudes. The asterix on the helicity amplitudes indicates a bad component of the Dirac field.

.7.1 Quark Distribution Functions

Table 1: **Quark distributions in a spin-0 hadron through twist-three.**

Twist	Name	Helicity Amplitude	Measurement	Chirality
Two	$f_1(x)$	$\mathcal{F}_{0\frac{1}{2},0\frac{1}{2}}$	Spin Average	Even
Three	$e(x)$	$\mathcal{F}_{0\frac{1}{2}^*,0\frac{1}{2}}$	Spin Average	Odd

Table 2: **Quark distributions in a nucleon through twist-three.**

twist $O(1/Q^{t-2})$	Name	Helicity Amplitude	Measurement	Chirality
Two	$f_1(x)$	$\mathcal{F}_{1\frac{1}{2},1\frac{1}{2}} + \mathcal{F}_{1-\frac{1}{2},1-\frac{1}{2}}$	Spin average	Even
Two	$g_1(x)$	$\mathcal{F}_{1\frac{1}{2},1\frac{1}{2}} - \mathcal{F}_{1-\frac{1}{2},1-\frac{1}{2}}$	Helicity difference	Even
Two	$h_1(x)$	$\mathcal{F}_{0\frac{1}{2},1-\frac{1}{2}}$	Helicity flip	Odd
Three	$e(x)$	$\mathcal{F}_{1\frac{1}{2}^*,1\frac{1}{2}} + \mathcal{F}_{1-\frac{1}{2},1-\frac{1}{2}}$	Spin average	Odd
Three	$h_L(x)$	$\mathcal{F}_{1\frac{1}{2}^*,1\frac{1}{2}} - \mathcal{F}_{1-\frac{1}{2},1-\frac{1}{2}}$	Helicity difference	Odd
Three	$g_T(x)$	$\mathcal{F}_{0\frac{1}{2}^*,1-\frac{1}{2}}$	Helicity flip	Even

Table 3: **Quark distributions in a spin-1 hadron through twist-three.**

Twist	Name	Helicity Amplitude	Measurement	Chirality
Two	$f_1(x)$	$\mathcal{F}_{1\frac{1}{2},1\frac{1}{2}} + \mathcal{F}_{1-\frac{1}{2},1-\frac{1}{2}} + \mathcal{F}_{0\frac{1}{2},0\frac{1}{2}}$	Helicity average	Even
Two	$b_1(x)$	$\mathcal{F}_{1\frac{1}{2},1\frac{1}{2}} + \mathcal{F}_{1-\frac{1}{2},1-\frac{1}{2}} - 2\mathcal{F}_{0\frac{1}{2},0\frac{1}{2}}$	Quadruple	Even
Two	$g_1(x)$	$\mathcal{F}_{1\frac{1}{2},1\frac{1}{2}} - \mathcal{F}_{1-\frac{1}{2},1-\frac{1}{2}}$	Helicity difference	Even
Two	$h_1(x)$	$\mathcal{F}_{0\frac{1}{2},1-\frac{1}{2}} + \mathcal{F}_{1-\frac{1}{2},0\frac{1}{2}}$	Helicity flip	Odd
Three	$e_1(x)$	$\mathcal{F}_{1\frac{1}{2}^*,1\frac{1}{2}} + \mathcal{F}_{1-\frac{1}{2}^*,1-\frac{1}{2}} + \mathcal{F}_{0\frac{1}{2}^*,0\frac{1}{2}}$	Spin Average	Odd
Three	$b_2(x)$	$\mathcal{F}_{1\frac{1}{2}^*,1\frac{1}{2}} + \mathcal{F}_{1-\frac{1}{2}^*,1-\frac{1}{2}} - 2\mathcal{F}_{0\frac{1}{2}^*,0\frac{1}{2}}$	Quadruple	Odd
Three	$h_2(x)$	$\mathcal{F}_{1\frac{1}{2}^*,1\frac{1}{2}} - \mathcal{F}_{1-\frac{1}{2}^*,1-\frac{1}{2}}$	Helicity difference	Odd
Three	$g_2(x)$	$\mathcal{F}_{0\frac{1}{2}^*,1-\frac{1}{2}} + \mathcal{F}_{1-\frac{1}{2}^*,0\frac{1}{2}}$	Helicity flip	Even
Three	$\Delta g_2(x)$	$\mathcal{F}_{0\frac{1}{2}^*,1-\frac{1}{2}} - \mathcal{F}_{1-\frac{1}{2}^*,0\frac{1}{2}}$	Helicity flip	Even

.7.2 Quark Fragmentation Functions

Table 4: **Quark fragmentations to a spin-0 hadron through twist-three.**

Twist	Name	Helicity Amplitude	Measurement	Chirality
Two	$\hat{f}_1(z)$	$\hat{\mathcal{F}}_{0\frac{1}{2},0\frac{1}{2}}$	Spin Average	Even
Three	$\hat{e}(z)$	$\hat{\mathcal{F}}_{0\frac{1}{2}^*,0\frac{1}{2}}$	Spin Average	Odd

Table 5: **Quark fragmentations to a spin-$\frac{1}{2}$ hadron through twist-three.**

twist $O(1/Q^{t-2})$	Name	Helicity Amplitude	Measurement	Chirality
Two	$\hat{f}_1(z)$	$\hat{\mathcal{F}}_{1\frac{1}{2},1\frac{1}{2}} + \hat{\mathcal{F}}_{1-\frac{1}{2},1-\frac{1}{2}}$	Spin average	Even
Two	$\hat{g}_1(z)$	$\hat{\mathcal{F}}_{1\frac{1}{2},1\frac{1}{2}} - \hat{\mathcal{F}}_{1-\frac{1}{2},1-\frac{1}{2}}$	Helicity difference	Even
Two	$\hat{h}_1(z)$	$\hat{\mathcal{F}}_{0\frac{1}{2},1-\frac{1}{2}}$	Helicity flip	Odd
Three	$\hat{e}(z)$	$\hat{\mathcal{F}}_{1\frac{1}{2}^*,1\frac{1}{2}} + \hat{\mathcal{F}}_{1-\frac{1}{2},1-\frac{1}{2}}$	Spin average	Odd
Three	$\hat{h}_L(z)$	$\hat{\mathcal{F}}_{1\frac{1}{2}^*,1\frac{1}{2}} - \hat{\mathcal{F}}_{1-\frac{1}{2},1-\frac{1}{2}}$	Helicity difference	Odd
Three	$\hat{g}_T(z)$	$\hat{\mathcal{F}}_{0\frac{1}{2}^*,1-\frac{1}{2}}$	Helicity flip	Even

Table 6: **Quark fragmentations in a spin-1 hadron through twist-three.**

Twist	Name	Helicity Amplitude	Measurement	Chirality
Two	$\hat{f}_1(z)$	$\hat{\mathcal{F}}_{1\frac{1}{2},1\frac{1}{2}} + \hat{\mathcal{F}}_{1-\frac{1}{2},1-\frac{1}{2}} + \hat{\mathcal{F}}_{0\frac{1}{2},0\frac{1}{2}}$	Helicity average	Even
Two	$\hat{b}_1(z)$	$\hat{\mathcal{F}}_{1\frac{1}{2},1\frac{1}{2}} + \hat{\mathcal{F}}_{1-\frac{1}{2},1-\frac{1}{2}} - 2\hat{\mathcal{F}}_{0\frac{1}{2},0\frac{1}{2}}$	Quadruple	Even
Two	$\hat{g}_1(z)$	$\hat{\mathcal{F}}_{1\frac{1}{2},1\frac{1}{2}} - \hat{\mathcal{F}}_{1-\frac{1}{2},1-\frac{1}{2}}$	Helicity difference	Even
Two	$\hat{h}_1(z)$	$\hat{\mathcal{F}}_{0\frac{1}{2},1-\frac{1}{2}} + \hat{\mathcal{F}}_{1-\frac{1}{2},0\frac{1}{2}}$	Helicity flip	Odd
Three	$\hat{e}_1(z)$	$\hat{\mathcal{F}}_{1\frac{1}{2}^*,1\frac{1}{2}} + \hat{\mathcal{F}}_{1-\frac{1}{2}^*,1-\frac{1}{2}} + \hat{\mathcal{F}}_{0\frac{1}{2}^*,0\frac{1}{2}}$	Spin Average	Odd
Three	$\hat{b}_2(z)$	$\hat{\mathcal{F}}_{1\frac{1}{2}^*,1\frac{1}{2}} + \hat{\mathcal{F}}_{1-\frac{1}{2}^*,1-\frac{1}{2}} - 2\hat{\mathcal{F}}_{0\frac{1}{2}^*,0\frac{1}{2}}$	Quadruple	Odd
Three	$\hat{h}_2(z)$	$\hat{\mathcal{F}}_{1\frac{1}{2}^*,1\frac{1}{2}} - \hat{\mathcal{F}}_{1-\frac{1}{2}^*,1-\frac{1}{2}}$	Helicity difference	Odd
Three	$\hat{g}_2(z)$	$\hat{\mathcal{F}}_{0\frac{1}{2}^*,1-\frac{1}{2}} + \hat{\mathcal{F}}_{1-\frac{1}{2}^*,0\frac{1}{2}}$	Helicity flip	Even
Three	$\Delta\hat{g}_2(z)$	$\hat{\mathcal{F}}_{0\frac{1}{2}^*,1-\frac{1}{2}} - \hat{\mathcal{F}}_{1-\frac{1}{2}^*,0\frac{1}{2}}$	Helicity flip	Even

.8 Spin Structure of the Nucleon in QCD

.8.1 Angular Momentum Operator in QCD[21]

In accordance with the Noether theorem, there exists a symmetry generator $T_{\mu\nu}$ associated with the translational invariance in QCD, which is conserved, $\partial_\mu T^{\mu\nu} = 0$. $T^{\mu\nu}$ is called as energy-momentum tensor, which is gauge invariant and symmetric, $T^{\mu\nu} = T^{\nu\mu}$. The Noether current associated with Lorentz transformations is a rank-3 tensor constructed entirely from $T^{\mu\nu}$[67],

$$M^{\mu\nu\lambda} \equiv x^\nu T^{\mu\lambda} - x^\lambda T^{\mu\nu} \tag{107}$$

It is very easy to verify that $M^{\mu\nu\lambda}$ is conserved because $T^{\mu\nu}$ is symmetric and conserved. $M^{\mu\nu\lambda}$ is gauge invariant and has no totally antisymmetric part,

$$\epsilon_{\alpha\mu\nu\lambda} M^{\mu\nu\lambda} = 0 \tag{108}$$

or equivalently

$$M^{\mu\nu\lambda} + M^{\lambda\mu\nu} + M^{\nu\lambda\mu} = 0. \tag{109}$$

The generators of Lorentz transformations are defined as

$$J^{\mu\nu} \equiv \int d^3x M^{0\mu\nu}. \tag{110}$$

It is very easy to verify that $J^{\mu\nu}$ is conserved, $\frac{d}{dt} J^{\mu\nu} = 0$, and obey the Lie algebra of the Poincaré group

$$\begin{aligned} [P^\mu, P^\nu] &= 0, \\ \left[J^{\mu\nu}, P^\lambda\right] &= i(g^{\mu\lambda} P^\nu - g^{\nu\lambda} P^\mu), \\ \left[J^{\mu\nu}, J^{\lambda\sigma}\right] &= i(g^{\mu\lambda} J^{\nu\sigma} - g^{\nu\lambda} J^{\mu\sigma} - g^{\mu\sigma} J^{\nu\lambda} + g^{\nu\sigma} J^{\mu\lambda}) \end{aligned} \tag{111}$$

where $P^\mu \equiv \int d^3x T^{0\mu}$ is the generator of the translation group.

The energy-momentum density tensor of QCD is as follows[68]

$$T^{\mu\nu}_{\rm QCD} = \frac{1}{2}\bar{\psi} i \overset{\leftrightarrow}{D}^{(\mu} \gamma^{\nu)}\psi + \frac{1}{4} g^{\mu\nu} F^{\alpha\beta}F_{\alpha\beta} - F^{\mu\alpha}F^{\nu}_{\alpha} \ , \tag{112}$$

where the covariant derivative $\overset{\leftrightarrow}{D} \equiv \vec{D} - \overset{\leftarrow}{D}$ with $\overset{\leftarrow}{D} = \overset{\leftarrow}{\partial} - igA$. The symmetrization of the indices μ and ν in the first term is indicated by$(\mu\nu)$.

Substituting Eq. (112) into Eq. (107), a short algebra yields the angular momentum density tensor for QCD as below,

$$\begin{aligned} M^{\mu\nu\lambda}_{\rm QCD} &= \frac{i}{4}\bar{\psi}x^{\nu}(\gamma^{\mu} \overset{\leftrightarrow}{D}^{\lambda} + \gamma^{\lambda} \overset{\leftrightarrow}{D}^{\mu})\psi - \frac{i}{4}\bar{\psi}x^{\lambda}(\gamma^{\mu} \overset{\leftrightarrow}{D}^{\nu} + \gamma^{\nu} \overset{\leftrightarrow}{D}^{\mu})\psi \\ &\quad - \left(x^{\nu}F^{\mu\alpha}F^{\lambda}_{\alpha} - x^{\lambda}F^{\mu\alpha}F^{\nu}_{\alpha} - \frac{1}{4}F^{\alpha\beta}F_{\alpha\beta}(x^{\nu}g^{\mu\lambda} - x^{\lambda}g^{\mu\nu}) \right) \ . \end{aligned} \tag{113}$$

Clearly, there is no breakup of the tensor into pieces that one can identify as being due to the quark spin, gluon spin, quark orbital angular momentum, and gluon orbital angular momentum. However, note that there is an arbitrariness in the definition of $M^{\mu\nu\lambda}$, that is, in the context of some field theory let $B^{[\mu\beta][\nu\lambda]}$ be some operator antisymmetric in (μ, β) and (ν, λ) ($B^{[\mu\beta][\nu\lambda]}$ may contain an explicit factor of the coordinate x), then we can define a new tensor by adding a superpotential

$$M'^{\mu\nu\lambda} \equiv M^{\mu\nu\lambda} + \partial_{\beta} B^{[\mu\beta][\nu\lambda]}, \tag{114}$$

which is conserved and antisymmetric in ν and λ, the Lorentz generators $J'^{\mu\nu}$ defined from $M'^{\mu\nu\lambda}$ are the same as $J^{\mu\nu}$,

$$J'^{\nu\lambda} = J^{\nu\lambda} + \int d^3x \partial_i B^{[0i][\nu\lambda]} = J^{\mu\nu} \tag{115}$$

for field configurations which vanish at spatial infinity. By choosing a suitable superpotential, one obtains[21]

$$\begin{aligned} M^{\alpha\mu\nu} = \quad & i\bar{\psi}\gamma^{\alpha}(x^{\mu}\partial^{\nu} - x^{\nu}\partial^{\mu})\psi + \frac{i}{4}\bar{\psi}\gamma^{\alpha}[\gamma^{\mu}, \gamma^{\nu}]\psi \\ & - F^{\alpha\sigma}(x^{\mu}\partial^{\nu} - x^{\nu}\partial^{\mu})A_{\sigma} - F^{\alpha\mu}A^{\nu} + F^{\alpha\nu}A^{\mu} \ . \end{aligned} \tag{116}$$

Now the terms in Eq. (116) correspond successfully to the spin and orbital angular momenta of the quarks and gluons.

.8.2 Angular Momentum Sum Rule[21, 31]

Now we apply the results of the previous section to the nucleon system. According to the definition, a nucleon moving in the z direction with momentum P^μ and helicity $1/2$ satisfies

$$J^{12}|P+\rangle = \frac{1}{2}|P+\rangle \ , \tag{117}$$

where $J^{12} = \int d^3x M^{012}$.

Thus one can write down a spin sum rule,

$$\begin{aligned} \frac{1}{2} &= \langle P+|J^{12}|P+\rangle/\langle P+|P+\rangle \\ &= \frac{1}{2}\Delta\Sigma + \Delta g + L_q + L_g \ , \end{aligned} \tag{118}$$

where the matrix elements are defined as ($\gamma_5 = \gamma^5 = i\gamma^0\gamma^1\gamma^2\gamma^3$),

$$\begin{aligned} \Delta\Sigma &= \langle P+|\hat{S}_{3q}|P+\rangle = \langle P+|\int d^3x\ \bar{\psi}\gamma^3\gamma_5\psi\ |P+\rangle \ , \\ \Delta g &= \langle P+|\hat{S}_{3g}|P+\rangle = \langle P+|\int d^3x\ (E^1A^2 - E^2A^1)\ |P+\rangle \ , \\ L_q &= \langle P+|\hat{L}_{3q}|P+\rangle = \langle P+|\int d^3x\ i\bar{\psi}\gamma^0(x^1\partial^2 - x^2\partial^1)\psi\ |P+\rangle \ , \\ L_g &= \langle P+|\hat{L}_{3g}|P+\rangle = \langle P+|\int d^3x\ E^i(x^2\partial^1 - x^1\partial^2)A^i\ |P+\rangle \ , \end{aligned} \tag{119}$$

where for simplicity we have neglected the normalization of the state. $E^{ia} \equiv -F^{0ia} = -(\partial^0 A^{ia} - \partial^i A^{0a} + ig_s f^{abc}A^{0b}A^{ic})$ is the color electric field.

It is clear from the above that $\Delta\Sigma$ and Δg are the quark and gluon helicity contributions to the nucleon spin, and L_q and L_g are the quark and gluon orbital angular momentum contributions. Apart from $\hat{S}_{3q}$, the other three operators $\hat{S}_{3g}$, $\hat{L}_{3q}$ and $\hat{L}_{3g}$ are not manifestly gauge invariant, and thus a decomposition of the nucleon spin is in general gauge-dependent. [Note that X.Ji gives a gauge invariant decomposition of angular momentum operator in his recent paper[69]. However, he

proved that the new gauge-invariant operators satisfy the same evolution equation as the old gauge-dependent ones. Therefore, here we will still use the gauge-dependent ones to demonstrate the calculations.] Furthermore, the matrix elements depend on the choice of Lorentz frame. Only in light-front coordinates and light-front gauge [70] Δg is the gluon helicity measured in high-energy scattering processes. We henceforth work in this coordinates and gauge [71] (the index 0 in Eq. (110) is now replaced by +).

.8.3 JTH Evolution Equation of Angular Momentum at Leading Order [31]

The evolution equation to leading-log order of quark and gluon angular momenta can be obtained by calculating the anomalous dimensions

$$\frac{d}{dt}\begin{pmatrix} \Delta\Sigma \\ \Delta G \\ L_q \\ L_g \end{pmatrix} = \begin{pmatrix} 0 & 0 & 0 & 0 \\ \frac{3}{2}C_F & \frac{\beta_0}{2} & 0 & 0 \\ -\frac{2}{3}C_F & \frac{n_f}{3} & -\frac{4}{3}C_F & \frac{n_f}{3} \\ -\frac{5}{6}C_F & -\frac{11}{2} & \frac{4}{3}C_F & -\frac{n_f}{3} \end{pmatrix}\begin{pmatrix} \Delta\Sigma \\ \Delta G \\ L_q \\ L_g \end{pmatrix}, \tag{120}$$

which contains the well-known Altarelli-Parisi evolution equation for the quark and gluon helicity contributions at leading-log[33]. The solution of this evolution equation can be obtained straightforwardly,

$$\begin{aligned} \Delta\Sigma(t) &= \text{const}\ , \\ \Delta g(t) &= -\frac{4\Delta\Sigma}{\beta_0} + \frac{t}{t_0}\left(\Delta g_0 + \frac{4\Delta\Sigma}{\beta_0}\right) \\ L_q(t) &= -\frac{1}{2}\Delta\Sigma + \frac{1}{2}\frac{3n_f}{16+3n_f} + (t/t_0)^{-2(16+3n_f)/(9\beta_0)}\left(L_q(0) + \frac{1}{2}\Delta\Sigma - \frac{1}{2}\frac{3n_f}{16+3n_f}\right)\ , \end{aligned}$$

$$L_g(t) = -\Delta g(t) + \frac{1}{2}\frac{16}{16+3n_f} + (t/t_0)^{-2(16+3n_f)/(9\beta_0)}\left(L_g(0) + \Delta g(0) - \frac{1}{2}\frac{16}{16+3n_f}\right). \tag{121}$$

Given a composition of the nucleon spin at some initial scale Q_0^2, the above equations yield the spin composition at any other perturbative scales in the leading-log approximation. From the expression for $L_g(t)$, it is clear that that the large gluon helicity at large Q^2 is canceled by an equally large, but negative, gluon orbital angular momentum.

Neglecting the sub-leading terms at large Q^2, we get,

$$\begin{aligned} J_q &= L_q + \frac{1}{2}\Delta\Sigma = \frac{1}{2}\frac{3n_f}{16+3n_f}\,, \\ J_g &= L_g + \Delta g = \frac{1}{2}\frac{16}{16+3n_f}\,. \end{aligned} \tag{122}$$

Thus partition of the nucleon spin between quarks and gluons follows the well-known partition of the nucleon momentum [34]. Mathematically, one can understand this from the expression for the QCD angular momentum density $M^{\mu\alpha\beta} = T^{\mu\alpha}x^\beta - T^{\mu\beta}x^\alpha$. When $M^{\mu\alpha\beta}$ and $T^{\alpha\beta}$ are each separated into gluon and quark contributions, the anomalous dimensions of the corresponding terms are the same because they have the same short distance behavior.

It is interesting to speculate phenomenological consequences of this asymptotic partition of the nucleon spin. Assuming, as found in the case of the momentum sum rule[72], that the evolution in Q^2 is very slow, then the above partition may still be roughly correct at low momentum scales, say, $Q^2 \sim 3$ GeV^2. If this is the case, from the experimentally measured $\Delta\Sigma$ we get an estimate of the quark orbital contribution at these scales,

$$L_q = 0.05 \sim 0.15\,. \tag{123}$$

To find a separation of the gluon contribution into spin and orbit parts, we need to know Δg, which shall be measurable in the future[73]. However, if Q^2 variation is rapid, the asymptotic result implies nothing about the low Q^2 spin structure of the

nucleon. Unfortunately, no one knows yet how to measure L_q to determine the role of Q^2 variation. In his recent paper, X.Ji related angular momenta of the nucleon to some form factors in the so-called deep virtual Compton scattering process[69]. He pointed out that some informations about the spin structure, especially orbital angular momenta, could be probed in this kind of process.

.9 Matrix representation for the tensor operators and corresponding helicity bases

.9.1 J=1/2

$$Q_0^0 = \begin{pmatrix} 1 & 0 \\ 0 & 1 \end{pmatrix}, \quad Q_0^1 = \begin{pmatrix} 1 & 0 \\ 0 & -1 \end{pmatrix}$$
$$Q_1^1 = \begin{pmatrix} 0 & -\sqrt{2} \\ 0 & 0 \end{pmatrix}, \quad Q_{-1}^1 = \begin{pmatrix} 0 & 0 \\ \sqrt{2} & 0 \end{pmatrix} \tag{124}$$

$$|\tfrac{1}{2}\tfrac{1}{2}>= \begin{pmatrix} 1 \\ 0 \end{pmatrix}, \quad |\tfrac{1}{2}-\tfrac{1}{2}>= \begin{pmatrix} 0 \\ 1 \end{pmatrix}. \tag{125}$$

.9.2 J=1

$$H_0^0 = \begin{pmatrix} 1 & 0 & 0 \\ 0 & 1 & 0 \\ 0 & 0 & 1 \end{pmatrix}, \qquad H_0^1 = \begin{pmatrix} 1 & 0 & 0 \\ 0 & 0 & 0 \\ 0 & 0 & -1 \end{pmatrix}, \qquad H_1^1 = \begin{pmatrix} 0 & -1 & 0 \\ 0 & 0 & -1 \\ 0 & 0 & 0 \end{pmatrix}$$

$$H_{-1}^1 = \begin{pmatrix} 0 & 0 & 0 \\ 1 & 0 & 0 \\ 0 & 1 & 0 \end{pmatrix}, \qquad H_0^2 = \begin{pmatrix} 1 & 0 & 0 \\ 0 & -2 & 0 \\ 0 & 0 & 1 \end{pmatrix}, \qquad H_2^2 = \sqrt{6}\begin{pmatrix} 0 & 0 & 1 \\ 0 & 0 & 0 \\ 0 & 0 & 0 \end{pmatrix}$$

$$H_1^2 = \sqrt{3}\begin{pmatrix} 0 & -1 & 0 \\ 0 & 0 & 1 \\ 0 & 0 & 0 \end{pmatrix}, \quad H_{-1}^2 = \sqrt{3}\begin{pmatrix} 0 & 0 & 0 \\ 1 & 0 & 0 \\ 0 & -1 & 0 \end{pmatrix}, \quad H_{-2}^2 = \sqrt{6}\begin{pmatrix} 0 & 0 & 0 \\ 0 & 0 & 0 \\ 1 & 0 & 0 \end{pmatrix} \tag{126}$$

$$|11>= \begin{pmatrix} 1 \\ 0 \\ 0 \end{pmatrix}, \quad |10>= \begin{pmatrix} 0 \\ 1 \\ 0 \end{pmatrix}, \quad |1-1>= \begin{pmatrix} 0 \\ 0 \\ 1 \end{pmatrix}. \tag{127}$$

.9.3 J=1(gluon case)

$$G_0^0 = \begin{pmatrix} 1 & 0 & 0 \\ 0 & 1 & 0 \\ 0 & 0 & 1 \end{pmatrix}, \qquad G_0^1 = \begin{pmatrix} 1 & 0 & 0 \\ 0 & 0 & 0 \\ 0 & 0 & -1 \end{pmatrix}$$

$$G_2^2 = \sqrt{6}\begin{pmatrix} 0 & 0 & 1 \\ 0 & 0 & 0 \\ 0 & 0 & 0 \end{pmatrix}, \quad G_{-2}^2 = \sqrt{6}\begin{pmatrix} 0 & 0 & 0 \\ 0 & 0 & 0 \\ 1 & 0 & 0 \end{pmatrix} \tag{128}$$

$$|11>= \begin{pmatrix} 1 \\ 0 \\ 0 \end{pmatrix}, \quad |1-1>= \begin{pmatrix} 0 \\ 0 \\ 1 \end{pmatrix}. \tag{129}$$

.9.4 $J = 0$ or 1(s and p wave interference)

$$H^1_1(01) = \begin{pmatrix} 0 & 0 & 0 & -1 \\ 0 & 0 & 0 & 0 \\ 0 & 0 & 0 & 0 \\ 0 & 0 & 0 & 0 \end{pmatrix}, \quad H^1_0(01) = \begin{pmatrix} 0 & 0 & 1 & 0 \\ 0 & 0 & 0 & 0 \\ 0 & 0 & 0 & 0 \\ 0 & 0 & 0 & 0 \end{pmatrix},$$

$$H^1_{-1}(01) = \begin{pmatrix} 0 & -1 & 0 & 0 \\ 0 & 0 & 0 & 0 \\ 0 & 0 & 0 & 0 \\ 0 & 0 & 0 & 0 \end{pmatrix} \quad H^1_1(10) = \begin{pmatrix} 0 & 0 & 0 & 0 \\ 1 & 0 & 0 & 0 \\ 0 & 0 & 0 & 0 \\ 0 & 0 & 0 & 0 \end{pmatrix}, \tag{130}$$

$$H^1_0(10) = \begin{pmatrix} 0 & 0 & 0 & 0 \\ 0 & 0 & 0 & 0 \\ 1 & 0 & 0 & 0 \\ 0 & 0 & 0 & 0 \end{pmatrix}, \quad H^1_{-1}(10) = \begin{pmatrix} 0 & 0 & 0 & 0 \\ 0 & 0 & 0 & 0 \\ 0 & 0 & 0 & 0 \\ 1 & 0 & 0 & 0 \end{pmatrix}$$

$$H_0^0(11) = \begin{pmatrix} 0 & 0 & 0 & 0 \\ 0 & 1 & 0 & 0 \\ 0 & 0 & 1 & 0 \\ 0 & 0 & 0 & 1 \end{pmatrix}, \quad H_0^1(11) = \begin{pmatrix} 0 & 0 & 0 & 0 \\ 0 & 1 & 0 & 0 \\ 0 & 0 & 0 & 0 \\ 0 & 0 & 0 & -1 \end{pmatrix},$$

$$H_1^1(11) = \begin{pmatrix} 0 & 0 & 0 & 0 \\ 0 & 0 & -1 & 0 \\ 0 & 0 & 0 & -1 \\ 0 & 0 & 0 & 0 \end{pmatrix} \quad H_{-1}^1(11) = \begin{pmatrix} 0 & 0 & 0 & 0 \\ 0 & 0 & 0 & 0 \\ 0 & 1 & 0 & 0 \\ 0 & 0 & 1 & 0 \end{pmatrix}, \tag{131}$$

$$H_0^2(11) = \begin{pmatrix} 0 & 0 & 0 & 0 \\ 0 & 1 & 0 & 0 \\ 0 & 0 & -2 & 0 \\ 0 & 0 & 0 & 1 \end{pmatrix}, \quad H_2^2(11) = \sqrt{6} \begin{pmatrix} 0 & 0 & 0 & 0 \\ 0 & 0 & 0 & 1 \\ 0 & 0 & 0 & 0 \\ 0 & 0 & 0 & 0 \end{pmatrix}$$

$$H^2_1(11) = \sqrt{3}\begin{pmatrix} 0 & 0 & 0 & 0 \\ 0 & 0 & -1 & 0 \\ 0 & 0 & 0 & 1 \\ 0 & 0 & 0 & 0 \end{pmatrix}, \quad H^2_{-1}(11) = \sqrt{3}\begin{pmatrix} 0 & 0 & 0 & 0 \\ 0 & 0 & 0 & 0 \\ 0 & 1 & 0 & 0 \\ 0 & 0 & -1 & 0 \end{pmatrix},$$

$$H^2_{-2}(11) = \sqrt{6}\begin{pmatrix} 0 & 0 & 0 & 0 \\ 0 & 0 & 0 & 0 \\ 0 & 0 & 0 & 0 \\ 0 & 1 & 0 & 0 \end{pmatrix} \qquad H^0_0(00) = \begin{pmatrix} 1 & 0 & 0 & 0 \\ 0 & 0 & 0 & 0 \\ 0 & 0 & 0 & 0 \\ 0 & 0 & 0 & 0 \end{pmatrix}. \tag{132}$$

$$|00>= \begin{pmatrix} 1 \\ 0 \\ 0 \\ 0 \end{pmatrix}, \quad |11>= \begin{pmatrix} 0 \\ 1 \\ 0 \\ 0 \end{pmatrix}, \quad |10>= \begin{pmatrix} 0 \\ 0 \\ 1 \\ 0 \end{pmatrix}, \quad |1-1>= \begin{pmatrix} 0 \\ 0 \\ 0 \\ 1 \end{pmatrix}. \tag{133}$$

.9.5 Angular momentum operators

$J = 1/2$

$$J_0 = \tfrac{1}{2}\begin{pmatrix} 1 & 0 \\ 0 & -1 \end{pmatrix}, \quad J_+ = \begin{pmatrix} 0 & 1 \\ 0 & 0 \end{pmatrix}, \quad J_- = \begin{pmatrix} 0 & 0 \\ 1 & 0 \end{pmatrix} \tag{134}$$

$J = 1$

$$J_0 = \begin{pmatrix} 1 & 0 & 0 \\ 0 & 0 & 0 \\ 0 & 0 & -1 \end{pmatrix}, \quad J_+ = \begin{pmatrix} 0 & \sqrt{2} & 0 \\ 0 & 0 & \sqrt{2} \\ 0 & 0 & 0 \end{pmatrix}, \quad J_- = \begin{pmatrix} 0 & 0 & 0 \\ \sqrt{2} & 0 & 0 \\ 0 & \sqrt{2} & 0 \end{pmatrix} \tag{135}$$

$J = 0, 1$ ***s* and *p* interference**

$$J_0 = \begin{pmatrix} 0 & 0 & 0 & 0 \\ 0 & 1 & 0 & 0 \\ 0 & 0 & 0 & 0 \\ 0 & 0 & 0 & -1 \end{pmatrix}, \quad J_+ = \begin{pmatrix} 0 & 0 & 0 & 0 \\ 0 & 0 & \sqrt{2} & 0 \\ 0 & 0 & 0 & \sqrt{2} \\ 0 & 0 & 0 & 0 \end{pmatrix}, \quad J_- = \begin{pmatrix} 0 & 0 & 0 & 0 \\ 0 & 0 & 0 & 0 \\ 0 & \sqrt{2} & 0 & 0 \\ 0 & 0 & \sqrt{2} & 0 \end{pmatrix} \tag{136}$$

Bibliography

[1] C. Itzykson and J. Zuber, *Quantum Field Theory*, McGraw-Hill, 1980. T.P. Cheng and L.F. Li, *Gauge theory of elementary particle physics*, Oxford University Press, 1984. Otto Nachtmann, *Elementary Particle Physics: Concepts and Phenomena*, Springer-Verlag, 1990. R. D. Field, *Applications of Perturbative QCD*, Addison-Wesley, 1989. T. Muta, *Foundations of Quantum Chromodynamics*, World Scientific, Singapore(1987). F. E. Close, *An Introduction to Quarks and Partons*, Academic Press, New York, 1979.

[2] M. Gell-Mann and Y. Ne'eman, *The Eightfold way*, W. A. Benjamin, New York and Amsterdam, 1964.

[3] M. Gell-Mann, Acta Physics Austriaca, Suppl.**9**(1972) 733. H. Fritzsch and M. Gell-Mann, in *Proc. XVth Intern. Conf. on High Energy Physics, Chicago-Batavia*, NAL, Batavia, 1973.

[4] W. Thirring, Acta Physics Austriaca, Suppl. **II**(1965) 205.

[5] D.J. Gross and F. Wilczek, Phys. Rev. Lett. **30**(1973)1343; Phys. Rev. **D8**(1973)3633; Phys. Rev. **D9**(1974)980. H.D. Politzer, Phys. Rev. Lett. **30**(1973) 1346;

[6] For a review, see R. L. Jaffe, in *Proceedings of the Ettore Majorana Intern ational School of Nucleon Structure: 1st Course: The Spin Structure of the Nucleon, Erice, Italy, 1995.*, `hep-ph/9602236`.

[7] K. Wilson, Phys. Rev. **179**(1969)1499; Phys. Rev. **D3**(1971)1818. W. Zimmermann, Ann. of Phys. **77**(1973)536, 570.

[8] J. D. Bjorken, Phys. Rev. **179**(1969) 1574.

[9] C. G. Callan and D. J. Gross, Phys. Rev. Lett. **22**(1969) 156.

[10] R. L. Jaffe and X. Ji, *Phys. Rev. Lett.* **67** (1991) 552.

[11] R. L. Jaffe, X. Ji, *Nucl. Phys.* **B375** (1992).

[12] X. Ji, *Phys. Rev.* **D49**, 114 (1994).

[13] J. Ashman et al., Phys. Lett. **B206** (1988) 364; Nucl. Phys. **B328** (1989) 1.

[14] J. Kodaira, Nucl. Phys. **B165**(1979)129.

[15] J. Kodaira, S. Matsuda, T. Muta, T. Uematsu and K. Sasaki, Phys. Rev. **D20** (1979)627; J. Kodaira, S. Matsuda, K. Sasaki and T. Uematsu, Nucl. Phys. **B159**(1979)99.

[16] S. L. Adler, Phys. Rev. **177**(1969) 2426; J. S. Bell and R. Jackiw, Nuovo Cimento **A51**(1967) 47.

[17] S. Okubo, Phys. Lett. **5**(1963)165; G. Zweig, CERN preprints 401, 412, (1964)(unpublished); J. Iizuki, Suppl. Theor. Phys. **37**(1966)21.

[18] J. Ellis and R. L. Jaffe, Phys. Rev. **D9**(1974) 3594.

[19] E143 Collaboration, K. Abe et al., SLAC-PUB-95-6997, hep-ex/9511015.

[20] R.L. Jaffe. MIT-CTP-2518, HUTP-96/A010, hep-ph/9603422(1996).

[21] R. L. Jaffe and A. Mahohar, Nucl. Phys. **B337**(1990) 509.

[22] B. Adeva ea al., Phys. Lett. **B302** (1993) 533; P. L. Anthony et al., Phys. Rev. Lett. **71** (1993) 959; K. Abe et al., Phys. Rev. Lett. **74** (1995) 346.

[23] J. Ellis and M. Karliner, CERN-TH/95-334, TAUP-2316-96, hep-ph/9601286; J. Ellis and M. Karliner, Phys. Lett. **B341**(1995)397.

[24] J. Bijnens, H. Sonoda, and M.B. Wise, Nucl. Phys. **B261**(1985)261.

[25] B. Ehrnsperger and A. Schafer, Phys. Lett.**B348**(1995) 619; J. Dai, R. Dashen, E. Jenkins and A. Manohar, Phys. Rev.**D53**(1996)273; J. Lichtenstadt and H.J. Lipkin, Phys. Lett.**B353**(1995)119.

[26] D.B. Kaplan and A. Manohar, Nucl. Phys. **B310**(1988)527; G.T. Garvey, W.C. Louis and D.H. White, Phys. Rev.**C48**(1993)761.

[27] F.E. Close and R.G. Roberts, Phys. Rev. Lett. **66**(1988) 1471.

[28] R.L. Jaffe, Phys. Lett. **B193**(1987)101.

[29] G. Altarelli and G. G. Ross, Phys. Lett.**B212**(1988) 391.

[30] R. D. Carlitz, J. C. Collins and A. H. Mueller, Phys. Lett. **B214**(1988) 229.

[31] X. Ji, J. Tang and P. Hoodbhoy, Phys. Rev. Lett. **76**(1996)740.

[32] X. Ji, Phys. Rev. Lett.**78**(1997)610; Phys.Rev.D**55**(1997)7114.

[33] G. Altarelli and G. Parisi, Nucl. Phys. **B126**(1977)298.

[34] D.Gross and F.Wilczek, Phys. Rev. **D9**(1974) 980.

[35] R.L. Jaffe, Xuemin Jin, and Jian Tang, Phys. Rev. Lett. **80**, 1166(1998); R.L. Jaffe, Xuemin Jin, and Jian Tang, Phys. Rev. **D57**, 5920(1998).

[36] Jian Tang, MIT-CTP-2769, hep-ph/9807560.

[37] K. Chen, G. R. Goldstein, R.L. Jaffe, X. Ji, Nucl. Phys. **B445**, 380 (1995).

[38] R. L. Jaffe, Phys. Rev. D**54**(1996)6581.

[39] R. Gastmanns and T. T. Wu, *The Ubiquitous Photon: The helicity Method for QED and QCD* (Clarnedon Press, Oxford, 1990).

[40] A. R. Edmonds, *Angular Momentum in Quantum Mechanics*, Princeton University Press(1960). J. J. Sakurai, *Modern Quantum Mechanics*, Addison-Wesley(1994).

[41] Particle Data Group, Phys. Rev. D**54**(1996) 1.

[42] R. L. Jaffe, MIT-CTP-2685, hep-ph/9710465.

[43] See, for example, V. W. Hughes and C. Cavata, *Internal Spin Structure of the Nucleon, Procedings of the Symposium on Internal Spin Structure of the Nucleon, New Haven, 1994* (World Scientific, Singapore, 1995). G. Altarelli and G. Ridolfi, *Nucl. Phys. Proc. Suppl.* **39BC** (1995) 106.

[44] J. Ralston and D. E. Soper, *Nucl. Phys.* **B152** (1979) 109.

[45] X. Artru and M. Mekhfi, *Z. Phys.* **C 45** (1990) 669.

[46] J. L. Cortes, B. Pire, J. P. Ralston, *Z. Phys.* **C 55** (1992) 409.

[47] SMC (D. Adams *et al.*), Phys. Lett. **B357**, 248 (1995); For a review, see *e.g.* G. Altarelli and G. Ridolfi, Nucl. Phys. Proc. Suppl. **39BC**, 106 (1995).

[48] W. Vogelsang, hep-ph/9706511. A. Hayashigaki, Y. Kanazawa, Y. Koike, hep-ph/9707208. S. Kumano and M. Miyana, hep-ph/9706420.

[49] J. Soffer, *Phys. Rev. Lett.* **74** (1995) 1292.

[50] H. He and X. Ji, Phys. Rev. D**52**(1995) 2960; Phys. Rev. D**54**(1996) 6897; X. Jin and J. Tang, Phys. Rev. D**56**(1997) 5618.

[51] S. Aoki, M. Doui, T. Hatsuda, Y. Kuramashi, *Phys. Rev.* **D56** (1997) 433.

[52] X. Ji, *Phys. Lett.* **B284** (1992) 137.

[53] R. L. Jaffe and N. Saito *Phys. Lett.* **B382** (1996) 165-172.

[54] J. C. Collins, *Nucl. Phys.* B396 (1993) 161; J. C. Collins, S. F. Heppelmann, and G. A. Ladinsky, *Nucl. Phys.* **B420** (1994) 565.

[55] B. Kamal, *Phys. Rev.* **D53** (1996) 1142.

[56] V. Barone, T. Calarco, A. Drago, *Phys. Rev.* **D56** (1997) 527.

[57] H. E. Conzett, Berkeley preprint, LBL-38589, Mar 1996.

[58] R. L. Jaffe, X. Jin, and J. Tang, in preparation.

[59] J. C. Collins and D. E. Soper, Nucl. Phys. **B194**, 445 (1982).

[60] M. L. Goldberger and K. M. Watson, *Collision Theory* (J. Wiley&Sons, New York, 1964).

[61] P. Estabrooks and A. D. Martin, Nucl. Phys. **B79**, 301 (1974).

[62] R. L. Jaffe, X. Jin, and J. Tang, in preparation.

[63] T. Gehrmann, W.J. Stirling, Phys.Rev.**D53**, 6100(1996).

chapter6

[64] J. C. Collins, Nucl. Phys. **B396**, 161 (1993).

[65] L. L. Frankfurt *et al.*, Phys. Lett. **B230**, 141 (1989).

[66] F. E. Close and R. G. Milner, Phys. Rev. **D 44**, 3691 (1991).

[67] See, for instance, S. Weinberg, *Gravitation and Cosmology*, Wiley, New York, 1972.

[68] See e.g. X. Ji, Phys. Rev. Lett. **74**(1995)1071; Phys. Rev. D**52** (1995)271.

[69] X. Ji, preprint MIT-CTP-2517, Cambridge(1996); hep-ph/9603249.

[70] I. Balitsky and V. Braun, Phys. Lett. **B267** (1991) 405.

[71] For a nice introduction to QCD in light-front coordinates, see the appendix of the paper by S. Brodsky and P. Lepage, in *Perturbative Quantum Chromodynamics*, ed. by A. Mueller, World Scientific, Singapore, 1989.

[72] See, for instance, T. Sloan, G. Smadja, and R. Voss, Phys. Rep. **162** (1988) 45.

[73] G. Bunce et al., Particle World 3 (1992) 1; The STAR and PHENIX spin proposals.